Role of radiation-induced immune changes for normal tissue toxicity with a focus on CD73/adenosine signaling and macrophages

Inaugural-Dissertation
zur
Erlangung des Doktorgrades

Dr. rer. nat.

der Fakultät für
Biologie

an der

Universität Duisburg-Essen

vorgelegt von

Simone de Leve
aus Nordhorn

Oktober 2016

Die der vorliegenden Arbeit zugrundeliegenden Experimente wurden am Institut für Zellbiologie (Tumorforschung) in der Arbeitsgruppe Molekulare Zellbiologie der Universität Duisburg-Essen durchgeführt.

1. Gutachter: Prof. Dr. Verena Jendrossek
2. Gutachter: Prof. Dr. Stefanie Flohé
3. Gutachter: Prof. Dr. Udo Gaipl
Vorsitzender des Prüfungsausschusses: Prof. Dr. Shirley Knauer
Tag der mündlichen Prüfung: 13.03.2017

Meiner Familie

Table of Contents

1 Introduction

1.1 Radiation treatment in cancer and normal tissue toxicity

More than 50% of all cancer patients receive radiotherapy (RT), at least once during their disease [6, 32]. Therefore, RT is one major treatment option for tumor patients besides surgery and chemotherapy. However, most often different treatment modalities are combined to achieve best tumor control and quality of life [78].

Radiation is applied with high-energy photons, charged particles like protons or heavy ions. RT is high effective in tumor cell killing because of its DNA damaging capacity. Especially DNA double strand breaks were identified as main contributors to the tumor cell killing characteristic of ionizing radiation (IR) [95]. RT triggers the generation of free radicals and reactive ions, particularly hydroxyl radicals. These molecules can cause further damage to cells resulting in a cellular stress response or cell death [13]. Due to its high potential to eradicate tumor cells, RT is one of the most effective cancer treatments [6].

Although there has been much technical improvement to administer the IR precisely to the tumor volume and spare as much healthy tissue as possible, normal tissue toxicity remains an important dose-limiting factor in RT [6]. The tolerance of the normal tissue to the toxic effects of IR is normally higher than the sensitivity of the tumor cells. The difference between the dose-response curves of the specific tumor type and the surrounding tissue defines the therapeutic window of RT (Figure 1) [78]. High intrinsic radioresistance of tumor

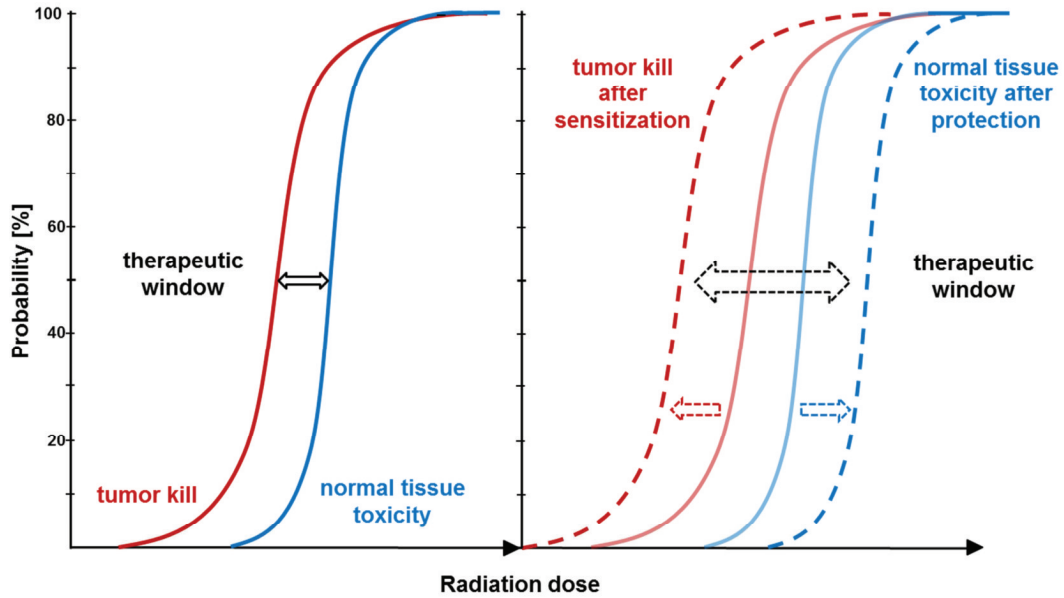

Figure 1: The therapeutic window in RT: The therapeutic window is defined by the difference between the probability of a certain radiation dose to kill the irradiated tumor cells and the probability to damage the normal tissue within the irradiation field. The wider the therapeutic window the more effective RT can be in tumor control and normal tissue toxicity (left part). Sensitizing tumor cells for irradiation and protecting normal tissue from irradiation can help to widen the therapeutic window (right part). Modified from [78] and [44]

cells, for example mediated through mutations or hypoxia, aggravates successful therapy outcomes [97]. Thus it is favorable to combine RT with other therapies to widen the therapeutic window, by sensitizing the tumor for RT-mediated cell death and/or by protecting the normal tissue from adverse effects of RT.

The lung is one of the most sensitive organs to radiation-induced damage. Nevertheless, RT is a standard treatment option for patients suffering from a neoplasm in the thoracic room e.g. lung tumor, head and neck cancer, or breast cancer. Also, patients who receive total body irradiation (TBI) in conditioning regimens for stem cell or bone marrow transplantations receive irradiation of the lung [69]. A major challenge for treating lung cancer is the high radioresistance of the tumors mediated for example through high intrinsic repair capabilities, hypoxia or a large tumor volume at the start of the treatment [159]. On the one hand, RT aims to achieve highest possible tumor control rates, by applying high radiation doses so that normal tissue toxicity cannot be excluded [122]. On the other hand, the high radiosensitivity of the normal lung tissue limits the applied dose, thereby enhancing the risk of local relapses and reducing tumor control [159].

Adverse side effects of RT are generally subdivided into early or acute toxicities and late or chronic toxicities [20, 69]. Regarding the normal lung tissue, side effects include acute inflammatory responses (pneumonitic phase) as well as chronic inflammatory responses, tissue remodeling and fibrosis development (fibrotic phase). Particularly these late side effects limit the total dose that is applied during the treatment as they are of a progressive nature [20, 156]. Radiation-induced pneumonitis and fibrosis are life-threatening adverse side effects of RT, but currently there are no therapies for a complete prevention or treatment of the diseases available [47]. Although already a lot of research has been done investigating and improving the direct damage of IR to tumor cells [38, 89], the side effects induced in the irradiated surrounding tissues are still not well understood. Consequently, there is a high need for the development of new treatment approaches to reduce normal tissue toxicity in RT.

1.2 Radiation-induced pneumopathy

1.2.1 Radiation-induced pneumonitis

Radiation-induced pneumonitis develops usually 4-12 weeks after radiation treatment and occurs in 5-20% of patients with lung or breast cancer in the irradiated and non-irradiated lung regions [47, 90, 119]. For patients receiving TBI the incidence of radiation pneumonitis was shown to be higher than 30% [69]. The damage of the lung tissue depends on the dose and volume of the irradiation field, but also on patient related factors like age, gender and performance status [122]. The symptoms of radiation-pneumonitis range from

low-grade fever and nonspecific respiratory symptoms up to dyspnea, non-productive cough, and chest pain [90, 119, 122]. During this acute phase of lung injury a massive infiltration of lymphocytes, monocytes, neutrophils and macrophages and subsequent changes in the cytokine and chemokine reservoir has been described from others and our lab [2, 17, 65, 125]. For details see section 1.3.2. Up to now, no causative but symptomatic treatment with glucocorticoids is available, which might reduce inflammation and inhibit endothelial cell toxicity [48]. Other anti-inflammatory agents (Azathioprine and cyclosporine) were shown to effectively dampen the symptoms of pneumonitis and could be used if glucocorticoids are not suitable [48, 110].

1.2.2 Radiation-induced lung fibrosis

Radiation-induced lung fibrosis (RILF) is the late adverse effect, limiting the treatment dose and enhancing the risk of tumor relapses simultaneously [20, 156]. Fibrosis development can occur in patients, who did not have pneumonitis before or were asymptomatic after acute pneumonitis [160]. Pulmonary fibrosis appears around six months up to years after irradiation. Major symptoms are breathing difficulties due to volume loss of the lung upon massive collagen deposition [20, 90]. So far, no treatment for patients suffering from RILF is available, but different approaches are in experimental investigations [20, 90, 160].

Fibrosis is characterized by accumulation of extracellular matrix (ECM) molecules in the lung tissue, leading to tissue scarring, progression of volume loss, and subsequent reduction of breathing ability (Figure 2) [165]. Fibrotic areas are mainly composed of collagens and fibronectin. Both proteins are known to be synthesized and secreted by fibroblasts. Various cell types are thought to impact on the development of RILF. One example are myofibroblasts, which can either derive from fibroblasts, circulating fibrocytes, or through epithelial-mesenchymal transition (EMT), a process in which epithelial cells undergo a transition to fibroblasts or myofibroblasts via migratory mesenchymal cells [120, 146, 161, 165]. Furthermore, radiation-induced damage to resident lung cells may lead to a delayed death of bronchiolar epithelial cells and result in a loss of barrier function [34]. Immune cells are recruited to the irradiated lung tissue and have been correlated to pathologic actions in patients with pulmonary fibrosis [65, 146]. The underlying mechanisms leading to pulmonary fibrosis are still not fully understood and although it is thought to be a deregulation of repair processes, potentially resulting from chronic inflammation, the contribution of the different immune cells to pathogenesis remains elusive [12, 16, 83, 165]. A detailed analysis of the different immune cells is described in the section 1.3.2.

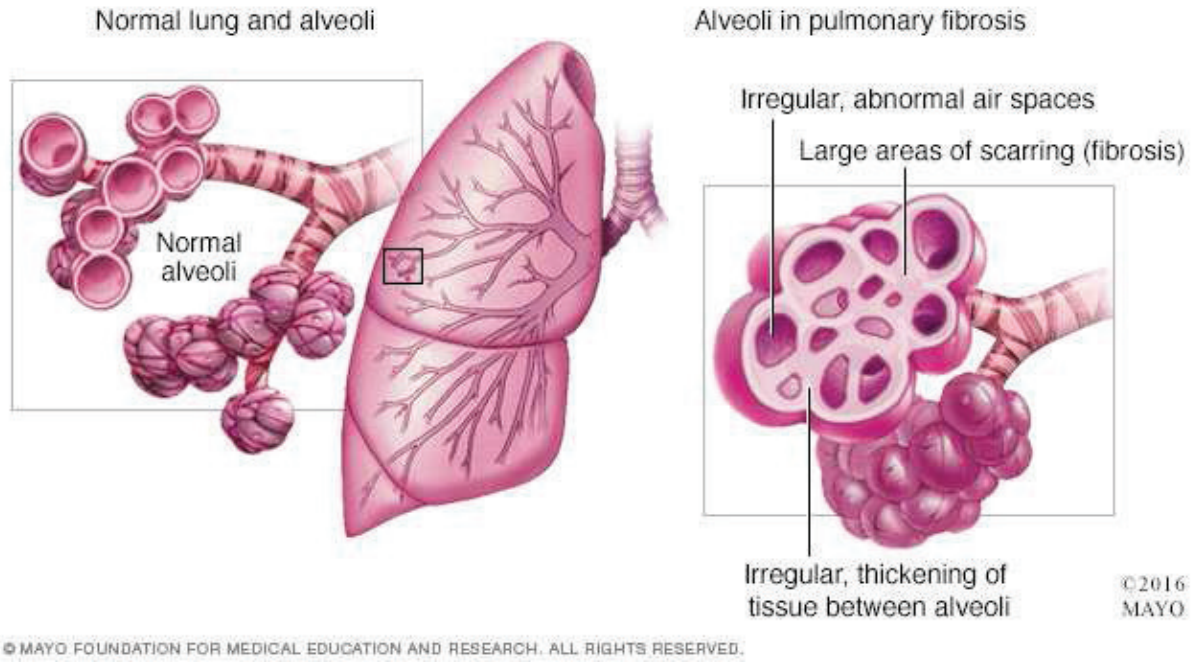

Figure 2: Schematic overview of a healthy lung and alveoli compared to alveoli in pulmonary fibrosis. The tissue between adjacent alveoli is thickened and irregular. Large areas of fibrosis, which mostly consist of collagen, can be found. The structure of the air spaces is irregular (http://www.mayoclinic.org/diseases-conditions/pulmonary-fibrosis/home/ovc-20211752).

1.2.3 Model systems to study radiation-induced normal tissue damage

The development of radiation-induced pneumonitis and lung fibrosis is a multicellular process that includes the complex interaction of various types of cells and soluble mediators. Model systems in the cell culture including two or three different cell types are not able to mimic the ongoing processes in the human body. Consequently, it is unavoidable to use *in vivo* model systems to study radiation-induced lung toxicity. One possible and most often used model organism that is also used by our lab is the mouse. Therefore, the following section focusses on murine models to investigate pulmonary fibrosis.

The most commonly used model to investigate different types of pulmonary injury (e.g. idiopathic pulmonary fibrosis (IPF) or chronic obstructive pulmonary disease (COPD)) is the bleomycin (BLM) model of lung injury [102]. BLM has been shown to induce lung injury as well as fibrosis in many model organisms like mice, rats, hamsters, dogs and primates, but is mostly used in murine studies [99, 102]. BLM is an antibiotic, produced by *Streptomyces verticillus* and used in cancer therapy, due to its tumor killing ability [54, 96]. It was shown that BLM induces single and double strand breaks in the DNA. Therefore, it is an useful agent to mimic irradiation-induced damage [137].

The model of BLM-induced lung fibrosis is separated further into different models. One intratracheal (i.t.) instillation of BLM leads to an acute lung injury (acute model) and to the development of fibrosis within 14 days which is mostly located bronchiocentric [23, 96]. It has been reported that in contrast to the human disease fibrosis can resolve in the i.t. model

of BLM-induced lung fibrosis [99]. More recently, a model of repetitive i.t. injections of BLM has been established and it was described to mimic the chronic aspect of pulmonary fibrosis more accurately [31]. Several intraperitoneal (i.p.) or intravenous (i.v.) injections of BLM result in lung inflammation and a more lasting fibrosis development around 28-33 days with subpleural scarring similar to the pathology in humans (chronic model) [23, 174].

Another *in vivo* model to study radiation-induced lung injury is a radiation-based model with a single high dose of IR. Thereby the mice undergo either a total body or whole thorax irradiation (WTI) with doses ranging from 12 to 15 Gy [99]. The irradiation model mimics the pathology observed in the clinics with a pneumonitic phase, one to three months after irradiation, and fibrosis development, after more than 6 months (24-30 weeks) [61, 99]. A disadvantage of the irradiation model with a single high dose is that the irradiation dose in cancer treatments is usually applied in fractionated doses to improve cytotoxic effects to the tumor and reduce normal tissue damage [19]. A more suitable model would therefore be a fractionated model. However, fractionated models of thorax irradiation are so far only reported in studies with rats and not mice [151, 153]. In the future, it will be necessary to establish also adequate murine models with fractionated irradiation schemes to improve the clinical relevance of the model.

It has been shown that fibrosis development after BLM treatment or thorax irradiation is strongly strain specific. In the model of BLM-induced lung fibrosis the murine strains CBA and C57BL/6 were shown to be fibrosis-prone, whereas BALB/c mice were fibrosis-resistant [96]. In the model of irradiation-induced fibrosis C3H/HeJ and CBA/J were shown to be fibrosis-resistant [99]. BALB/c mice developed only small areas with mild fibrosis after thorax irradiation [61], whereas C57BL/6 mice are reported to be fibrosis prone [60, 99]. All experiments in this project were conducted with the fibrosis-prone mice strain C57BL/6 and by irradiating the mice over their whole thorax with a single high dose of 15 Gy from a Cobalt-60 source.

1.3 Driving forces of inflammation and repair processes upon irradiation injury

1.3.1 Soluble mediators

Initially, IR causes DNA single- and double-strand breaks as well as reactive oxygen and nitric oxide species (ROS and NOS) [13]. ROS and NOS can induce further DNA damage or damage to ECM components. Even more, these highly reactive molecules initiate stress responses and immune responses. Unrepaired DNA damage might lead to cell death, which in turn causes an immune response initiating the elimination of damaged cells and debris and the repair and regeneration of the wound [134].

Danger-associated molecule patterns (DAMPs) are endogenous molecules created and released upon tissue damage. Examples for DAMPs are heat shock protein 70 (HSP70), high mobility group box 1 protein (HMGB1), surfactant protein A, adenosine triphosphate (ATP) and hyaluronan (HA) fragments [112, 149]. They are known as key molecules in the initiation of tissue repair. DAMPs act via toll-like receptors (TLRs) and lead to two main intrinsic pathways depending on the receptor and the associated proteins they bind to [149]. The first pathway leads, via several stages, to the activation of nuclear factor kappa-light-chain-enhancer of activated B cells (NF-κB) and results in the expression of pro-inflammatory cytokines. The second pathway results in the synthesis of pro-inflammatory interferons (IFN) [112]. However, DAMPs are reported to be highly upregulated in many pathologic conditions revealing an important role for regulated DAMP secretion/production [144, 149].

Furthermore, irradiation induces rapid changes in cytokine/chemokine expression and redox-sensitive proteins, where the latter could be a result of pro-inflammatory cytokines/chemokines [128]. Generation of ROS through cytokines causes enhanced cell death and DNA damage [128]. The main goal of cytokine/chemokine release upon irradiation is the restoration of tissue homeostasis as well as the orchestration of cell communications between mesenchymal, epithelial and immune cells [128]. Cytokines, chemokines and DAMPs work closely together to fulfill this task. [108]. It is also known that cytokine cascades that are initially driven by DAMPs drive inflammatory tissue damage [129]. Release of cytokines, chemokines and DAMPs trigger immune cell infiltration to the damage site. During regeneration anti-inflammatory cells infiltrate to the tissue and help to orchestrate the substitution of damaged areas by secretion of ECM components [128]. The first cytokines being released are among others interleukin 1, 6 (IL-1, IL-6) and tumor necrosis factor alpha (TNFα). Those are able to activate especially the resident immune cells like lymphocytes and macrophages [128] and can be found increased in plasma shortly after irradiation [119]. Mediated through cytokines and chemokines, adhesion molecules on the endothelial membranes are upregulated to facilitate the infiltration of more lymphocytes, monocytes and macrophages into the lung tissue from the blood [119].

1.3.2 The Immune cells

Irradiation within the thoracic room leads to an influx of diverse types of immune cells that orchestrate a complex interaction with resident cells as well as with each other. Among them are T lymphocytes and myeloid cells/ macrophages which are in the focus of this thesis. T-lymphocytes as well as myeloid cells and neutrophils were found to be elevated after radiation treatment in breast cancer patients [85]. We and others showed in a preclinical mouse model that WTI leads to an infiltration of activated T cells [17, 22, 64, 105]. Similarly, in a study with rats undergoing hemithorax irradiation an influx of $CD4^+$ T cells was observed

at 4 weeks after irradiation. A depletion of those cells resulted in reduced alveolar thickening [157]. In a patient based study RT also led to an increase in $CD4^+$ and $CD8^+$ T cells in bronchoalveolar lavages (BAL). Patients who were later diagnosed with pneumonitis were characterized by higher total cell counts and higher proportions of T-lymphocytes [105]. Similar results were obtained by two other studies analyzing BAL samples of irradiated and non-irradiated patients. Interestingly, pneumonitis could be detected in both lung lopes although irradiation was limited to one half [85, 121]. Also in a murine model, inflammation could be observed in all lopes of the lung although only the right hemithorax received radiation treatment [35]. Taken together, the data suggest an important role for inflammatory T-lymphocytes in radiation-induced pneumonitis and indicate the inclusion of systemic effects. Our lab could furthermore show that the loss of mature T and B-lymphocytes in recombination activating gene 2 (RAG2) deficient mice was accompanied by an early onset of fibrosis [17]. Moreover, important roles for $CD4^+$ T cell subsets in pro-fibrotic actions have also been proposed, for example through the secretion of IL-4, IL-5 or IL-13 [163]. These data indicate crucial roles for T-lymphocytes in early and late events after WTI.

Besides lymphocytes also myeloid cells and macrophages infiltrate into the lung upon irradiation [17, 63, 87]. Macrophages are the first line of defense and responsible for the orchestration of the immune response. One of their major functions is the phagocytosis of apoptotic neutrophils that infiltrate into the lung upon tissue injury [56]. In previous studies from our lab hemithorax irradiation of C57BL/6 mice led to increased levels of various macrophage-related cytokines and chemokines in BAL. Elevated mediators include macrophage-colony stimulating factor (M-CSF), macrophage chemoattractant protein-1 (MCP-1; CCL-2), macrophage inflammatory proteins (MIP)-1ß and MIP-2. Moreover, irradiation led to the formation of lipid-loaded macrophages, indicating a disturbed lipid metabolism [17].

Alveolar macrophages infiltrate into the airways shortly after birth. Once in the lung tissue they are known to be able to undergo self-renewal [50, 52]. But in the case of depletion of alveolar macrophages through IR it has been shown, that circulating monocytes can contribute at least partially to a repopulation [86]. Pulmonary macrophages are the first line of defense, phagocyting cell debris and pathogens [81]. In general, macrophages show a high plasticity and rapidly respond to changes in their microenvironment [45, 56, 113]. Therefore, they have been subdivided into classically and alternatively activated macrophages. The classical activation refers to a pro-inflammatory phenotype and is also named M1 phenotype, whereas the alternative activation refers to an anti-inflammatory macrophage phenotype and is also named M2 phenotype [45, 113]. It has been suggested that pro-inflammatory macrophages contribute to radiation-induced pneumonitis, whereas anti-inflammatory macrophages contribute to RILF [34].

Activation of TLRs through DAMPS or the cytokine IFN-γ, which is released upon tissue injury, can drive the polarization into a pro-inflammatory macrophage phenotype. Pro-inflammatory macrophages show improved phagocytic capacity and production of pro-inflammatory cytokines to recruit further immune cells from the circulation to the site of injury [56, 81, 138]. A study from Savani and colleagues revealed that i.t. injection of BLM in rats resulted in an influx of macrophages [127]. Furthermore, in a study with C57BL/6 mice receiving 12 Gy WTI macrophages expressed the inducible nitric oxide synthase (iNOS) a known marker of the pro-inflammatory phenotype of macrophages early after irradiation [171].

Apart from that, the accumulation of macrophages and their mediators is also one characteristic feature of chronic inflammatory diseases [91]. The source of enhanced chemokines in chronically inflamed tissues (e.g. in patients with IPF [18], rheumatoid arthritis [71] or BLM-induced lung injury in mice [132]) could be attributed to activated macrophages [91]. Macrophages have been reported to drive fibroblast recruitment and activation during fibrotic diseases [164]. The secretion of pro-fibrotic mediators like osteopontin (OPN), transforming growth factor beta (TGFβ) and platelet derived growth factor (PDGF) has also been attributed to macrophages in fibrotic tissues [143, 163].

Interestingly in pathologic conditions that include chronic inflammation, macrophages with an anti-inflammatory phenotype were found. Alternative activated macrophages are suspected to drive IPF, COPD [173] and potentially RILF [171, 173]. Moreover, macrophages in irradiation-induced fibrotic lung tissues were found to express arginase-1 (ARG1), a protein that competes with iNOS for its substrate L-Arginine. The products emerging from the metabolism of L-Arginine through ARG1 drive cell growth and collagen synthesis. Therefore, ARG1 activity is a feature of anti-inflammatory macrophages [171].

Prominent roles for macrophages, especially alternatively activated macrophages, and T-lymphocytes in the development of pulmonary fibrosis have been suggested. However, the underlying mechanisms are not yet understood. Particularly their role in RILF remains elusive and further investigations are required.

1.4 Signaling molecules investigated in the present thesis

1.4.1 Purinergic signaling

ATP and adenosine play an important role in the orchestration of inflammation and repair in the lung [33]. ATP is actively or passively released upon cell death, damage or stress induced for example by IR [167]. Extracellular ATP is a “danger” signal and belongs to the earlier mentioned DAMPs [112]. First of all, extracellular ATP can initiate a pro-inflammatory immune response that leads to the infiltration of pro-inflammatory immune cells

[68]. ATP can act via direct binding to receptors, namely P2X and P2Y receptors, or it can be converted via membrane bound enzymes [33]. The ectonucleoside triphosphate diphosphohydrolase-1 also known as CD39 is an enzyme located on the cell surface of many immune cells, like neutrophils [37], lymphocytes [4] and dendritic cells [7] but also epithelial cells and fibroblasts [15] or vascular endothelial and smooth muscle cells [167]. CD39 hydrolyzes extracellular ATP to adenosine diphosphate (ADP) and is also capable of hydrolyzing ADP to adenosine monophosphate (AMP). The produced AMP can subsequently be converted via the ecto-5'-nucleotidase (CD73) to adenosine. CD73 is found on the cell membrane of immune cells like neutrophils [36], dendritic cells [7], macrophages [173] and lymphocytes [4] but also on vascular endothelial cells [167]. Extracellular adenosine can pursue three different ways: enzymatic inactivation, cellular uptake or action through receptor binding. The adenosine deaminase (ADA) can convert adenosine to inosine, a process that can happen extra- as well as intracellularly [33]. Adenosine may also be transported into its target cells via four different adenosine transporters, the so called equilibrative nucleoside transporter (ENT). The third possibility is the binding of extracellular adenosine to one of four different adenosine receptors namely A_1, A_{2A}, A_{2B} and A_3 (from here on ADORA1, ADORA2A, ADORA2B and ADORA3) to induce cellular responses (Figure 3) [33, 41].

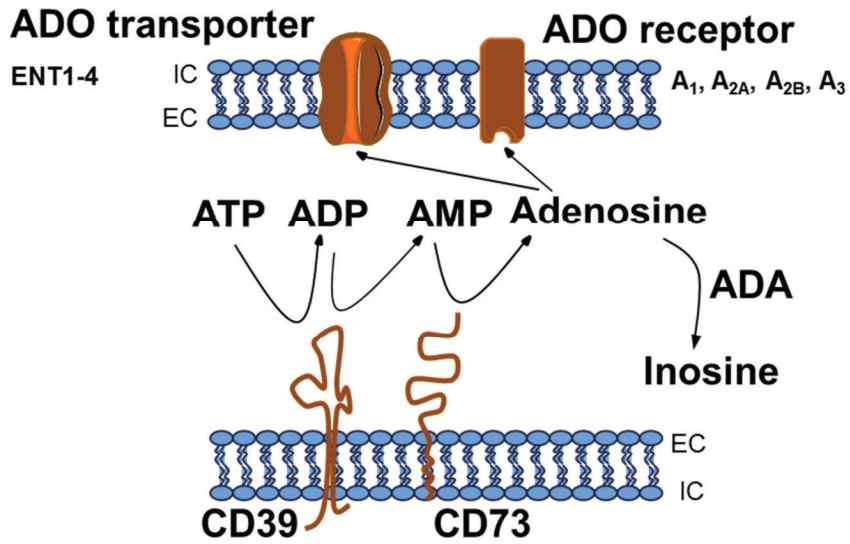

Figure 3: Schematic overview of the purinergic system. ATP is released into the extracellular room upon stress induction or cell death. ATP can be converted from CD39 via ADP to AMP. AMP is converted to adenosine by CD73. Adenosine can be further converted through the adenosine deaminase (ADA) to inosine (extra- and intracellular), it can bind to one of four different adenosine receptors (ADO receptor) or it can be transported into its target cells via adenosine transporters (ADO transporter, ENT1-4).

All receptors are G-protein coupled receptors and are expressed on various cell types including immune cells [33]. Within the immune cells neutrophils [21], mast cells [84], monocytes [172], macrophages [14], dendritic cells [111], T-lymphocytes [57, 94], B-lymphocytes [43] and natural killer cells [117] have been shown to express adenosine receptors. Details are nicely reviewed in a recent publication [15]. ADORA1 and ADORA2A

are high affinity receptors responding to low concentrations of extracellular adenosine, while ADORA2B and ADORA3 are low affinity receptors and are mainly addressed if the extracellular adenosine concentration rises [33, 41]. Adenosine is known to be responsible in dampening the initial inflammatory response in the lung upon stress or injury. Therefore, it has a function in the protection of the tissue from massive inflammation [33, 152].

1.4.2 Role of CD73 and adenosine in pneumopathy

CD73 and adenosine are found to be elevated in BALs from patients suffering from asthma, IPF and COPD [67]. I.t. administration of BLM to C57BL/6 wildtype mice resulted in enhanced levels of adenosine and CD73 activity [152]. Challenging CD73 knockout ($CD73^{-/-}$) mice with BLM i.t. abrogated adenosine accumulation almost completely and led to enhanced inflammation as well as fibrosis development. The study revealed a protective role for adenosine in the BLM i.t. model of lung injury [152]. In addition, a recent study showed that blocking nucleoside transporters with dipyridamole in BLM-induced lung injury inhibited the resolution of fibrosis that can normally be observed in the i.t. model. Furthermore, treatment with dipyridamole worsened the fibrosis in the chronic model (i.p. injection), indicating that long lasting high adenosine levels impact on fibrosis outcome [82].

Besides the different models of BLM-induced pneumopathy, the role of chronic enhanced levels of adenosine can also be studied in the model of ADA knockout mice ($ADA^{-/-}$). In the $ADA^{-/-}$ mouse model adenosine highly accumulates, due to the deficiency of the adenosine converting enzyme ADA [11, 25]. The affected animals die within three weeks of age due to respiratory distress [11]. Partially ADA deficient mice also have high levels of lung adenosine and enhanced levels of alveolar macrophages are found in the BAL at six weeks of age [25]. Severe pulmonary fibrosis and enhanced levels of myofibroblasts could be found in these mice at 15 weeks of age. Furthermore, various immune cells like macrophages, lymphocytes, eosinophils, and neutrophils infiltrated into the lung tissue [24].

Important roles for CD73 and adenosine have been suggested in patients with chronic inflammatory lung diseases like IPF and COPD and in the murine BLM model of lung injury. However, at the beginning of this project nothing was known about the impact of CD73/adenosine on the development of radiation-induced pneumopathy. Database research did not show any hits for the combination of RILF or radiation fibrosis lung with adenosine. We speculated, as RILF is also a process of chronic inflammation, that extracellular adenosine might accumulate in the lung and promotes disease development. There is a high interest to uncover the underlying mechanisms of radiation-induced lung injury, especially fibrosis, due to its poor clinical prognosis. Therefore, the investigation of the role of CD73 and adenosine in the model of RILF is of great importance.

1.4.3 Hyaluronan

HA is another important modulator of lung homeostasis. As part of the ECM it influences lung elasticity, airway resistance and compliance [158]. HA is also called hyaluronic acid and composed of polymers from D-glucoronic acid and D-N-acetylglucosamin linked via alternating β-1,4 and β-1,3 glycosidic bonds. It is a nonsulfated glycosaminoglycan and can be found in various tissues all over the human body. Unlike other glycosaminoglycans HA is not synthesized in the golgi, but three HA synthases (Has1-3) produce HA molecules at the inner surface of the plasma membrane (Figure 4) [140]. While Has1 and Has2 synthesize high molecular weight (HMW) HA molecules, Has3 produces HA chains of low molecular weight (LMW) [58, 155]. Every day approximately one third of the whole HA content is renewed, although it is known that ROS triggers an enhanced HA turnover [40, 133]. HA can be degraded to oligosaccharides by the enzymatic reaction of hyaluronidases (HYAL) [140]. In humans and mice six HYAL genes code for enzymes with distinct catalytic characteristics. Nevertheless, it is thought that HYAL1 and HYAL2 are the most abundant and active proteins [27].

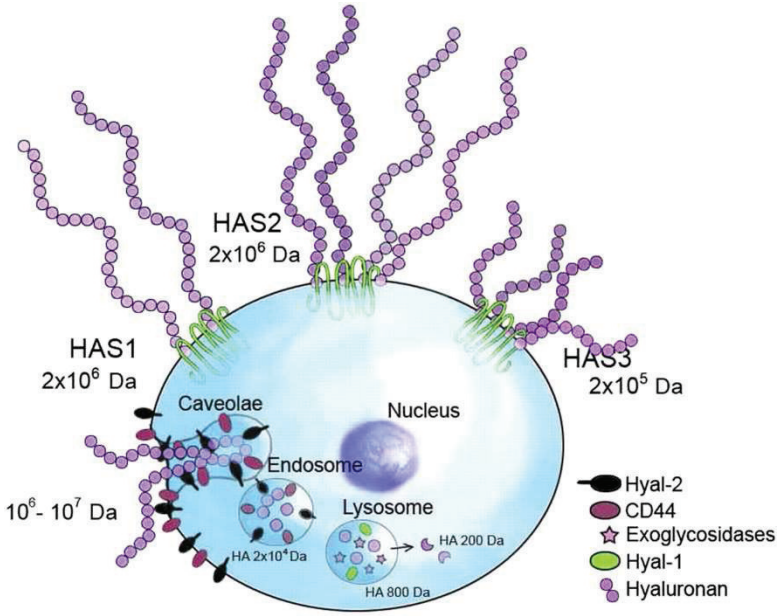

Figure 4: Synthesis and degradation of HA. HA is synthesized by one of three different HA synthases (Has1-3) in the cell membrane. Has1 and Has2 produce HMW HA, whereas Has3 produces LMW HA molecules. Degradation of HA is initialized by HYAL2 on the plasma membrane with the help of CD44. HA is fragmented and internalized. Later on, in lysosomes, HYAL1 and the low pH will degrade HA in small fragments (Stridh 2012 [140]).

Common HA receptors are CD44 and the receptor for HA-mediated motility (RHAMM). CD44 is expressed on hematopoietic cells, fibroblasts and various tumor cells. It is a cell surface glycoprotein and is known to be a HA receptor, while binding of HA to CD44 is dependent on the activation state of the receptor [75]. HMW HA as well as LMW HA can

bind to CD44 [140]. Besides HA, CD44 is able to bind to proteins of the ECM as well as cytokines and chemokines and growth factors [106, 114]. RHAMM, which is also named CD168, can be found on the cell surface, in the nucleus and in the cytoplasm of a cell [88]. Surface RHAMM is GPI-anchored and plays an important role in cell motility as well as wound healing in interaction with CD44 [150].

In the healthy lung tissue HA is found in the basement membrane. Fibroblasts are the main producers of the ECM molecule HA, but HA is also produced and secreted by smooth muscle cells [115]. During tissue homeostasis HA exists as a HMW polymer with a size of more than 10^6 Dalton [92]. Inflammation causes a depolymerization of HMW HA, for example through oxygen radicals, leading to the formation of LMW HA fragments with a size around $2x10^5$ Dalton [107, 115]. The functions of the high and low molecular weight form of HA differ a lot. HMW HA is known to be a hydrating and structural polymer with anti-inflammatory capacities. LMW HA has pro-inflammatory effects, promotes proliferation, and acts in combination with specific receptors (CD44, RHAMM, TLRs) [104, 139, 145]. In response to IR HA polymers are fragmented to LMW HA, which function as an early danger signal, since they belong to the earlier mentioned DAMPs [133, 149]. DAMPs induce an immune response that needs to be regulated and controlled. Failure of immune regulation will contribute to a chronic inflammation and tissue fibrosis [116, 147].

1.4.4 Role of the hyaluronic system in pneumopathy

It is suggested that impaired ECM function can lead to lung fibrosis and potentially loss of function [158]. It was shown that the levels of HA in BAL samples from IPF patients are elevated [10] and that HA is accumulating before fibrosis and prior to the influx of inflammatory cells [92]. BLM-induced lung injury in the rat also confirmed enhanced HA levels, and especially accumulation of LMW HA fragments, in the lung tissue as well as the BAL fluid [55]. Furthermore, HA seems to impact on TGFβ-driven pro-fibrotic processes like the transition of primary human lung fibroblasts to myofibroblasts [93].

CD44 is a main contributor to HA clearance after lung injury and can thereby counteract chronic inflammatory stages and fibrosis development [170]. Furthermore, lung fibrosis is characterized by the abundance of myofibroblasts that express Has2 and are invasive. Vice versa the HA receptor CD44 was shown to be important to recruit fibroblasts and to contribute to the invasive phenotype of myofibroblasts [77]. The expression of the HA receptor RHAMM is also elevated upon BLM-induced lung tissue injury. RHAMM is essential in tissue repair processes and the interaction between HA and RHAMM is necessary for macrophage chemotaxis towards injured lungs [170]. The loss of RHAMM is associated with decreased levels of TGFβ upon injury, thereby preventing a fibroblast into myofibroblast differentiation [147]. Macrophages seem to be the main cell type executing the observed

effects of LMW HA in response to lung tissue injury [107, 127]. Macrophages and HA co-localize in the injured lung tissue upon i.t. BLM treatment in rats. The accumulation of macrophages in the injured lung was abolished by treatment with a HA-binding peptide mimicking the binding domain of RHAMM [127].

So far, not much research has been done to define a potential role the HA system in radiation-induced pneumopathy. In breast cancer patients that underwent RT, enhanced levels of HA were found in the BAL [9]. In a radiation-induced lung disease model in the rat also elevated levels of HA were found in the BAL, serum and lung tissue [123]. One murine based radiation-induced lung injury study with a single dose of 10 Gy reported enhanced levels of HA only at 12 hours after RT within an observation period up to 12 weeks [59]. Although HA is associated with different fibrotic diseases of the lung, its impact on RILF has been rarely studied so far.

2 Aim of the project

Radiation-induced pneumonitis and pulmonary fibrosis are severe and dose-limiting side effects of thoracic irradiation for cancer treatment and of TBI in conditioning regimens for hematopoietic stem cell transplantation. To improve treatment outcome there is high interest in the development of new strategies to either sensitize the tumor tissue to the toxic effect of IR or to protect the normal tissue from the adverse radiation effects. However, the signaling molecules associated with infiltration/inflammation and the disease-promoting capabilities of diverse immune cells are still largely unknown. Therefore the identification of new biomarkers and therapeutic targets for prediction, prevention or treatment of radiation-induced pneumonitis and fibrosis are important.

In this context studies with preclinical rodent models and patient data identified a complex response of the lung tissue after RT with multiple interactions between resident lung cells and infiltrating immune cells. The role of the different types of immune cells during pneumopathy is still poorly defined. Previous work from our group using a murine model of radiation-induced pneumopathy revealed alterations in leukocyte-associated cytokines/chemokines as well as in immune cell recruitment (lymphocytes and myeloid cells) during radiation-induced pneumonitis [17]. Preclinical murine studies as well as patient studies suggested a contribution of lymphocytes and macrophages in fibrotic pulmonary diseases, but a potential contribution and underlying mechanism in radiation-induced lung injury remained unknown. Moreover, studies identified CD73 and/or adenosine as well as HA as important factors contributing to fibrosis development in other types of lung injury.

Thus, the aim of my project was the detailed characterization of immune cells, especially macrophages, and the identification of the impact of CD73/adenosine and HA during radiation-induced lung damage using our murine *in vivo* model of radiation-induced pneumopathy. This project is of great importance to understand the disease progression and for the identification of promising candidates for prevention as well as the development of treatment options for counteracting disease-promoting immune changes.

3 Results

3.1 Publication overview

Thorax irradiation triggers a local and systemic accumulation of immunosuppressive CD4+ FoxP3+ regulatory T cells.

Wirsdörfer F*, Cappuccini F*, Niazman M, de Leve S, Westerndorf AM, Lüdemann L, Stuschke M, Jendrossek V.
Radiation Oncology 2014, 9:98
* Equal contributors

Extracellular adenosine production by ecto-5'-nucleotidase (CD73) enhances radiation-induced lung fibrosis.

Wirsdörfer F*, de Leve S*, Cappuccini F*, Eldh T, Meyer AV, Gau E, Thompson LF, Chen NY, Karmouty-Quintana H, Fischer U, Kasper M, Klein D, Ritchey JW, Blackburn MR, Westendorf AM, Stuschke M, Jendrossek V.
Cancer Res May 15, 2016 76; 3045.
* Equal contributors

Loss of CD73 prevents accumulation of alternatively activated macrophages and the formation of pre-fibrotic macrophage clusters in irradiated lungs

de Leve S*, Wirsdörfer F*, Cappuccini F, Schütze A, Meyer AV, Röck K, Thompson LF, Fischer JW, Jendrossek V
submitted manuscript: *FASEB Journal, 10th of November 2016*
* Equal contributors

Radiation-induced pneumonitis and pulmonary fibrosis are dose-limiting side effects of thoracic irradiation, but its pathogenesis remains poorly understood and no effective treatment is available. The following publications give new insights for a better understanding of the pathogenic processes and offer potential treatment approaches to reduce normal tissue toxicity in the lung. We used the murine model of radiation-induced pneumopathy and irradiated C57BL/6 wildtype mice with a single high dose of 15 Gy over their whole thorax to study radiation-induced pneumonitis and fibrosis. Since the infiltration of various immune cells is a common feature of pneumonitis and fibrosis, we analyzed T cells with a focus on Treg and macrophages in irradiated versus non-irradiated mice. Furthermore, there were hints from other types of pulmonary fibrosis that altered signaling pathways, e.g. purinergic and hyaluronic signaling, contribute to the microenvironmental changes observed during fibrosis. Therefore, we included $CD73^{-/-}$ mice in our studies of radiation-induced fibrosis and analyzed components of the hyaluronic signaling pathway.

Thorax irradiation of C57BL/6 mice altered the composition of T cell populations locally and systemically (cervical lymph nodes and spleen). Lung irradiation led to increased levels of Treg and to upregulation of CD103, cytotoxic T-lymphocyte-associated protein4 (CTLA-4) and CD73 on T cells at 3 weeks after IR. These markers are known to promote recruitment and immunosuppressive activity. At six and twelve weeks post irradiation (pneumonitic phase) an influx of $CD3^{+}$ T cells was observed. In addition to an increased CD73 expression on T cells, CD73 expression and activity was also upregulated on other immune cells and non-leukocytes in the irradiated lung. Elevated levels of Treg were also found during the fibrotic phase. The upregulation of CD73 was paralleled by progressively accumulating levels of extracellular adenosine. CD73 deficient mice failed to accumulate adenosine in BALF and exhibited significantly less RILF. Furthermore, treatment of wild-type mice with pegylated ADA (PEG-ADA) or a CD73 antibody (TY/23) significantly reduced RILF. The development of RILF in WT mice was accompanied by the accumulation of macrophages within organized clusters expressing pro-fibrotic marker proteins such as TGFβ, alpha smooth muscle actin (α-SMA) and ARG1. Interestingly, in $CD73^{-/-}$ mice no organized macrophage clusters and no upregulation of anti-inflammatory markers on macrophages were observed during the fibrotic phase. Furthermore, $CD73^{-/-}$ mice showed a differential expression of the HA synthases and the receptors CD44 and RHAMM.

In sum, the data reveal that immune cells of the innate and adaptive immune system as well as the purinergic and hyaluronic system impact on radiation-induced pneumonitis and fibrosis and suggest a cross-talk between the investigated components.

3.2 Thorax irradiation triggers a local and systemic accumulation of immunosuppressive CD4+ FoxP3+ regulatory T cells.

Contribution to present publication:

- Contribution to data collection (approx. one of two or three repeated experiments for the 21, 42 and 84 days time points)
    - Isolation of spleen and lung
    - Isolation of immune cells from spleen, lymph nodes and lung (tissue digestion, filtration steps, erythrocyte lysis)
    - Staining of isolated immune cells for flow cytometric analysis: surface staining as well as intracellular staining
- Writing Material and Methods (part: Phenotyping of leukocytes by flow cytometry)
- Proof reading of the manuscript

The above listed contributions of Simone de Leve to the publication are correct.

Essen, den _____ _____

Unterschrift der Doktorandin

Essen, den _____ _____

Unterschrift des wissenschaftl. Betreuers/
Mitglieds der Universität Duisburg-Essen

Wirsdörfer et al. Radiation Oncology 2014, 9:98
http://www.ro-journal.com/content/9/1/98

RADIATION ONCOLOGY

RESEARCH Open Access

Thorax irradiation triggers a local and systemic accumulation of immunosuppressive CD4+ FoxP3+ regulatory T cells

Florian Wirsdörfer[1†], Federica Cappuccini[1†], Muska Niazman[1], Simone de Leve[1], Astrid M Westendorf[2], Lutz Lüdemann[3], Martin Stuschke[3] and Verena Jendrossek[1*]

Abstract

Background: Lymphocyte infiltration is a common feature of radiation-induced pneumonitis and fibrosis, but their contribution to the pathogenic processes is still unclear. Here, we addressed the impact of thorax irradiation on the T cell compartment with a focus on immunosuppressive regulatory T cells (Treg).

Methods: C57BL/6 wild type mice (WT) received anesthesia only (sham controls, 0 Gy) or were exposed to a single dose of whole thorax irradiation (15 Gy). Immune cells from lung tissue, spleen, and cervical lymph nodes were collected 10 to 84 days post-irradiation and phenotypically characterized by flow cytometry.

Results: Whole thorax irradiation provoked an increased influx of CD3+ T cells at 42 and 84 days post-irradiation. In contrast, local irradiation caused a sustained reduction in CD3+ T cells in peripheral lymphoid tissues. Interestingly, we observed a significant local and systemic increase in the fraction of CD4+ T cells expressing the transcription factor forkhead box P3 (FoxP3), the phenotypic marker for murine Treg, at day 21 post-irradiation. The accumulation of Treg was associated with increased levels of T cells expressing surface proteins characteristic for recruitment and immunosuppressive activity, e.g. CD103, CTLA-4 and CD73. Importantly, Treg isolated at this time point were able to suppress CD4+ effector T cells to a similar extent as Treg isolated from control mice.

Conclusions: The response of the adaptive immune system to whole thorax irradiation is characterized by local immunoactivation and systemic immunosuppression. The transient accumulation of immunosuppressive CD4+ FoxP3+ Treg may be required to protect the lung against excessive inflammation-induced tissue damage. Further investigations shall define the mechanisms underlying the accumulation of Treg and their role for the pathogenesis of radiation-induced lung disease.

Keywords: Thorax irradiation, Regulatory T cells, T-lymphocytes, Pneumonitis, Fibrosis

Introduction

Radiotherapy is an integral part of current standard treatment concepts in oncology and provides a broad contribution to cancer cure alone and in combined treatment regimens. However, despite the high therapeutic potential of radiotherapy alone and in multimodal combinations with surgery, chemotherapy, or targeted drug therapy, a low tolerance of the normal tissue to radiotherapy can considerably limit the success of radiotherapy: Acute and late toxicity to normal tissues within the irradiated volume not only decreases the quality of life but also precludes the application of a curative radiation dose to the tumor resulting in local relapse particularly in tumors with high intrinsic radiation resistance. Hence, researchers aim to improve the therapeutic ratio by technical and physical innovations in treatment delivery, e.g. intensity-modulated radiation therapy (IMRT) or particle therapy, as well as by developing effective biology-based strategies to prevent or treat the toxic effects of ionizing radiation affecting normal tissues without increasing radiation resistance of the tumor cells.

* Correspondence: verena.jendrossek@uni-due.de
†Equal contributors
[1]Department of Molecular Cell Biology, Institute of Cell Biology (Cancer Research), Medical Faculty, University of Duisburg-Essen, Virchowstrasse 173, 45122, Essen, Germany
Full list of author information is available at the end of the article

As a clinically relevant example the lung constitutes a highly radiosensitive tissue with little repair capacity. As a consequence, radiation-induced pneumonitis and fibrosis are observed as severe dose-limiting complications of total body irradiation (TBI) or radiotherapy of thorax-associated neoplasms [1-3]. However, so far there is no available effective pharmacotherapy suited to specifically prevent or treat radiation-induced lung disease in the clinical setting so that a symptomatic anti-inflammatory therapy remains standard of care, though its use is disputed [4].

Depending on the total radiation dose and the irradiated volume, patients develop a toxic inflammation of the lung parenchyma (pneumonitis) within 4 to 12 weeks post-irradiation without or with subsequent lung fibrosis. Radiation-induced lung fibrosis is mostly observed 6 to 24 months after radiotherapy and may become chronic in patients with a large irradiated lung volume [4]. Interestingly, experimental models using whole thorax or hemithorax irradiation of fibrosis-sensitive mice (C57BL/6) mimic human disease with respect to the time course and major symptoms so that they can be used to define the underlying mechanisms as well as disease biomarkers [5-8].

Investigations in patient probes and animal models demonstrate a complex response of the lung tissue with multiple interactions between resident cells (alveolar epithelial cells I and II, endothelial cells, fibroblasts), stromal factors and infiltrating immune cells [9,10]. It is assumed that radiation-induced pulmonary fibrosis may originate from a disturbed balance between tissue inflammation and repair as it has been described for other fibrotic diseases [11]. However, it is still controversial whether cells from the innate and adaptive immune system directly contribute to radiation-induced tissue damage or only modulate disease progression.

In this regard there is evidence from preclinical and clinical investigations that T cells constitute an important part of the immune cells infiltrating the lung tissue upon irradiation of the thoracic region [6,12-15]. Even more important, the presence of CD4+ T-lymphocytes in the bronchioalveolar lavage fluid (BALF) of irradiated breast or lung cancer patients correlated with a pneumonitic reaction [13,15]. A radiation-induced increase in T-lymphocytes in the lung tissue, particularly CD4+ T-lymphocytes, during the pneumonitic phase was confirmed in rodent models [7,16,17]. Of note, depletion of CD4+ T cells during the pneumonitic phase decreased radiation-induced lung fibrosis pointing to a contribution of these cells to disease pathogenesis [16]. In contrast, lung fibrosis upon whole thorax irradiation was aggravated in *recombination-activating gene 2* (RAG2)-deficient mice; these mice lack mature T- and B-lymphocytes suggesting that lymphocytes may also have beneficial effects in radiation-induced lung disease [18]. Interestingly, in further own investigations thorax irradiation triggered the early appearance of two distinct types of T-helper cells in C57BL/6 mice, namely interleukin 17 (IL-17)-expressing CD4+ T cells and CD4+ FoxP3+ T-lymphocytes in the lung tissue [18]. The above data suggest a causal link between the recruitment or local expansion of specific T-lymphocyte populations and the course of radiation-induced lung disease. In the present investigation we addressed the potency of ionizing radiation to induce local and systemic changes in the T cell compartment with a focus on regulatory T cells (Treg) using a C57BL/6-based murine model. Treg specifically express the transcription factor FoxP3 which activates genes that silence many effector T cell genes and suppress T cell proliferation and activation in the periphery by secreting inhibitory cytokines such as transforming growth factor beta1 (TGF-β1) and IL-10 [19].

Here, we show that radiation-induced pneumonitis is associated with specific local and systemic time-dependent changes in the T cell compartment. Importantly, whole thorax irradiation (WTI) triggered the local and systemic accumulation of CD4+ FoxP3+ Treg with immunosuppressive capacities during the early pneumonitic phase. These immunosuppressive cells may be necessary to keep in check effector T cells with tissue destructive activity, such as T_H1 cells or IL-17-expressing T_H17 cells. An improved understanding of the underlying mechanisms and of the role of these regulatory cells during radiation-induced pneumonitis may open novel routes to prevent or treat radiation-induced pneumonitis and fibrosis.

Material and methods

Mouse strains

Eight-to-twelve weeks-old C57BL/6 wild-type mice (WT) were enrolled in the study. All animals were bred and housed under specific pathogen-free conditions in the Laboratory Animal Facility of the University Hospital Essen. Food consisting of a commercial laboratory animal diet and drinking water were provided *ad libitum*. The animal facility and all protocols were approved by the Universities Animal Protection Boards in conjunction with the Landesamt für Natur, Umwelt und Verbraucherschutz Nordrhein-Westfalen (LANUV) according to the German animal welfare regulations (AZ.8.87-51.04.20.09.333).

Experimental setup for whole thorax irradiation (WTI)

For whole thorax irradiation, groups of four mice were irradiated in parallel. Animals were anesthetized with 2% isoflurane, placed in holders and irradiated simultaneously with a single dose of 0 Gy (sham control) or 15 Gray (Gy) over their whole thorax. The radiation dose was applied using a Cobalt-60 source (Phillips, Hamburg, Germany). The irradiation was performed using a field

size of 23.3 cm × 2 cm at the focus target distance of 58 cm. The field size was additionally reduced to 23.3 cm × 1.5 cm field size (full width half maximum) using two Lipowitz metal absorber blocks (5.3 cm thickness) at focus surface distance of 44 cm. The beam collimation allowed for the irradiation of an axial 1.5 cm thick slice covering the lungs of 4 mice fixed in parallel position at a time. The mouse lung position within the dedicated mice holders were validated once with a CT scan of the complete positioning setup.

Dosimetry was performed with a type 31016 pin point "3D chamber" (0.016 cm^3), a reference semiflex chamber type 31003 (0.3 cm^3) and an electrometer type UNIDOS (PTW, Freiburg, Germany). Dose was applied with an accuracy of 3% (+3% for the two mice with 3 cm distance to central beam axis, -3% for the two mice with 9 cm distance to central beam axis). The body dose outside the irradiation field was found 1.3% of the prescribed dose. The Co-60 source provided a dose rate of approximately 0.5 Gy/min at the target.

Collection of bronchoalveolar lavage fluid (BALF)

To obtain BAL fluid (BALF), a horizontal incision was made in the dissected tracheal tube. A syringe needle was connected and fixed by two surgical knots and the lungs were lavaged three times with 0.4 mL PBS. All fluid collected from one mouse was pooled and 50 μL were cytospun onto glass slides at 400 rpm/5 min with a Shandon Cytospin 4 (Thermo Scientific, USA). Slides were allowed to air dry for several minutes and were then Giemsa-stained. Stainings were further analysed via bright-field microscopy.

Isolation of lymphocytes from spleen, cervical lymph nodes and lungs

Mice were sacrificed at days 10, 21, 42, or 84 post-irradiation and lung tissue, cervical lymph nodes and spleen were collected for further analysis as follows:

Isolation from spleen

Spleens were rinsed with an erythrocyte lysis buffer (containing 0.15 M NH_4Cl, 10 mM $KHCO_3$, and 0.5 M EDTA), meshed through a 70 μm cell strainer, passed through a 30 μm cell strainer and washed with complete medium (RPMI medium supplemented with 10% fetal calf serum, Penicilline and Streptomycine).

Isolation from cervical lymph nodes

Cervical lymph node cells (cLN) were disrupted with two 23G needles in PBS containing 2 mM EDTA and 2% fetal calf serum or complete medium respectively, and collected in complete medium for further analysis.

Isolation from lungs

Lungs were cut into pieces and digested in 1 mg/mL Collagenase D and 10 μg/mL DNAse for 45 min at 37°C and the cell suspension filtered (70 μm cell strainer) and subsequently centrifuged by 1500 rpm for 6 min. Total lung cells (TLC) were then rinsed with an erythrocyte lysis buffer (containing 0.15 M NH_4Cl, 10 mM $KHCO_3$, and 0.5 M EDTA), passed through a 30 μm cell strainer and washed with complete medium for subsequent phenotyping.

Phenotyping of leukocytes by flow cytometry

Lung cells were stained with anti-mouse CD45 Pacific Blue (30-F11) for determination of leukocytes in the lung tissue. Splenocytes, cLN cells, and lung cells were further fluorochrome-labeled with anti-mouse CD3ε (145-2C11), CD4 (RM4-5), CD8 (53-6.7), CD45R/B220 (RA3-6B2), CD39 (24DMS1), CD73 (TY/11.8) and CD103 (M290). Detection of FoxP3 and CTLA-4 was performed using the FoxP3 staining kit from eBioscience (Frankfurt, Germany) with anti-mouse FoxP3 (FJK-16 s) and anti-mouse CTLA-4 (UC10-4B9), according to the manufacturer's recommendations. All antibodies used in this study, were obtained from BD Biosciences (Heidelberg, Germany), BioLegend (Fell, Germany) or eBioscience (Frankfurt, Germany).

RNA isolation, cDNA synthesis and RT-PCR analysis

For RNA isolation *ex vivo* isolated lung tissues were lysed in RLT-buffer using an ULTRA-TURRAX® UTC (IKA, Staufen, Germany). RNA was isolated using RNeasy Mini kit (Qiagen, Hilden, Germany) according to the manufacturer's instruction. Total RNA (1 μg) was used for reverse transcription (RT) with Superscript™-II reverse transcriptase (Qiagen) using oligo-dT primers according to the manufacturer's instructions. 0.5 μL of obtained cDNA was used for PCR reaction as previously described [20]. Analysis was carried out using the oligonucleotide primers FoxP3_sense CTGGCGAAGGGCTCGGTAGTCCT, FoxP3_antisense CTCCCAGAGCCCATGGCAGAAGT; βActin_sense GGCTGTATTCCCCTCCATCG; βActin_antisense CCAGTTGGTAACAATGCCATGT.

Suppression assay

CD4+ CD25hi Treg were separated from cLNs and spleen of mice that received 0 Gy or 15 Gy whole thorax irradiation using a FACSAria II cell sorter (BD Biosciences). As responder T cells, CD4+ T cells were purified from spleens of naive WT mice using the CD4+ T cell isolation kit II (Miltenyi Biotec, Bergisch-Gladbach, Germany) and were labeled with Carboxyfluorescein succinimidyl ester (CFSE) (Invitrogen). CD4+ responder T cells (1×10^5) were either cultured alone or co-cultured with CD4+ CD25hi Treg (1×10^5) for 4 days in the presence of 1 μg/mL anti-CD3 (2C11; BD Biosciences). Irradiated splenocytes from naive C57BL/6 mice served as antigen-presenting cells (APCs) (3×10^5).

Statistical analysis

If not otherwise indicated, data were obtained from 2 – 3 independent experiments with at least 3 mice each. Mean values were calculated and used for analysis of standard deviation (SD) or standard error (SEM) and statistical significance. Differences were assessed by 2-way ANOVA followed by Bonferroni's multiple comparison test. Data analysis was performed with Prism 5.0 software (GraphPad, La Jolla, CA). Statistical significance was set at the level of $p < 0.05$.

Results

WTI induces time-dependent changes in the immune cell composition of the lung tissue

In a first set of experiments we compared radiation-induced local changes in immune cell composition within the lung tissue during the pneumonitic phase. To this end, we exposed C57BL/6 wild type mice to a single dose of WTI with 0 Gy or 15 Gy. Using flow cytometry we subsequently analyzed phenotypic markers of leukocytes isolated from the lung tissue 10 to 84 days post-irradiation. While the fraction of total leukocytes (CD45+ cells; gating strategy: Figure 1A) in the lung tissue was comparable to sham controls until 21 days after WTI with 15 Gy, a significant increase of CD45+ cells in the lung tissue was observed at 42 and 84 days post-irradiation (Figure 1B). The fraction of B-lymphocytes (B220+ cells) in the irradiated lung tissue also remained relatively constant during the early pneumonitic phase, but a significant increase in B220+ cells was detected at 84 days post-irradiation (Figure 1C). Finally, we also observed a pronounced increase in CD3+ T cells at 42 and 84 days post-irradiation compared to sham controls. Interestingly, the increase in CD3+ T cells was paralleled by a comparable increase in the amount of CD4+ T cells, whereas the levels of CD8+ T cells in the lungs of irradiated mice and the sham controls did not differ significantly (Figure 1D-F). Analysis of cells present in the bronchioalveolar lavage fluid (BALF) of irradiated mice and sham controls corroborated the above findings of increased immune cell infiltration into the irradiated lungs at 21 days post-irradiation (Figure 1G).

WTI triggers distinct time-dependent changes in the T cell compartment of peripheral lymphoid organs

Next we examined the potential of WTI to induce systemic changes in the T cell compartment. To this end, we isolated lymphocytes from spleen and cervical lymph nodes (cLN) and analyzed the fraction of CD3+ T-lymphocytes, CD4+ T-lymphocytes and CD8+ T-lymphocytes using flow cytometry. As shown in Figure 2A and B, WTI led to a significant reduction of CD3+ T cells particularly the cervical lymph nodes (cLN) and less pronounced in the spleen of irradiated mice as compared to sham controls. The early drop in CD3+ T cells at days 10 and 21 post-irradiation involved reduction of both CD4+ and CD8+ T cells (Figure 2C-F). However, while the loss of CD4+ T cells was only transient and normal levels were reconstituted within 42 days post-irradiation, the suppressive effect of irradiation on CD8+ T cells was long-lasting and a significant reduction in the fraction of CD8+ T cells was still observed at 42 days post-irradiation, particularly in the cervical lymph nodes (Figure 2C-F).

Thorax irradiation triggers a local and systemic accumulation of CD4+ FoxP3+ T regulatory cells

Since our earlier investigations suggested the generation of Treg in the lungs of mice exposed to hemithorax irradiation [18], we next examined time-dependent local and systemic changes in the amount of Treg in the lung tissue and peripheral lymphoid organs of mice exposed to WTI with 15 Gy. FoxP3 is considered as a reliable phenotypic marker of Treg, at least in mice [21-23]. Therefore, we examined the fraction of CD4+ FoxP3+ T cells in lung tissue, cervical lymph nodes and spleen until 84 days post-irradiation (gating strategy Figure 3A). Interestingly, we observed a significant increase in the levels of CD4+ FoxP3+ T cells in the lungs of mice exposed to WTI compared to sham irradiated mice at 21 days post-irradiation. However this increase was only transient and levels of CD4+ FoxP3+ T cells in the lung tissue reached values of sham controls within 42 days post-irradiation (Figure 3B). The accumulation of CD4+ FoxP3+ T cells at 21 days post-irradiation could be confirmed by RT-PCR mRNA analysis of FoxP3 expression levels in total lung RNA isolated from control and whole thorax irradiated animals (Figure 3C). Interestingly, a significant accumulation of CD4+ FoxP3+ T cells at day 21 post-irradiation was also observed in the analysis of lymphocytes from cervical lymph nodes and spleen of irradiated mice. Similarly to what was observed in lung tissues this effect was only transient, though a trend to higher levels of CD4+ FoxP3+ T cells in the peripheral lymphoid organs could be already observed at 10 days post-irradiation (Figure 3D-E).

Treg isolated from irradiated mice have normal immunosuppressive function

Our data indicated that WTI leads to a local and systemic accumulation of CD4+ FoxP3+ T cells in the CD4+ T cell compartment during the early pneumonitic phase at 21 days post-irradiation. Next we aimed to explore whether CD4+ FoxP3 + cells that accumulate in the lung tissue at 21 days post-irradiation also express specific surface molecules associated with immunosuppressive activity of Treg, such as the adenosinergic ectoenzymes CD39 and CD73 [24,25]. Therefore, we performed a detailed analysis of the fraction of CD4+ T cells expressing

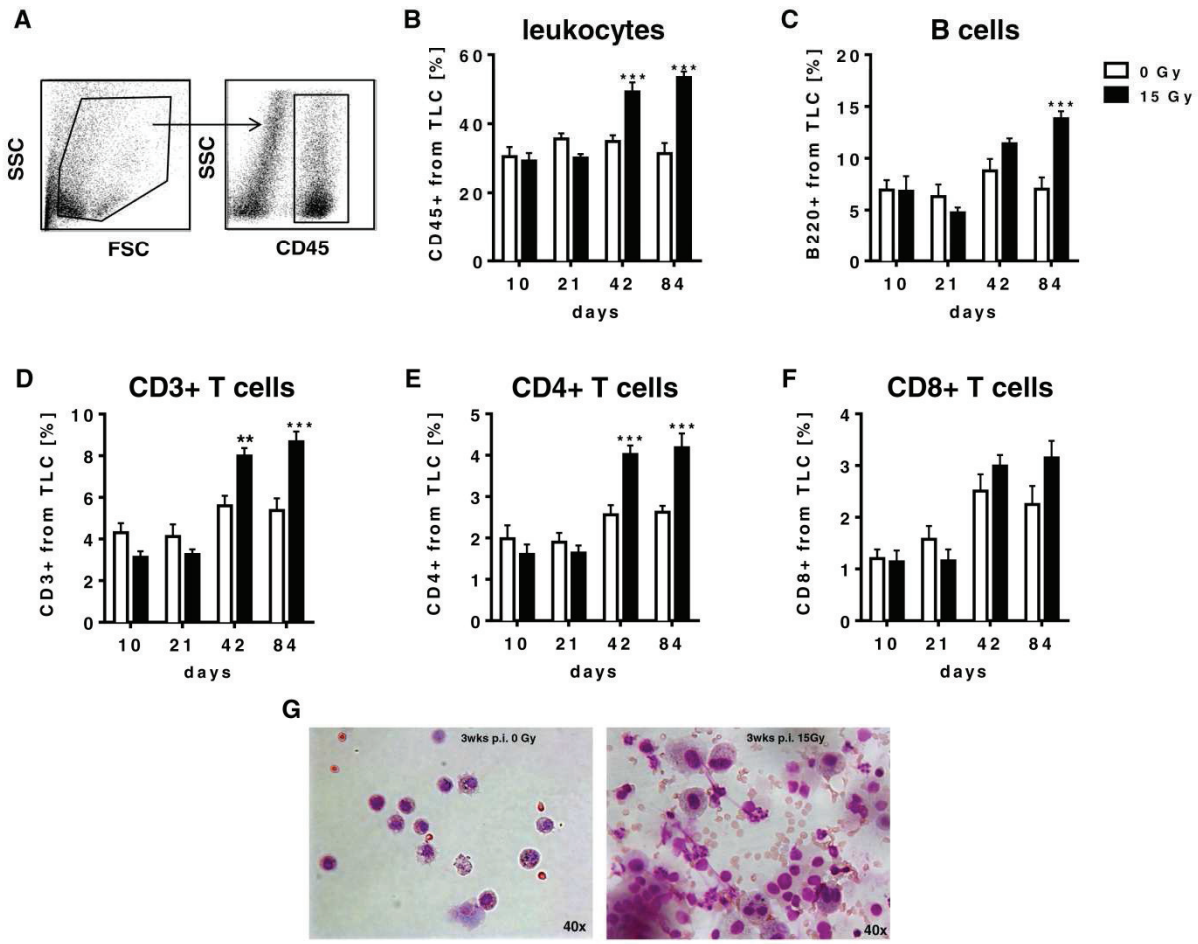

Figure 1 Whole thorax irradiation (WTI) induces time-dependent local changes in the T cell compartment of the lung tissue. C57BL/6 mice received 0 Gy or 15 Gy whole thorax irradiation. At specified time points cells were isolated from lung tissue and stained with antibodies against distinct leukocyte populations as indicated. **(A)** Gating strategy for lung cells: Living total lung cells were gated and further characterized by gating on CD45+ cells (leukocytes). All subpopulations were then gated on the CD45+ population. At different time points, cells were isolated from lung tissue, stained with antibodies against **(B)** total leukocytes (CD45+), **(C)** B-lymphocytes (B220+), **(D)** T-lymphocytes (CD3+), **(E)** CD4+ T-helper cells (CD4+) and **(F)** CD8+ T cells (CD8+) and analyzed by flow cytometry. Timelines of the indicated cell populations are shown with mean values ± SEM of percentages calculated on total lung cells (TLC). Cells of 6-9 mice per group were analyzed, ** $p \leq 0.01$; *** $p \leq 0.001$, two-way ANOVA followed by post-hoc Bonferroni test. **(G)** BALF (bronchoalveolar lavage fluid) was collected at 21 days post-irradiation from lungs of C57BL/6 mice irradiated with 15 Gy (right panel) and sham controls (left panel). Cytospin of BALF probes were stained with Giemsa and analyzed via bright-field microscopy: left panel: BALF from a sham control; right panel BALF from a lung irradiated with 15 Gy (40 × magnification). Pictures show one representative slide.

CD39 and CD73 in the lungs of mice exposed to WTI and of sham controls. While levels of CD39+ CD4+ cells remained mostly unaffected (Figure 4A) we observed an increase in CD73+ CD4+ T cells in the lungs of mice exposed to WTI as compared to sham controls (Figure 4B). The time course of the increased surface expression of CD73 on CD4+ T cells followed the time course observed for the accumulation of CD4+ FoxP3+ T cells in the irradiated mice with a maximum at 21 days post-irradiation. Moreover, we noted a transient increase in CD4+ T cells and CD4+ FoxP3+ Treg expressing the marker proteins CTLA-4 (Figures 4C and 5A) and CD103, respectively (Figures 4D and 5B), indicative for increased recruitment and activation of these cells into the lung tissue [21,26].

Finally we explored whether Treg from irradiated mice are functional and exert suppressive activity. For this we used CD4+ CD25hi cells since sorting of viable Treg via the intracellular marker FoxP3 (fixation step) is impossible. Indeed, when comparing the phenotype and inhibitory capacity of CD4+ CD25hi cells isolated by FACS sorting from peripheral lymphoid organs of mice exposed to WTI and sham controls at 21 days post-

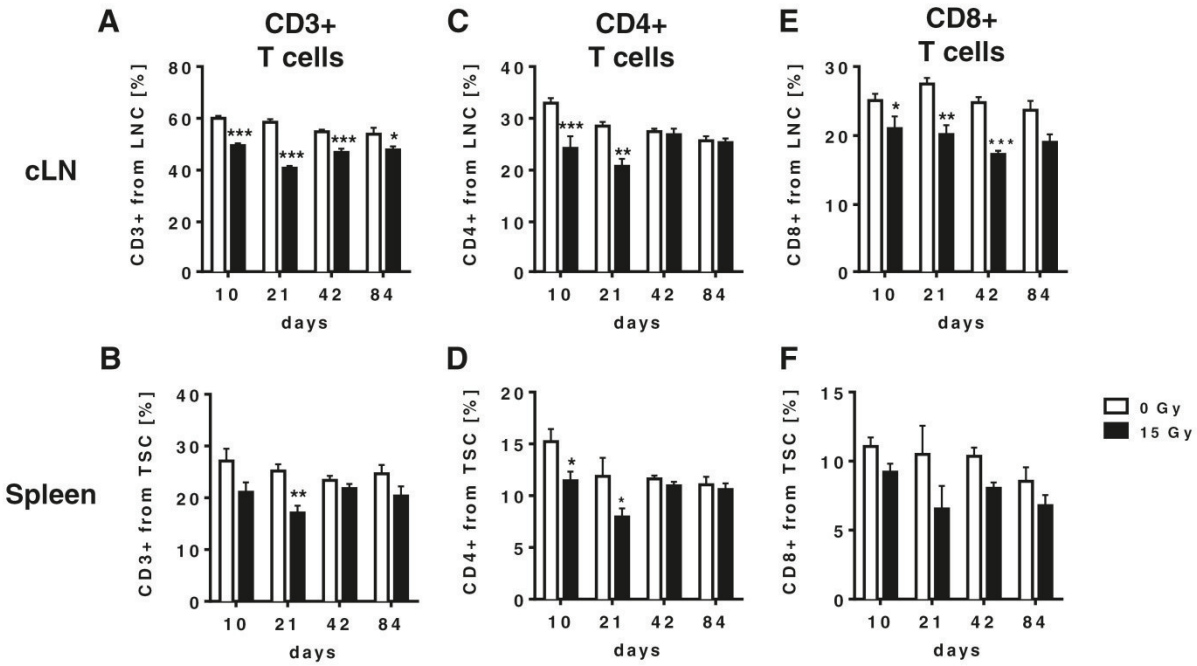

Figure 2 WTI triggers distinct time-dependent changes in the T cell compartment of peripheral lymphoid organs. C57BL/6 mice received 0 Gy or 15 Gy whole thorax irradiation. At different time points, cells were isolated from cervical lymph nodes (cLN) and spleen (TSC) and stained with antibodies against **(A/B)** CD3+ T cells (cLN and spleen), **(C/D)** CD4+ T-helper cells (cLN and spleen), **(E/F)** CD8+ T cells (cLN and spleen) as indicated. Cells were analyzed by flow cytometry and timelines of the indicated cell populations are shown with mean values ± SEM of percentages calculated on lymph node cells (LNC) or total spleen cells (TSC). Cells of 6-9 mice per group were analyzed, * $p \leq 0.05$; ** $p \leq 0.01$; *** $p \leq 0.001$, two-way ANOVA followed by post-hoc Bonferroni test.

irradiation, more than 90% of CD4+ CD25hi sorted cells expressed FoxP3 and could thus be considered as functional Treg (Figure 5C). Importantly, CD4+ CD25hi Treg isolated from cervical lymph nodes (Figure 5D left panel) or spleen (Figure 5D right panel) of mice exposed to WTI (black bars) were able to suppress proliferation of untreated CD4+ T responder cells with similar potency as CD4+ CD25hi Treg from sham controls (white bars). These results indicate that WTI triggers accumulation of Treg and that irradiation *in vivo* does not affect their immunosuppressive capacity.

Discussion

Exposure of the thoracic region to ionizing radiation triggers time-dependent leukocyte infiltration into the lung, including lymphocytes. We show here that irradiation of the thoracic region exerts dual effects on the adaptive immune system: While WTI caused a sustained reduction in CD3+ T cells in peripheral lymphoid tissues it provoked an increased recruitment of CD4+ T cells to the lung tissue at 6 and 12 weeks post-irradiation. Importantly, we demonstrate that radiation-induced local immunoactivation was associated with local and systemic accumulation of cells with the phenotype of immunosuppressive Treg. This assumption is based on the following findings: i) WTI triggered a transient increase in the CD4+ FoxP3+ cell fraction in the lungs and the peripheral lymphoid organs of mice compared to sham controls with a maximum at 21 days post-irradiation; ii) at the time of increased FoxP3-expression the levels of CD73, CD103 and of CTLA4 on CD4+ T cells were also increased; iii) FoxP3+ expressing CD4+ CD25hi cells isolated from irradiated mice displayed enhanced expression of the marker proteins CTLA-4 and CD103 and exhibited unrestrained immunosuppressive activity.

In more detail, local irradiation of the thoracic region caused a sustained systemic suppression of CD3+ T cells in peripheral lymphoid organs that was characterized by a transient decrease in CD4+ T cells and a long-lasting reduction of CD8+ T cell numbers. These observations suggest a more pronounced sensitivity of CD8+ T cells to the cytotoxic action of IR *in vivo* compared to CD4+ T cells. Pronounced cytotoxic effects of local irradiation on the circulating lymphocyte pool had already been observed by others and had been attributed to blood flow through the radiation field [27]. In contrast, after an initial slight decrease of lymphocyte numbers in the lung tissue we observed increased levels of CD3+ T cells in the lung tissue at 42 and 84 days post-irradiation, presumably caused by an increased influx of CD4+ T cells.

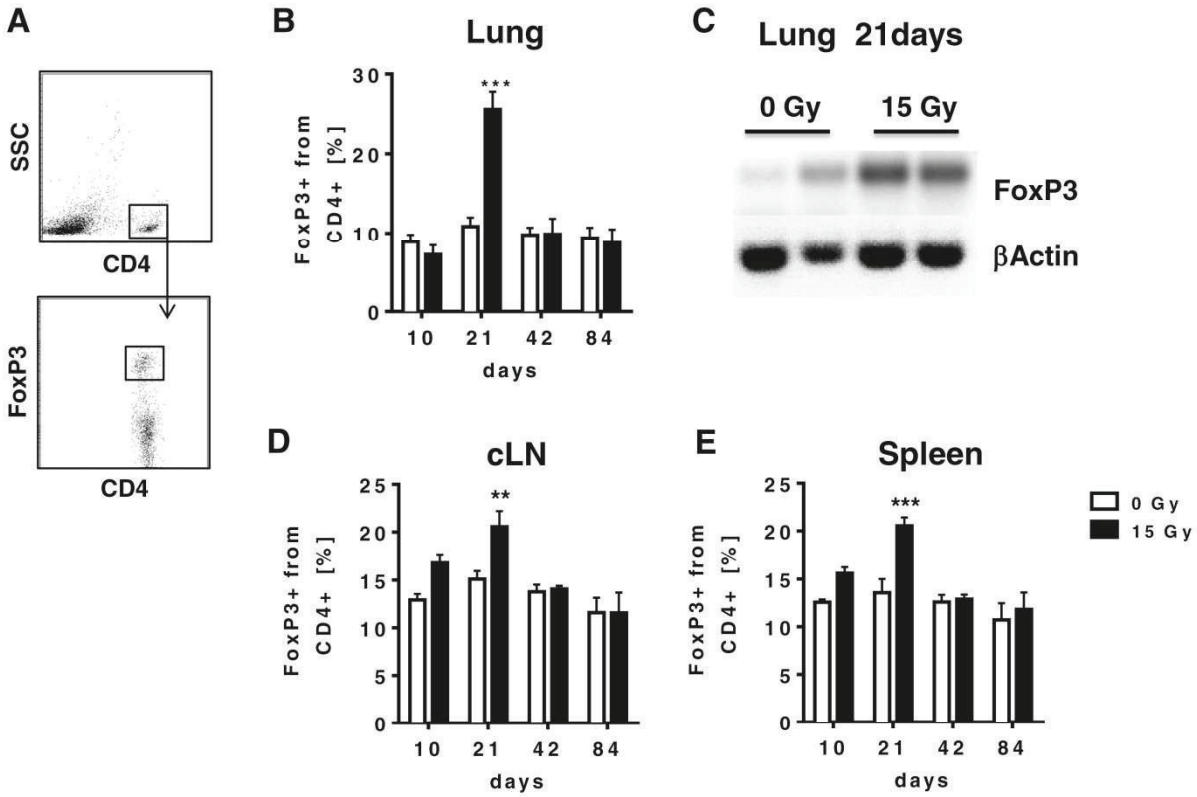

Figure 3 WTI triggers a local and systemic accumulation of FoxP3+ T regulatory cells. C57BL/6 mice received 0 Gy or 15 Gy whole thorax irradiation. At indicated time points, immune cells were isolated from lung tissue, spleen and cervical lymph nodes (cLN) and stained for flow cytometric analysis. **(A)** Gating strategy for the detection of FoxP3 on CD4+ T cells. **(B)** Treg (CD4+ FoxP3+) cells change in the lung during pneumopathy. Mean values ± SEM of the expression of FoxP3 are shown as percentages from CD4+ lung cells. **(C)** RT-PCR mRNA analysis of FoxP3 expression levels of total lung RNA isolates derived from control as well as whole thorax irradiated animals 21 days after irradiation. βActin was included as control. Two images per condition are shown. **(D/E)** Timelines of FoxP3 on gated CD4+ T cells in the cLN **(D)** and spleen **(E)** during pneumopathy. Shown are mean values ± SEM of percentages calculated on CD4+ LNC and TSC. Cells of 6-9 mice/group were analyzed; ** $p \leq 0.01$, *** $p \leq 0.001$, two-way ANOVA followed by post-hoc Bonferroni test.

Thus, lymphocyte influx correlated to the time of radiation-induced pneumonitis defined by maximum impairment of lung function in our earlier investigations [6,28]. Our present data corroborate earlier findings from rodent models of thorax irradiation showing that lymphocyte numbers increase after an initial early depletion by 3 to 6 weeks post-irradiation [7,17].

It is known from preclinical and clinical investigations that CD4+ and CD8+ T-lymphocytes constitute a significant part of the immune cell infiltrate in the lung tissue of irradiated breast and lung cancer patients with a predominance of the CD4+ subset [12-16]. Of note, the increase in numbers of activated CD4+ T-lymphocytes in the BALF is more pronounced in symptomatic patients than in asymptomatic patients [13,15]. Vice-versa, increased apoptosis of peripheral blood lymphocytes, particularly CD8+ T cells, after curative radiation therapy is associated with reduced late toxicity [29]. In line with these findings, depletion of CD4+ T cells during pneumonitis decreased radiation-induced lung fibrosis in preclinical investigations in rats [16]. These findings indicate that infiltration of CD4+ T cells is a common feature of radiation-induced pneumonitis and that these cells may play a role for disease progression. Thus, CD4+ T cells may be promising targets for the modulation of radiation-induced late effects in the lung. However, so far little was known about the phenotype and function of CD4+ T-lymphocytes recruited to the lung tissue in response to thoracic irradiation. This is of particular interest because these cells depending on the microenvironment can differentiate into diverse subsets with opposing pro-inflammatory or immunosuppressive function, e.g. T_H1, T_H2 or T_H17 cells and Treg, respectively.

Here we demonstrate for the first time that WTI leads to a selective accumulation of CD4+ FoxP3+ T cells both in lungs and peripheral lymphoid organs of mice at 21 days post-irradiation. These findings corroborate our recent observation about the appearance of CD4+ FoxP3+

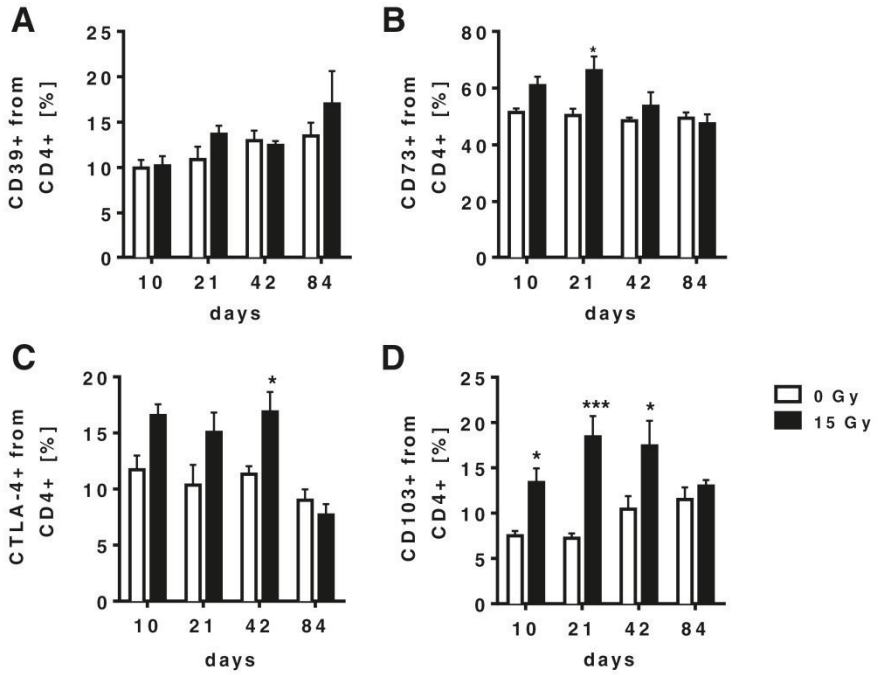

Figure 4 WTI-induced changes in the T cell phenotype are associated with altered surface expression of immunoregulatory molecules on CD4+ T cells. C57BL/6 mice received 0 Gy or 15 Gy whole thorax irradiation. At different time points, immune cells were isolated from lung tissue and stained for flow cytometric analysis. **(A)** Expression of CD39 on gated CD4+ T cells in the lung. **(B)** Expression of CD73 on gated CD4+ T cells in the lung. **(C)** Detection of CTLA-4 expression on gated CD4+ T cells in the lung. **(D)** Expression of CD103 on gated CD4+ T cells in the lung. Timelines of the indicated cell populations are shown as mean values ± SEM of percentages calculated on total lung cells. Cells of 4-6 mice per group were analyzed, * $p \leq 0.05$; *** $p \leq 0.001$, two-way ANOVA followed by post-hoc Bonferroni test.

T-lymphocytes in the lung tissue of mice exposed to hemithorax irradiation [18]. However, it had not yet been shown that local irradiation of the thoracic region also triggers a time-dependent accumulation of CD4+ FoxP3+ T-lymphocytes in cervical lymph nodes and in the spleen. The observation that local thorax irradiation also affects the T cell compartment in peripheral lymphoid organs supports earlier findings about systemic effects of a local irradiation: In this regard, irradiation of prostate tumors grown on the hint-leg of C57BL/6 mice resulted in the accumulation of CD4+ CD25hi FoxP3+ lymphocytes in peripheral lymphoid organs [30]. Moreover, others and we have shown that lymphocyte infiltration after thorax irradiation is not exclusively confined to the radiation field but can also be observed in non-irradiated parts of the lung further corroborating a systemic response of the immune system to local irradiation [6,12,13,31].

Since thorax irradiation led to a decrease in CD3+ T cells by tendency at 21 days post-irradiation, it may be speculated that the radiation-induced accumulation of Treg during the pneumonitic phase may at least partially be due to increased survival of Treg compared to T effector lymphocytes. Such enhanced resistance of CD4+ FoxP3+ cells and of CD4+ CD25hi FoxP3+ cells to ionizing radiation compared to other T-lymphocytes has recently been reported *in vitro* and *in vivo* in different experimental models [30,32-36] and had been attributed among others to enhanced expression of anti-apoptotic Bcl-2 and therefore increased resistance to apoptosis [32,33]. However, T-lymphocytes are generally characterized by a high intrinsic sensitivity to ionizing radiation so that only a minor population will survive WTI with 15 Gy. Certainly, thorax irradiation is known to provoke an increase in the levels of TGF-β1 [37], a cytokine involved in the differentiation of Treg [38-40]. Thus, radiation-induced changes in the lung microenvironment may alternatively trigger a local expansion of CD4+ FoxP3+ T-lymphocytes recruited to the lung tissue.

Of note, our data also demonstrate that Treg isolated from the lymphoid tissues of irradiated mice are fully functionally active: The CD4+ FoxP3 T cell fraction displayed up-regulated expression of surface molecules associated with recruitment and immunosuppressive function, namely CD103 and CTLA-4 [26,41,42]. In this scenario, up-regulation of CD103 on both, CD4+ T cells and CD4+ FoxP3+ suggests that Treg originate from CD4+ T cells newly recruited to the lung tissue whereas up-regulation

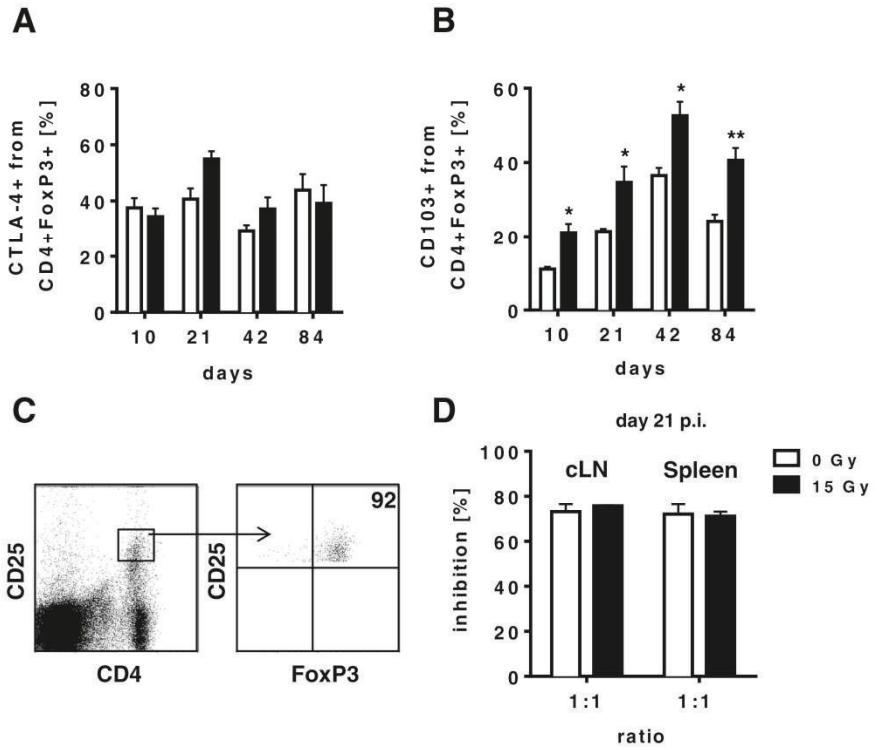

Figure 5 Treg isolated from irradiated mice have normal immunosuppressive function. C57BL/6 mice received 0 Gy or 15 Gy whole thorax irradiation. At different time points, immune cells were isolated from lung tissue and stained for flow cytometric analysis. **(A)** Detection of CTLA-4 on CD4+ FoxP3+ Treg in the lung. **(B)** Expression of CD103 on CD4+ FoxP3+ Treg in the lung. Timelines are shown as mean values ± SEM of percentages calculated on total lung cells. Cells of 4-6 mice per group were analyzed (* $p \leq 0.05$; ** $p \leq 0.01$; two-way ANOVA followed by post-hoc Bonferroni test). **(C)** Gating strategy for FACS-sorting of Treg from cervical lymph nodes and spleen. CD4+ CD25hi cells are 92% FoxP3+. Shown are dotplots from one representative experiment. **(D)** To determine the suppressive capability of regulatory T cells *in vitro* CD4+ CD25hi T cells (Treg) from cervical lymph nodes and spleens of 0 Gy or 15 Gy whole thorax irradiated mice were isolated at 21 days post-irradiation by FACS sorting. Treg were co-cultured at a ratio of 1:1 with CFSE-labeled CD4+ responder T cells and with antigen-presenting cells in the presence of αCD3. Proliferation of responder T cells was measured by loss of the fluorescent dye CFSE and inhibition was calculated accordingly. Data from three individual hosts are shown with mean values ± SEM.

of the adenosinergic ectoenzyme CD73 hints to immunosuppressive activity of the CD4+ FoxP3+ Treg via extracellular generation of adenosine from adenine nucleotides [24,25,43]. Our observation may provide an explanation for the suggested role of adenosine as an important mediator of tissue protection from radiation-induced injury [44,45]. Finally, the CD4+ FoxP3+ T cells isolated from irradiated mice exhibited a pronounced suppression of T effector cell proliferation that was comparable to the suppression exhibited by Treg isolated from cervical lymph nodes and spleen of sham controls.

Up to now only sparse data are available about the radiation-induced accumulation of Treg and contradictory data have been published regarding their function in the regulation of local and systemic responses to ionizing radiation. Consistent with our findings, numbers of lymphocyte subsets in peripheral blood, lymph nodes, spleens and thymuses of C57BL/6 mice decreased 2 weeks after exposure to TBI with 5 Gy, whereas the fractions of CD4+ CD25hi and CD4+ CD25hi FoxP3+ T cells in the CD4+ T cell compartment increased [32]. Though CD4+ CD25hi Treg turned out to be functional, the authors claimed a reduced immunosuppressive activity compared to Treg isolated from non-irradiated mice. Similarly, the fraction of CD4+ FoxP3+ T cells within the proliferating CD4+ T cell pool increased in response to TBI with 2 Gy but these cells displayed a reduced capacity to suppress T effector cell proliferation [33]. In line with these *in vivo* observations, human Treg isolated from the peripheral blood of healthy donors displayed a dose-dependent reduction in proliferation and immunosuppressive capacity upon *in vitro* irradiation compared to non-irradiated controls [46]. In contrast, though local irradiation of the legs of C57BL/6 mice bearing subcutaneous tumors also led to a rapid and transient increase of CD4+ FoxP3+ and CD4+ CD25hi FoxP3+ T cells in the

lung and peripheral lymphoid organs, functional activity of these CD4+ FoxP3+ cells exposed to ionizing radiation *in vivo* was not affected in this experimental setting which is consistent with our present findings [30]. Altogether, these data indicate that transient local and systemic accumulation of CD4+ FoxP3+ Treg seems to constitute a common immune response to irradiation *in vivo*, though the kinetics and the functional state may depend on the radiation dose and the target tissue, respectively.

In general, Treg induced in the periphery may be considered as readout for the initiation of cytotoxic effector T cell responses known to play a key role in the maintenance of immune homeostasis and the suppression of pro-inflammatory reactions [19,47]. We therefore speculate that accumulation of Treg upon local irradiation contributes to the control of radiation-induced pneumonitis. Functional Treg may be required to keep in check effector cells of the innate and adaptive immune system, e.g. T_H1, T_H17 cells, thereby limiting inflammation-associated tissue damage and balancing tissue homeostasis [18,48-50].

However, when considering to target Treg for modulating the outcome of radiation-induced normal tissue toxicity it has to be taken into account that CD4+ FoxP3+ Treg may have a distinct contribution for shaping the immune response during the pneumonitic phase, which has many characteristics of acute inflammation, and the fibrotic phase characterized by chronic inflammation and tissue repair with excessive deposition of extracellular matrix and remodeling of the lung architecture, respectively [51]. In this regard, Treg dampened lung inflammation in a model of silica-induced lung disease, whereas depletion of this cell population attenuated lung fibrosis through maintenance of a T_H1-dominated pro-inflammatory state [52]. We assume that the action of Treg in the context of radiation-induced lung disease may be similarly complex and requires further definition.

Conclusion

Whole thorax irradiation exerts a dual effect on the adaptive immune system characterised by local immunoactivation and systemic immunosuppression. Moreover, local irradiation of the thoracic region led to a local and systemic expansion of immunosuppressive CD4+ FoxP3+ cells during the early pneumonitic phase. We speculate that these cells are needed to restrain the local cytotoxic effector T cell response induced in the lung in response to ionizing radiation thereby limiting excessive inflammation-associated lung damage and re-establishing tissue homeostasis. Further investigations shall identify the origin of these cells and the mechanisms governing their local and systemic accumulation. Moreover, the identification of the role of Treg during radiation-induced pneumonitis and fibrosis is required if we aim to exploit radiation-induced immune changes for developing effective strategies to prevent or treat radiation-induced adverse effects in the lung.

Abbreviations

APC: Antigen presenting cell; BALF: Bronchoalveolar lavage fluid; CD39: Ectoapyrase; CD73: 5'Ectonucleotidase; CFSE: Carboxyfluorescein succinimidyl ester; cLN: Cervical lymph node; CTLA-4: Cytotoxic T-Lymphocyte Antigen 4; FoxP3: Forkhead box protein 3; Gy: Gray; IL: Interleukin; IMRT: Intensity-modulated radiation therapy; LNC: Lymph node cells; RAG2: Recombination-activating gene 2; TBI: Total body irradiation; TGF-β: Transforming growth factor beta; TLC: Total lung cells; Treg: Regulatory T cells; TSC: Total spleen cells; WT: Wild type; WTI: Whole thorax irradiation.

Competing interest

No competing interest does exist for any of the authors.

Authors' contributions

VJ and FW conceived the study. FW, FC, MN and SdL participated in data collection. VJ and FW performed statistical analysis, data evaluation, and drafted the manuscript. LL helped in the experimental setup and drafting the manuscript. AW and MS critically revised the manuscript. All authors read and approved the final manuscript.

Acknowledgements

We thank Dr. Ali Sak and Michael Groneberg for support with the irradiation of mice, and Eva Gau for excellent technical support. The work was supported by grants of the DFG (GRK1739/1) and of the BMBF (ZISS - FKZ: 02NUK024-D).

Author details

[1]Department of Molecular Cell Biology, Institute of Cell Biology (Cancer Research), Medical Faculty, University of Duisburg-Essen, Virchowstrasse 173, 45122, Essen, Germany. [2]Department of Infection Immunology, Institute of Microbiology, Medical Faculty, University of Duisburg-Essen, Essen, Germany. [3]Department of Radiotherapy, Medical Faculty, University of Duisburg-Essen, Essen, Germany.

Received: 15 January 2014 Accepted: 9 April 2014
Published: 25 April 2014

References

1. Ghafoori P, Marks LB, Vujaskovic Z, Kelsey CR: **Radiation-induced lung injury. Assessment, management, and prevention.** *Oncology (Williston Park)* 2008, **22**(1):37–47. discussion 52-33.
2. Tsoutsou PG, Koukourakis MI: **Radiation pneumonitis and fibrosis: mechanisms underlying its pathogenesis and implications for future research.** *Int J Radiat Oncol Biol Phys* 2006, **66**(5):1281–1293.
3. Kristensen CA, Nottrup TJ, Berthelsen AK, Kjaer-Kristoffersen F, Ravn J, Sorensen JB, Engelholm SA: **Pulmonary toxicity following IMRT after extrapleural pneumonectomy for malignant pleural mesothelioma.** *Radiother Oncol J European Soc Therap Radiol Oncol* 2009, **92**(1):96–99.
4. Graves PR, Siddiqui F, Anscher MS, Movsas B: **Radiation pulmonary toxicity: from mechanisms to management.** *Semin Radiat Oncol* 2010, **20**(3):201–207.
5. Travis EL, Vojnovic B, Davies EE, Hirst DG: **A plethysmographic method for measuring function in locally irradiated mouse lung.** *British J Radiol* 1979, **52**(613):67–74.
6. Eldh T, Heinzelmann F, Velalakan A, Budach W, Belka C, Jendrossek V: **Radiation-induced changes in breathing frequency and lung histology of C57BL/6J mice are time- and dose-dependent.** *Strahlentherapie und Onkologie: Organ der Deutschen Rontgengesellschaft [et al]* 2012, **188**(3):274–281.
7. Chiang CS, Liu WC, Jung SM, Chen FH, Wu CR, McBride WH, Lee CC, Hong JH: **Compartmental responses after thoracic irradiation of mice: strain differences.** *Int J Radiat Oncol Biol Phys* 2005, **62**(3):862–871.
8. O'Brien TJ, Letuve S, Haston CK: **Radiation-induced strain differences in mouse alveolar inflammatory cell apoptosis.** *Can J Physiol Pharmacol* 2005, **83**(1):117–122.
9. Trott KR, Herrmann T, Kasper M: **Target cells in radiation pneumopathy.** *Int J Radiat Oncol Biol Phys* 2004, **58**(2):463–469.
10. Rube CE, Uthe D, Wilfert F, Ludwig D, Yang K, Konig J, Palm J, Schuck A, Willich N, Remberger K, Rübe C: **The bronchiolar epithelium as a**

prominent source of pro-inflammatory cytokines after lung irradiation. *Int J Radiat Oncol Biol Phys* 2005, **61**(5):1482–1492.
11. Todd NW, Luzina IG, Atamas SP: **Molecular and cellular mechanisms of pulmonary fibrosis.** *Fibrogenesis Tissue Repair* 2012, **5**(1):11.
12. Gibson PG, Bryant DH, Morgan GW, Yeates M, Fernandez V, Penny R, Breit SN: **Radiation-induced lung injury: a hypersensitivity pneumonitis?** *Ann Intern Med* 1988, **109**(4):288–291.
13. Martin C, Romero S, Sanchez-Paya J, Massuti B, Arriero JM, Hernandez L: **Bilateral lymphocytic alveolitis: a common reaction after unilateral thoracic irradiation.** *Eur Respir J* 1999, **13**(4):727–732.
14. Roberts CM, Foulcher E, Zaunders JJ, Bryant DH, Freund J, Cairns D, Penny R, Morgan GW, Breit SN: **Radiation pneumonitis: a possible lymphocyte-mediated hypersensitivity reaction.** *Ann Intern Med* 1993, **118**(9):696–700.
15. Nakayama Y, Makino S, Fukuda Y, Min KY, Shimizu A, Ohsawa N: **Activation of lavage lymphocytes in lung injuries caused by radiotherapy for lung cancer.** *Int J Radiat Oncol Biol Phys* 1996, **34**(2):459–467.
16. Westermann W, Schobl R, Rieber EP, Frank KH: **Th2 cells as effectors in postirradiation pulmonary damage preceding fibrosis in the rat.** *Int J Radiat Biol* 1999, **75**(5):629–638.
17. Johnston CJ, Williams JP, Elder A, Hernady E, Finkelstein JN: **Inflammatory cell recruitment following thoracic irradiation.** *Exp Lung Res* 2004, **30**(5):369–382.
18. Cappuccini F, Eldh T, Bruder D, Gereke M, Jastrow H, Schulze-Osthoff K, Fischer U, Kohler D, Stuschke M, Jendrossek V: **New insights into the molecular pathology of radiation-induced pneumopathy.** *Radiother Oncol J European Soc Therap Radiol Oncol* 2011, **101**(1):86–92.
19. Sakaguchi S, Yamaguchi T, Nomura T, Ono M: **Regulatory T cells and immune tolerance.** *Cell* 2008, **133**(5):775–787.
20. Klein D, Demory A, Peyre F, Kroll J, Augustin HG, Helfrich W, Kzhyshkowska J, Schledzewski K, Arnold B, Goerdt S: **Wnt2 acts as a cell type-specific, autocrine growth factor in rat hepatic sinusoidal endothelial cells cross-stimulating the VEGF pathway.** *Hepatology* 2008, **47**(3):1018–1031.
21. Chen X, Oppenheim JJ: **Resolving the identity myth: key markers of functional CD4 + FoxP3+ regulatory T cells.** *Int Immunopharmacol* 2011, **11**(10):1489–1496.
22. Fontenot JD, Gavin MA, Rudensky AY: **Foxp3 programs the development and function of CD4 + CD25+ regulatory T cells.** *Nat Immunol* 2003, **4**(4):330–336.
23. Hori S, Nomura T, Sakaguchi S: **Control of regulatory T cell development by the transcription factor Foxp3.** *Science* 2003, **299**(5609):1057–1061.
24. Deaglio S, Dwyer KM, Gao W, Friedman D, Usheva A, Erat A, Chen JF, Enjyoji K, Linden J, Oukka M, Kuchroo VK, Strom TB, Robson SC: **Adenosine generation catalyzed by CD39 and CD73 expressed on regulatory T cells mediates immune suppression.** *J Exp Med* 2007, **204**(6):1257–1265.
25. Kobie JJ, Shah PR, Yang L, Rebhahn JA, Fowell DJ, Mosmann TR: **T regulatory and primed uncommitted CD4 T cells express CD73, which suppresses effector CD4 T cells by converting 5'-adenosine monophosphate to adenosine.** *J Immunol* 2006, **177**(10):6780–6786.
26. Allakhverdi Z, Fitzpatrick D, Boisvert A, Baba N, Bouguermouh S, Sarfati M, Delespesse G: **Expression of CD103 identifies human regulatory T-cell subsets.** *J Allergy Clinical Immunol* 2006, **118**(6):1342–1349.
27. Schaue D, Xie MW, Ratikan JA, McBride WH: **Regulatory T cells in radiotherapeutic responses.** *Frontiers Oncol* 2012, **2**:90.
28. Heinzelmann F, Jendrossek V, Lauber K, Nowak K, Eldh T, Boras R, Handrick R, Henkel M, Martin C, Uhlig S, Köhler D, Eltzschig HK, Wehrmann M, Budach W, Belka C: **Irradiation-induced pneumonitis mediated by the CD95/CD95-ligand system.** *J Natl Cancer Inst* 2006, **98**(17):1248–1251.
29. Ozsahin M, Crompton NE, Gourgou S, Kramar A, Li L, Shi Y, Sozzi WJ, Zouhair A, Mirimanoff RO, Azria D: **CD4 and CD8 T-lymphocyte apoptosis can predict radiation-induced late toxicity: a prospective study in 399 patients.** *Clinical Cancer Res Off J Am Assoc Cancer Res* 2005, **11**(20):7426–7433.
30. Kachikwu EL, Iwamoto KS, Liao YP, DeMarco JJ, Agazaryan N, Economou JS, McBride WH, Schaue D: **Radiation enhances regulatory T cell representation.** *Int J Radiat Oncol Biol Phys* 2011, **81**(4):1128–1135.
31. Formenti SC, Demaria S: **Systemic effects of local radiotherapy.** *Lancet Oncol* 2009, **10**(7):718–726.
32. Qu Y, Jin S, Zhang A, Zhang B, Shi X, Wang J, Zhao Y: **Gamma-ray resistance of regulatory CD4 + CD25 + Foxp3+ T cells in mice.** *Radiat Res* 2010, **173**(2):148–157.
33. Balogh A, Persa E, Bogdandi EN, Benedek A, Hegyesi H, Safrany G, Lumniczky K: **The effect of ionizing radiation on the homeostasis and functional integrity of murine splenic regulatory T cells.** *Inflammation Res Off J European Histamine Res Soc [et al]* 2013, **62**(2):201–212.
34. Kusunoki Y, Yamaoka M, Kubo Y, Hayashi T, Kasagi F, Douple EB, Nakachi K: **T-cell immunosenescence and inflammatory response in atomic bomb survivors.** *Radiat Res* 2010, **174**(6):870–876.
35. Nakatsukasa H, Tsukimoto M, Tokunaga A, Kojima S: **Repeated gamma irradiation attenuates collagen-induced arthritis via up-regulation of regulatory T cells but not by damaging lymphocytes directly.** *Radiat Res* 2010, **174**(3):313–324.
36. Weng L, Williams RO, Vieira PL, Screaton G, Feldmann M, Dazzi F: **The therapeutic activity of low-dose irradiation on experimental arthritis depends on the induction of endogenous regulatory T cell activity.** *Ann Rheum Dis* 2010, **69**(8):1519–1526.
37. Martin M, Lefaix J, Delanian S: **TGF-beta1 and radiation fibrosis: a master switch and a specific therapeutic target?** *Int J Radiat Oncol Biol Phys* 2000, **47**(2):277–290.
38. Heiber JF, Geiger TL: **Context and location dependence of adaptive Foxp3(+) regulatory T cell formation during immunopathological conditions.** *Cell Immunol* 2012, **279**(1):60–65.
39. Curotto de Lafaille MA, Lafaille JJ: **Natural and adaptive foxp3+ regulatory T cells: more of the same or a division of labor?** *Immunity* 2009, **30**(5):626–635.
40. Chen W, Jin W, Hardegen N, Lei KJ, Li L, Marinos N, McGrady G, Wahl SM: **Conversion of peripheral CD4 + CD25- naive T cells to CD4 + CD25+ regulatory T cells by TGF-beta induction of transcription factor Foxp3.** *J Exp Med* 2003, **198**(12):1875–1886.
41. Tai X, Van Laethem F, Pobezinsky L, Guinter T, Sharrow SO, Adams A, Granger L, Kruhlak M, Lindsten T, Thompson CB, Feigenbaum L, Singer A: **Basis of CTLA-4 function in regulatory and conventional CD4(+) T cells.** *Blood* 2012, **119**(22):5155–5163.
42. Wing K, Onishi Y, Prieto-Martin P, Yamaguchi T, Miyara M, Fehervari Z, Nomura T, Sakaguchi S: **CTLA-4 control over Foxp3+ regulatory T cell function.** *Science* 2008, **322**(5899):271–275.
43. Zarek PE, Huang CT, Lutz ER, Kowalski J, Horton MR, Linden J, Drake CG, Powell JD: **A2A receptor signaling promotes peripheral tolerance by inducing T-cell anergy and the generation of adaptive regulatory T cells.** *Blood* 2008, **111**(1):251–259.
44. Hosek B, Bohacek J, Sikulova J, Pospisil M, Vacek A: **Protection of early cellular damage in 1 Gy-irradiated mice by the elevation of extracellular adenosine.** *Radiat Environ Biophys* 1992, **31**(4):289–297.
45. Pospisil M, Hofer M, Netikova J, Pipalova I, Vacek A, Bartonickova A, Volenec K: **Elevation of extracellular adenosine induces radioprotective effects in mice.** *Radiat Res* 1993, **134**(3):323–330.
46. Cao M, Cabrera R, Xu Y, Liu C, Nelson D: **Gamma irradiation alters the phenotype and function of CD4 + CD25+ regulatory T cells.** *Cell Biol Int* 2009, **33**(5):565–571.
47. Schaue D, Comin-Anduix B, Ribas A, Zhang L, Goodglick L, Sayre JW, Debucquoy A, Haustermans K, McBride WH: **T-cell responses to survivin in cancer patients undergoing radiation therapy.** *Clinical cancer Res Off J Am Assoc Cancer Res* 2008, **14**(15):4883–4890.
48. MacConmara MP, Tajima G, O'Leary F, Delisle AJ, McKenna AM, Stallwood CG, Mannick JA, Lederer JA: **Regulatory T cells suppress antigen-driven CD4 T cell reactivity following injury.** *J Leukoc Biol* 2011, **89**(1):137–147.
49. Chaudhry A, Samstein RM, Treuting P, Liang Y, Pils MC, Heinrich JM, Jack RS, Wunderlich FT, Bruning JC, Muller W, Rudensky AY: **Interleukin-10 signaling in regulatory T cells is required for suppression of Th17 cell-mediated inflammation.** *Immunity* 2011, **34**(4):566–578.
50. Peterson RA: **Regulatory T-cells: diverse phenotypes integral to immune homeostasis and suppression.** *Toxicol Pathol* 2012, **40**(2):186–204.
51. Wynn TA: **Integrating mechanisms of pulmonary fibrosis.** *J Exp Med* 2011, **208**(7):1339–1350.
52. Liu F, Liu J, Weng D, Chen Y, Song L, He Q, Chen J: **CD4 + CD25 + Foxp3+ regulatory T cells depletion may attenuate the development of silica-induced lung fibrosis in mice.** *PLoS One* 2010, **5**(11):e15404.

doi:10.1186/1748-717X-9-98
Cite this article as: Wirsdörfer *et al.*: Thorax irradiation triggers a local and systemic accumulation of immunosuppressive CD4+ FoxP3+ regulatory T cells. *Radiation Oncology* 2014 **9**:98.

3.3 Extracellular adenosine production by ecto-5'-nucleotidase (CD73) enhances radiation-induced lung fibrosis.

Contribution to present publication:

- Writing and reviewing of the manuscript
    - Introduction: literature research and critical review
    - Materials and Methods: writing the Histopathology section
    - Results: Writing with Wirsdörfer, Cappuccini and Jendrossek, critical reviewing
    - Discussion: writing 5%, literature research and critical review
- Isolation of lung tissue for histological analysis and CD73 activity measurements Figure 1A, 1B, 1D, 3C, 4D, 4F+G, 5A+B, 6C, 6E (with Wirsdörfer and Cappuccini)
    - Performed Ashcroft Scoring in Figure 4C, 6D (all slices; one of four independent observers together with Wirsdörfer, Meyer and Gau)
    - IHC staining Figure 4G, 5B
- Collecting BALF (with Wirsdörfer and Cappuccini)
    - 9 weeks stay in Houston in the lab of Prof. Blackburn to learn and perform the measurement of ATP and adenosine in BALF
    - measurement of extracellular adenosine in BALF (approx. 30% of the samples) for Figure 1C, 4A+B, 6B
- Data collection for flow cytometry (with Wirsdörfer and Cappuccini)
    - Isolation of lung
    - Isolation of immune cells lung (tissue digestion, filtration steps, erythrocyte lysis)
    - Staining of isolated immune cells for flow cytometric analysis: surface staining as well as intracellular staining
    - Analyses of flow cytometry data: Figure 2, 3D
- RNA isolation and QPCR analyses Figure 4E, 5C+D, 6F
    - established method to isolate RNA from murine tissue samples with the biopulverizer
    - primer design and optimization for QPCR
    - Performed QPCR for Figure 4E, 5D, 6F
- Administration of PBS, PEG-ADA and TY/23 to mice for Figure 6 (with Wirsdörfer and Meyer)

The above listed contributions of Simone de Leve to the publication are correct.

Essen, den _____ _____

Unterschrift der Doktorandin

Essen, den _____ _____

Unterschrift des wissenschaftl. Betreuers/
Mitglieds der Universität Duisburg-Essen

Cancer Research

Extracellular Adenosine Production by ecto-5′-Nucleotidase (CD73) Enhances Radiation-Induced Lung Fibrosis

Florian Wirsdörfer[1], Simone de Leve[1], Federica Cappuccini[1], Therese Eldh[2], Alina V. Meyer[1], Eva Gau[1], Linda F. Thompson[3], Ning-Yuan Chen[4], Harry Karmouty-Quintana[4], Ute Fischer[5], Michael Kasper[6], Diana Klein[1], Jerry W. Ritchey[7], Michael R. Blackburn[4], Astrid M. Westendorf[8], Martin Stuschke[9], and Verena Jendrossek[1]

Abstract

Radiation-induced pulmonary fibrosis is a severe side effect of thoracic irradiation, but its pathogenesis remains poorly understood and no effective treatment is available. In this study, we investigated the role of the extracellular adenosine as generated by the ecto-5′-nucleotidase CD73 in fibrosis development after thoracic irradiation. Exposure of wild-type C57BL/6 mice to a single dose (15 Gray) of whole thorax irradiation triggered a progressive increase in CD73 activity in the lung between 3 and 30 weeks postirradiation. In parallel, adenosine levels in bronchoalveolar lavage fluid (BALF) were increased by approximately 3-fold. Histologic evidence of lung fibrosis was observed by 25 weeks after irradiation. Conversely, CD73-deficient mice failed to accumulate adenosine in BALF and exhibited significantly less radiation-induced lung fibrosis ($P < 0.010$). Furthermore, treatment of wild-type mice with pegylated adenosine deaminase or CD73 antibodies also significantly reduced radiation-induced lung fibrosis. Taken together, our findings demonstrate that CD73 potentiates radiation-induced lung fibrosis, suggesting that existing pharmacologic strategies for modulating adenosine may be effective in limiting lung toxicities associated with the treatment of thoracic malignancies. *Cancer Res; 76(10); 1–12. ©2016 AACR.*

Introduction

Radiotherapy is an integral part of standard treatment for thorax-associated neoplasms. Unfortunately, adverse late effects in the highly radiosensitive lung limit the radiation dose, resulting in suboptimal local control, metastases, and decreased quality of life (1, 2). Lung toxicity also limits the dose of total body irradiation in conditioning regimens for hematopoietic stem cell transplantation (3). Acute damage to resident cells induced by thorax irradiation triggers complex reciprocal interactions between damaged resident lung cells, recruited immune cells, extracellular matrix molecules, secreted cytokines/chemokines, growth factors, and proteases, resulting in a disturbed balance between inflammatory and repair processes, tissue disorganization, pathologic remodeling, and lung fibrosis (2, 4, 5). As a consequence, pneumonitis and pulmonary fibrosis develop within 12 weeks and 6 to 24 months after radiotherapy, respectively, in patients and mice with symptoms including nonproductive cough, dyspnea, and respiratory insufficiency and a lethality rate up to 10% (1–3, 6). As no available therapies completely prevent or treat these potentially life-threatening adverse late effects, there is a great need for a better understanding of the underlying mechanisms (7, 8).

Ecto-5′-nucleotidase (NT5E, CD73) and adenosine play critical roles in balancing tissue inflammation and repair processes in pulmonary fibrosis, regulating leukocyte extravasation and function, and modulating epithelial cell behavior, vascular function, and cell death (9–16). Herein, CD73 is found on the surface of various cell types in the lung. It acts in concert with ectonucleoside triphosphate diphosphohydrolase 1 (ENTPD1, CD39) to generate adenosine from extracellularly released ATP/ADP. Extracellular adenosine levels are usually low due to rapid cellular uptake by nucleoside transporters and catabolic conversion by adenosine deaminase (ADA) or adenosine kinase to inosine or AMP, respectively. However, they can rapidly increase in response to stress or tissue injury through either direct release from damaged cells or ATP/ADP catabolism by

[1]Institute of Cell Biology (Cancer Research), Medical School, University of Duisburg-Essen, Essen, Germany. [2]Department of Radiation Oncology, University Hospital Tübingen, Tübingen, Germany. [3]Immunobiology and Cancer Program, Oklahoma Medical Research Foundation, Oklahoma City, Oklahoma. [4]Department of Biochemistry and Molecular Biology, University of Texas Health Science Center, Houston, Texas. [5]Department of Pediatric Oncology, Hematology and Clinical Immunology, University Children's Clinic, Medical Faculty, Heinrich-Heine-University, Düsseldorf, Germany. [6]Institute of Anatomy, Medical Faculty Carl Gustav Carus, Technische Universität Dresden, Dresden, Germany. [7]Department of Veterinary Pathobiology, Center for Veterinary Health Sciences, Oklahoma State University, Stillwater, Oklahoma. [8]Department of Infection Immunology, Institute of Medical Microbiology, Medical Faculty, University of Duisburg-Essen, Essen, Germany. [9]Department of Radiation Oncology, University Hospital Essen, Essen, Germany.

F. Wirsdörfer, S. de Leve, and F. Cappuccini contributed equally to this article.

Current address for F. Cappuccini: ORCRB, The Jenner Institute, University of Oxford, Oxford, United Kingdom.

Corresponding Author: Verena Jendrossek, University of Duisburg-Essen, Medical School, Virchowstrasse 173, Essen 45122, Germany. Phone: 49-201-723-3380; Fax: 49-201-723-5904; E-mail: verena.jendrossek@uni-due.de

doi: 10.1158/0008-5472.CAN-15-2310

CD39 and CD73 (9, 10). Extracellular adenosine acts through four different G protein–coupled adenosine receptors (ADORA1, ADORA2A, ADORA2B, ADORA3) that are widely expressed and have various biologic functions aimed at maintaining or restoring tissue homeostasis (9, 10, 17). Though CD73 and adenosine are crucial for the regulation of lung homeostasis, their role during radiation-induced pneumopathy is unknown. As earlier reports showed both tissue-protective and profibrotic effects of CD73 and adenosine in pulmonary fibrosis (18–20), we asked whether they would be protective or harmful in radiation-induced lung disease and evaluated their potential as therapeutic targets.

Materials and Methods

Mice

C57BL/6 wild-type (WT; Charles River Laboratories) and CD73$^{-/-}$ (*Nt5e*$^{-/-}$) mice on the C57BL/6 background (12) were bred and housed under specific pathogen-free conditions in Laboratory Animal Facilities of the University Hospitals Tübingen and Essen. Experimental protocols were approved by the appropriate animal protection boards.

In vivo treatment

Eight- to twelve-week-old mice were anesthetized with 2% isoflurane, placed in holders, and irradiated either with a single dose of 0 (sham control) or 15 Gray (Gy) over their right hemithorax, using a linear accelerator (4.7 Gy/minute), or over their whole thorax (WTI) using a Cobalt-60 source (Philips; 0.5 Gy/minute) as described previously (21, 22).

Some WT mice were exposed to WTI and subsequently treated twice weekly from week 16 to week 25 or 26 postirradiation by intraperitoneal injection with 100 μL PBS (solvent), 5 units of pegylated ADA (PEG-ADA) to catabolize adenosine (23), or 100 μg of anti-CD73 mAb TY/23 to inhibit CD73 function (24).

Mice were sacrificed at 3, 6, 12, 16, 20, 24, or 25 to 30 weeks postirradiation and blood serum, lung tissue, and/or bronchoalveolar lavage fluid (BALF) were collected.

CD73 enzyme assay

CD73 ecto-5′-nucleotidase enzyme activity was evaluated in frozen lung tissue by measuring the proportion of [^{14}C]IMP converted to [^{14}C]inosine that could be inhibited by the specific CD73 inhibitor adenosine 5′-(α,β-methylene)diphosphate (APCP, Sigma-Aldrich) as described previously (12, 25). CD73 activity was expressed as μmol IMP hydrolyzed/h/mg protein.

Determination of albumin in BALF

Albumin levels in BALF were determined using the Albumin ELISA Quantification Kit Mouse (Bethyl Laboratories) according to the manufacturer's instructions (26).

Quantification of apoptosis in BALF

Active caspase-3 in BALF was detected using Caspase-Glo 3/7 Kit (Promega) as described previously (26).

Nucleotide and nucleoside quantification

AMP and adenosine were measured in BALF by reverse-phase high-performance liquid chromatography as described previously (27). For this, lungs were lavaged 4× with 0.3 mL of PBS with 10 μmol/L dipyridamole, 10 μmol/L APCP, and 10 μmol/L ADA inhibitor 2′-deoxycoformycin (Sigma-Aldrich) to prevent adenosine degradation.

Histopathology

Paraffin-embedded tissue. Lungs were isolated from euthanized mice after intratracheal perfusion with 4% paraformaldehyde in PBS (pH 7.2) and fixed overnight in the same solution. Upon dehydration, lungs were embedded in paraffin and sectioned into 5-μm slices.

Frozen tissue. Lungs of euthanized mice were inflated with a 1:1 mixture of Tissue-Tek O.C.T. Compound (Sakura Finetek) and PBS, isolated and placed in optimal cutting temperature embedding medium, precooled on dry ice, and stored at −80°C. Frozen tissue was cut into 7-μm cryosections.

Caspase-3 (CASP3). Immunohistochemical staining of paraffin-embedded lung tissue was performed as described before (26) using an active caspase-3 antibody (New England Biolabs), anti-rabbit IgG, Streptavidin AP Complex ready to use, and Fast Red Staining (Roche).

Osteopontin (SPP1, OPN), collagen type 1 (COL1A1). Tissue slides were deparaffinized, rehydrated and steam boiled in citrate buffer pH 6. After blocking endogenous peroxidase with 3% H_2O_2, sections were blocked for 20 minutes with 2% FCS (osteopontin) or 2% normal goat serum (collagen), and subsequently incubated with anti-osteopontin (R&D Systems) or anti-collagen type 1 antibodies (Rockland Immunochemicals Inc.) overnight at 4°C. Primary antibodies were detected by secondary antibodies linked to horseradish peroxidase and subsequent DAB staining.

TGFβ (TGFB1), α-SMA (ACTA2). Immunohistochemical staining of paraffin-embedded lung tissue slides was performed using the Mouse on Mouse (M.O.M.) ImmPRESS HRP (peroxidase) Polymer Kit (Vector Laboratories) according to the manufacturer's instructions. Anti-TGFβ (R&D Systems) and anti-smooth muscle actin (α-SMA; Merck Millipore) were used as mouse primary antibodies. ImmPACT VIP Peroxidase (HRP) Substrate Kit (Vector Laboratories) was used to detect TGFβ and α-SMA according to the manufacturer's instructions. Stained sections were counterstained with hematoxylin.

Fibrosis. Lung sections were stained with hematoxylin and eosin (H&E) or Masson Goldner Trichrome (MT; Carl Roth Karlsruhe), and scored by three individuals blinded to the genotype and treatment group. Ten random, nonoverlapping fields (magnification, ×200) of lung parenchyma from each specimen were photographed and lung fibrosis was scored using a 0 to 8 point Ashcroft scale (28). The mean scores for each observer were averaged to yield the final score for each specimen.

CD73 histochemistry. CD73 ecto-5′-nucleotidase enzyme activity was visualized on tissue sections by histochemistry as described previously (29). For a negative control, 5′-AMP was replaced by nonhydrolyzable 3′-AMP. In other experiments, the CD73 inhibitor APCP (Sigma-Aldrich) was added.

qPCR

RNA was isolated using RNeasy Mini Kit (74106, Qiagen) according to the manufacturer's instructions. Expression levels were normalized to the reference gene (β-actin; set as 1). qPCR was carried out using specific oligonucleotide primers [β-Actin (*Actb*): fw, CCAGAGCAAGAGAGGTATCC; rev, CTGTGGTGGTGAAGC-TGTAG; Fibronectin (*Fn1*): fw, GAAACCTGCTTCAGTGTGTCTG; rev, TTGAATTGCCACCATAAGTCTG; osteopontin (*Spp1*): fw, ATCTCCTTGCGCCACAGAAT; rev, CTGCCCTTTCCGTTGTT-GTC; TGFβ−1 (*Tgfb1*): fw, ACCTGGGTTGGAAGTGGAT; rev, GAAGCGCCCGGGTTGTGTTGGTT] using qPCR MasterMix for SYBR Assay ROX (SN2X-03T, Eurogentec) according to the manufacturer's instructions.

Lung leukocyte phenotyping

Lung cells were isolated as described previously (22) and stained with anti-CD45 PacificBlue (30-F11), anti-CD11c APC (N418), anti-CD4 APC (RM4-5), anti-CD8 PE (53-6.7), anti-FoxP3 PE (FJK-16s), and/or anti-CD73 PECy7 (TY/11.8). Antibodies were obtained from BD Biosciences, BioLegend, or eBioscience. Flow cytometry was performed on a LSRII flow cytometer using FACS DIVA software (BD Biosciences) and FlowJo (Tree Star).

Statistical Analysis

Statistical analyses were performed using Prism 5.0 (GraphPad). For normalization, sham control values were set to 100% and values for irradiated animals were displayed as percent of sham controls. Student two-tailed unpaired *t* tests were used to compare differences between two groups. One-way ANOVA followed by Newman–Keuls multiple comparison tests were used to compare more than two groups. Two-way ANOVA with *post hoc* Bonferroni multiple comparison tests were used to compare groups split on two independent variables. Statistical significance was set at $P < 0.05$.

Results

Thorax irradiation triggers upregulation of CD73, progressive adenosine accumulation in the lung, and pulmonary fibrosis

To gain insight into the role of CD73 in radiation-induced pneumopathy, we first examined the effects of a single high dose (15 Gy) WTI on CD73 expression in lungs of WT C57BL/6 mice. We used a histochemical CD73 assay in which the released inorganic phosphate from the exogenously added substrate 5′-AMP is converted into an insoluble black lead sulfide precipitate. CD73 activity was barely detectable in lungs of control mice at all timepoints (Fig. 1A). In contrast, we observed a time-dependent increase in lead sulfide precipitation indicative of enhanced AMPase activity in the lung tissue of mice exposed to WTI (Fig. 1A). There was no nonspecific nucleotidase activity as evidenced by a lack of 3′-AMP hydrolysis (Fig. 1A, right).

Next we examined whether upregulation of CD73 expression was associated with increased generation of adenosine by comparing time-dependent changes in lung CD73 enzymatic activity and adenosine levels in the BALF of mice exposed to 0 or 15 Gy WTI. Irradiated mice displayed a time-dependent progressive increase in lung CD73 enzyme activity compared with sham controls culminating in a 3.7-fold rise by 25 to 30 weeks; no significant differences were seen in control mice (Fig. 1B). WTI also led to time-dependent adenosine accumulation in the BALF, suggesting that radiation-induced upregulation of CD73 triggers enhanced generation of adenosine. This started at 16 weeks postirradiation and persisted until the end of the observation time (Fig. 1C).

There was no significant increase in AMPase activity that was not inhibited by the CD73 inhibitor APCP, suggesting that CD73 is the main AMPase contributing to increased adenosine production after WTI (data not shown).

Although the first signs of matrix deposition were detectable at 20 weeks (but not at 16 weeks) postirradiation, histologic signs of lung fibrosis became clearly visible in irradiated WT mice only at 24 to 30 weeks (Fig. 1D). These findings demonstrate that CD73 activity increases prior to the development of lung fibrosis.

WTI led to an increase in the percentage of $CD73^+$ lung cells and the level of CD73/cell compared with sham controls; Fig. 2A depicts a representative histogram of whole lung cells isolated 6 weeks postirradiation. We observed an increase in $CD45^+$ leukocytes in the lungs of WT mice at 12 to 24 weeks postirradiation that was paralleled by a gradual increase in cells with CD73 surface expression reaching a maximum at weeks 25 to 30 postirradiation (Fig. 2B and D). Instead, $CD45^-$ cells showed a temporary increase in the proportion of $CD73^+$ cells at week 12 postirradiation that was however associated with a transient drop in their number in lung tissue during this intermediate phase (Fig. 2C and E).

The above data suggested a contribution of $CD45^+$ cells in radiation-induced CD73 upregulation. We next evaluated the specific roles of $CD4^+$ and $CD8^+$ lymphocytes and alveolar macrophages, as these are major immune cells infiltrating the irradiated lung (22). Although the percentages of $CD73^+CD4^+$ T cells were increased at most time points (Fig. 2F), the percentages of $CD73^+CD8^+$ T cells did not change (Fig. 2G). In contrast, the percentages of $CD73^+$ alveolar macrophages were transiently increased at 6 and 12 weeks postirradiation (Fig. 2H). Notably, we found largely increased percentages of $CD4^+FoxP3^+$ regulatory T cells (Tregs) during the pneumonitic (early) and fibrotic (late) phases (Fig. 2I). Tregs generally express CD73 (14; Fig. 2J), and may thus be a major source of adenosine production from $CD45^+$ cells during the fibrotic phase.

Genetic deficiency of CD73 partially protects from early radiation-induced injury

Early damage to resident cells is thought to be linked to fibrosis development (2, 4, 26). For example, fibrosis-prone C57BL/6 mice develop a transient disturbance of blood air barrier function and increased apoptosis of bronchial epithelial cells 3 weeks after hemithorax irradiation (26). To determine whether CD73 influences these early pathophysiologic alterations associated with radiation-induced lung disease, we compared albumin levels in the BALF of WT and $CD73^{-/-}$ mice 3 weeks postirradiation. Albumin leakage into the BALF was significantly reduced in $CD73^{-/-}$ mice compared with WT mice (Fig. 3A), indicating that loss of CD73 provides partial protection from radiation-induced barrier dysfunction.

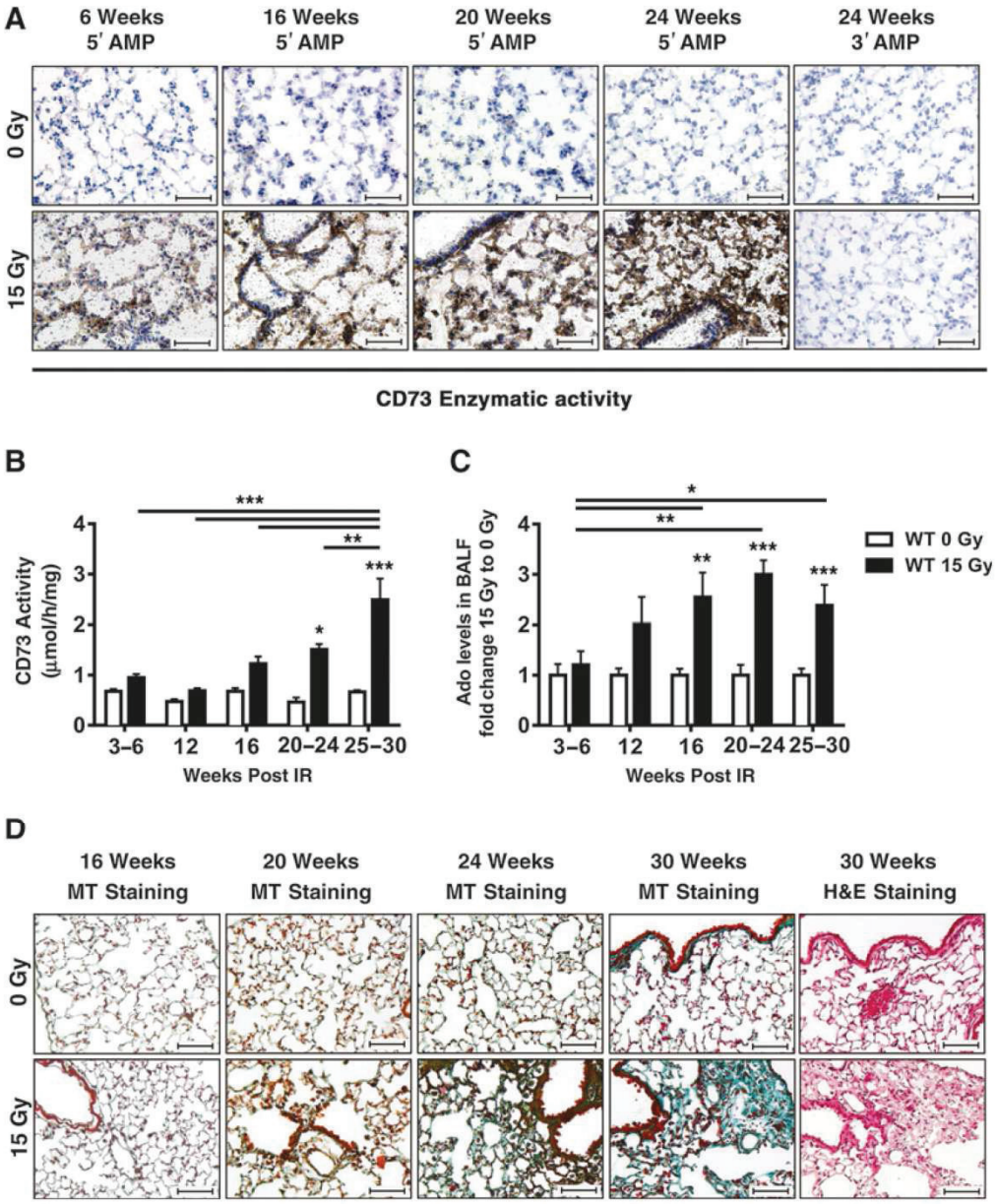

Figure 1.
Radiation induces upregulation of CD73, adenosine accumulation, and lung fibrosis. C57BL/6 WT mice received 0 or 15 Gy WTI and were sacrificed at the indicated time points postirradiation. A, CD73 histochemistry on lung frozen sections of irradiated and control mice using 5′-AMP or 3′-AMP (negative control) as substrates. CD73 activity is visualized by the black lead sulfide precipitate. B, lung CD73 enzyme activity at the indicated time points [n = 12/12, 9/9, 10/9, 5/4, 19/13 (0/15 Gy)]. C, fold change of BALF adenosine levels (mean ± SEM) of irradiated versus control mice. Means of control values were between 41 and 149.5 nmol/L [n = 9/10, 7/7, 10/9, 8/7, 20/11 (0/15 Gy)]. *, $P \leq 0.05$; **, $P \leq 0.01$; ***, $P \leq 0.001$ by two-way ANOVA followed by *post hoc* Bonferroni test. D, Masson Goldner Trichrome (MT) and H&E staining of paraffin-embedded lung sections (scale bar, 100 μm).

WTI also triggered a significant increase in active caspases in the BALF of WT and CD73$^{-/-}$ mice after 3 weeks, but the absolute levels of caspase activation were again significantly lower in knockout mice (Fig. 3B). Consistent with these findings, more bronchial epithelial cells expressed high levels of active caspase-3 in tissue sections of irradiated WT than CD73$^{-/-}$ mice (Fig. 3C). The higher sensitivity of CD73$^{+/+}$ bronchial epithelial cells to radiation-induced apoptosis may contribute to the more pronounced barrier function disturbance observed in WT mice.

In contrast, there were no significant differences in the percentages of CD45^{+} cells in the lungs of WT and CD73$^{-/-}$ mice after WTI (Fig. 3D). These data demonstrate that loss of CD73 partially protects mice from radiation-induced early damage to resident cells without influencing radiation-induced leukocyte recruitment.

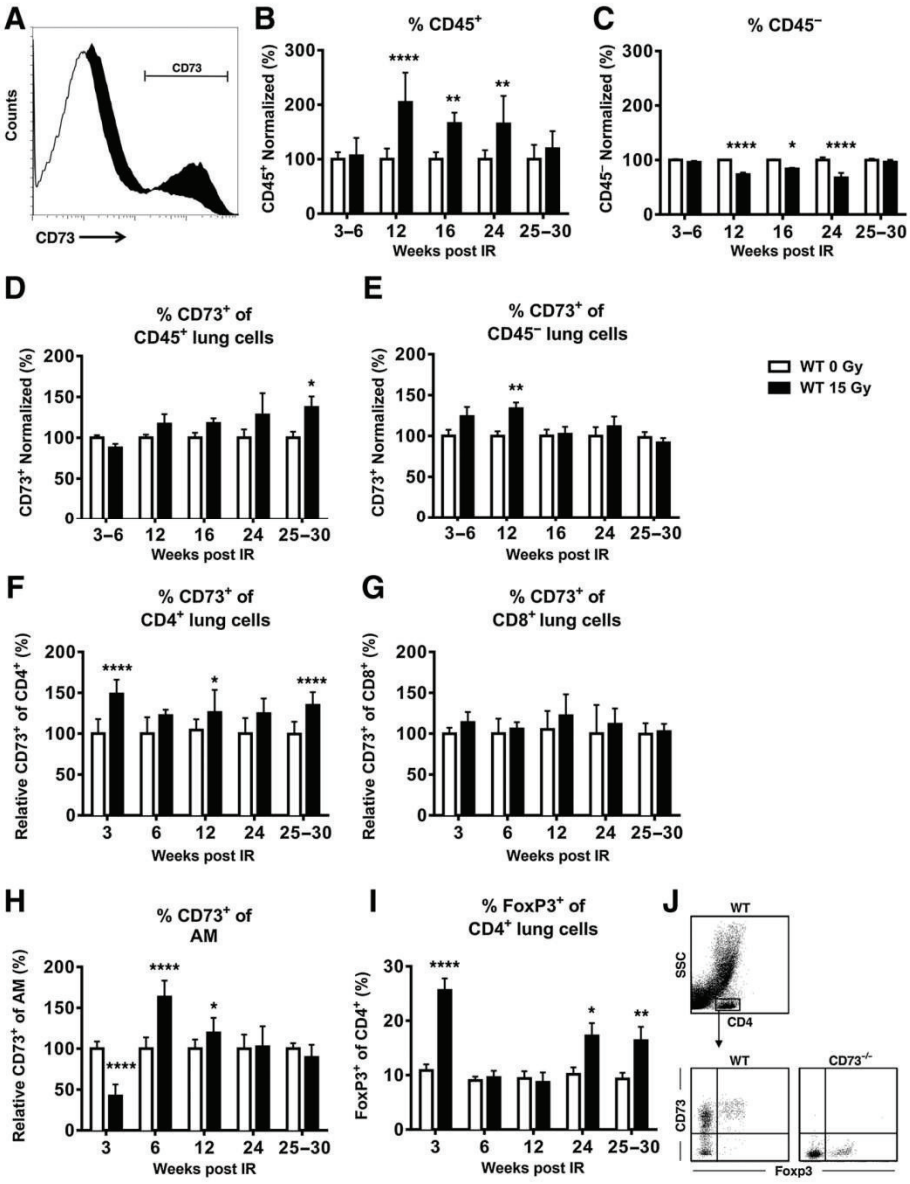

Figure 2.
Thoracic irradiation triggers time-dependent alterations in CD73 expression on resident cells and immune cells. C57BL/6 WT mice received 0 or 15 Gy WTI and were sacrificed at the indicated time points postirradiation. Whole lung cell CD45 and/or CD73 expression were analyzed by flow cytometry. A, CD73 expression in whole lung cells is shown in the black histogram. B and C. normalized percentages of $CD45^+$ (B, $n = 11/11$, 16/16, 6/6, 6/5, 10/12) or $CD45^-$ (C, $n =$ 15/11, 16/16, 6/6, 6/5, 10/12) whole lung cells. D—H, normalized percentages of $CD45^+$, $CD45^-$, $CD4^+$, $CD8^+$ cells and alveolar macrophages ($CD11c^{hi}$ autofluorescent; ref. 55) with CD73 surface expression (D, $n = 11/11$, 16/16, 6/6, 6/5, 10/12; E, $n = 11/11$, 16/16, 6/6, 6/5, 9/11; F and G, $n = 7/7$, 7/7, 14/14, 6/6, 15/15; H, $n = 10/10$, 8/8, 12/12, 6/4, 6/4). I, percentages of lung $CD4^+$ regulatory T cells ($FoxP3^+$; $n = 7/6$, 11/11, 9/9, 7/7, 13/8). Mean ± SEM. *, $P \leq 0.05$; **, $P \leq 0.01$; ****, $P \leq 0.0001$ by unpaired two-tailed t test. J, gating strategy of $CD4^+$ cells for CD73 and $FoxP3^+$ expression evaluation. IR, irradiation.

$CD73^{-/-}$ mice show reduced adenosine levels and lung fibrosis after WTI

To determine whether CD73 is required for radiation-induced adenosine accumulation, we compared radiation-induced changes in the relative levels of adenosine and its precursor AMP in $CD73^{+/+}$ and $CD73^{-/-}$ mice. As our initial data indicated pronounced CD73 activity at the time of fibrosis development, we performed these investigations 30 weeks after irradiation. WT mice accumulated high levels of BALF adenosine at this time point whereas AMP levels were low (Fig. 4A); in contrast, irradiated $CD73^{-/-}$ mice had low levels of BALF adenosine but high levels of AMP (Fig. 4B). These findings strongly suggest that the elevated adenosine levels in lungs of irradiated WT mice result indeed from CD73-mediated enzymatic conversion of AMP to adenosine.

To examine the role of CD73 in radiation-induced lung fibrosis, we next compared histologic changes in WT and $CD73^{-/-}$ mice 30 weeks after WTI using H&E- and MT-stained lung sections (Fig. 4C and D). We observed slightly increased thickening of alveolar septa in nonirradiated $CD73^{-/-}$ mice perhaps due to higher levels of basal tissue inflammation; however, there was little collagen deposition visible in nonirradiated WT or $CD73^{-/-}$ mice (Fig. 4D, left). Importantly, lung sections from irradiated WT mice revealed a prominent thickening of alveolar septa, increased collagen deposition, and multiple fibrotic foci, well-known fibrosis-associated lung lesions (28); in contrast, lung sections of irradiated $CD73^{-/-}$ mice displayed fewer and less

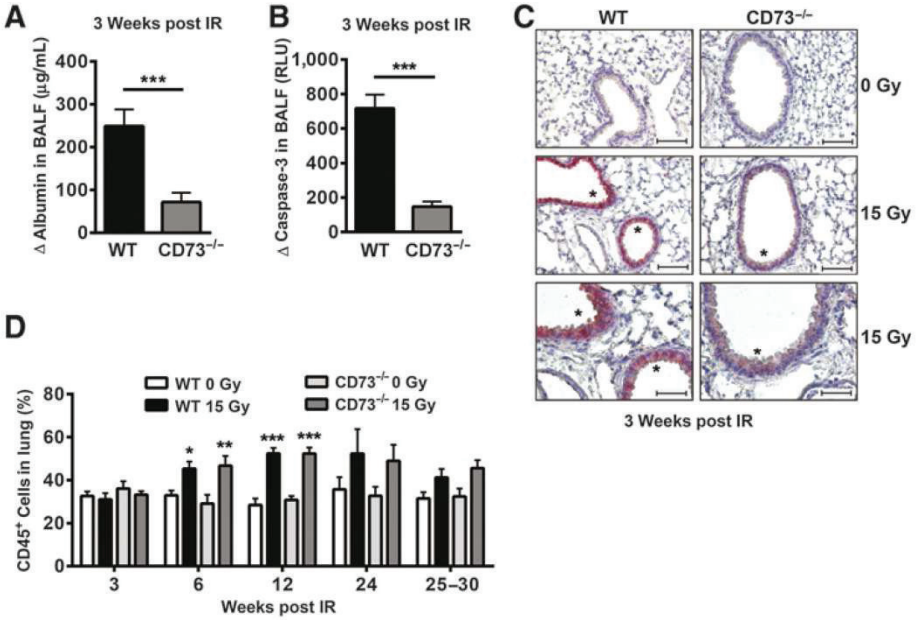

Figure 3.
CD73$^{-/-}$ mice exhibit decreased early damage to resident cells, but have similar leukocyte recruitment in response to ionizing radiation. C57BL/6 WT and CD73$^{-/-}$ mice received 0 or 15 Gy hemithorax irradiation (A and B) or WTI (C and D). A, differences in BALF albumin levels of irradiated WT versus CD73$^{-/-}$ mice (Δ albumin) at 3 weeks postirradiation by ELISA ($n = 4/5$). B, differences in BALF active caspase-3 of WT versus CD73$^{-/-}$ mice (Δ caspase-3) by luminescence (RLU) at 3 weeks postirradiation ($n = 3/3$). C, active caspase-3 on paraffin-embedded lung sections (bottom panels are a 2× enlargement of middle panels; top and middle panels, scale bar, 100 μm; bottom panels, scale bar, 50 μm). Asterisks depict regions with active caspase-3. D, time course of radiation-induced infiltration of CD45$^+$ cells (%) in WT and CD73$^{-/-}$ mice [$n = 10/10/10/10, 10/10/10/10, 12/12/12/11, 6/4/6/5, 10/8/8/9$ (WT 0 Gy/WT 15 Gy/CD73$^{-/-}$ 0 Gy/CD73$^{-/-}$ 15 Gy)]. Data show means ± SD (A and B) or means ± SEM (D). *, $P \leq 0.05$; **, $P \leq 0.01$; ***, $P \leq 0.001$ by unpaired two-tailed t test (A and B) or two-way ANOVA followed by *post hoc* Bonferroni test (D). IR, irradiation.

severe lesions yielding a significantly lower Ashcroft score (Fig. 4C and D).

To corroborate our findings, we quantified the fibrosis-associated proteins fibronectin, collagen type 1 (COL1A1) and α-SMA during the fibrotic phase. Although WTI triggered a significant increase in fibronectin mRNA expression in WT mice, it enhanced fibronectin mRNA expression in CD73$^{-/-}$ mice to a lesser degree (Fig. 4E). Similarly, a significant accumulation of Col1a1 and α-SMA protein occurred only in lungs of irradiated WT mice, particularly in fibrotic areas. In contrast, only low levels of Col1a1 were detected in the lung sections of irradiated CD73$^{-/-}$ mice and α-SMA expression was hardly detectable except for vascular structures (Fig. 4F and G).

To strengthen the above observations, we additionally analyzed the expression of the profibrotic cytokines osteopontin (OPN) and TGFβ, known to be associated with fibrosis development in patients (30, 31). WTI induced higher levels of OPN and TGFβ in paraffin-embedded tissue sections of WT mice compared with CD73$^{-/-}$ mice at ≥ 25 weeks postirradiation, particularly in the fibrotic areas (Fig. 5A and B). These findings were confirmed by qPCR analysis of their mRNA expression levels in whole lung tissue (Fig. 5C and D).

Taken together, the inability of CD73$^{-/-}$ mice to accumulate adenosine in response to WTI correlates with a significant reduction in the expression of fibrosis-associated proteins and a significant attenuation of radiation-induced lung fibrosis. In line with these observations, CD73$^{-/-}$ mice also showed improved survival after irradiation (88% vs. 76% for WT mice) and improved health as shown by normal weight gain. In contrast, WT mice exposed to WTI displayed a significantly reduced weight gain at 30 weeks postirradiation (108% ± 6.5%) compared with 135% ± 18% for nonirradiated controls.

Targeting adenosine accumulation or CD73 attenuates radiation-induced lung fibrosis

To confirm the involvement of adenosine and CD73 in the pathogenesis of radiation-induced lung fibrosis, we treated WT mice with either PEG-ADA, to catabolize adenosine (23) or with CD73 mAb TY/23 that has proven activity for therapeutic inhibition of CD73 function in mice (32). On the basis of the kinetics of CD73 increase and adenosine accumulation (Fig. 1B and C), treatment was initiated 16 weeks after WTI (Fig. 6A). PEG-ADA significantly reduced BALF adenosine levels and almost completely abrogated the radiation-induced increase in lung CD73 activity (Fig. 6B and C). Even more important, PEG-ADA reduced the severity of radiation-induced lung fibrosis (represented by the Ashcroft score) in all treated mice by almost 40% ($P < 0.01$; Fig. 6D and E) and also significantly reduced fibronectin mRNA expression (Fig. 6F). Similarly, TY/23 significantly reduced lung CD73 activity (Fig. 6C). Although TY/23 did not significantly decrease BALF adenosine levels (data not shown), it significantly reduced fibronectin expression and severity of radiation-induced lung fibrosis in all

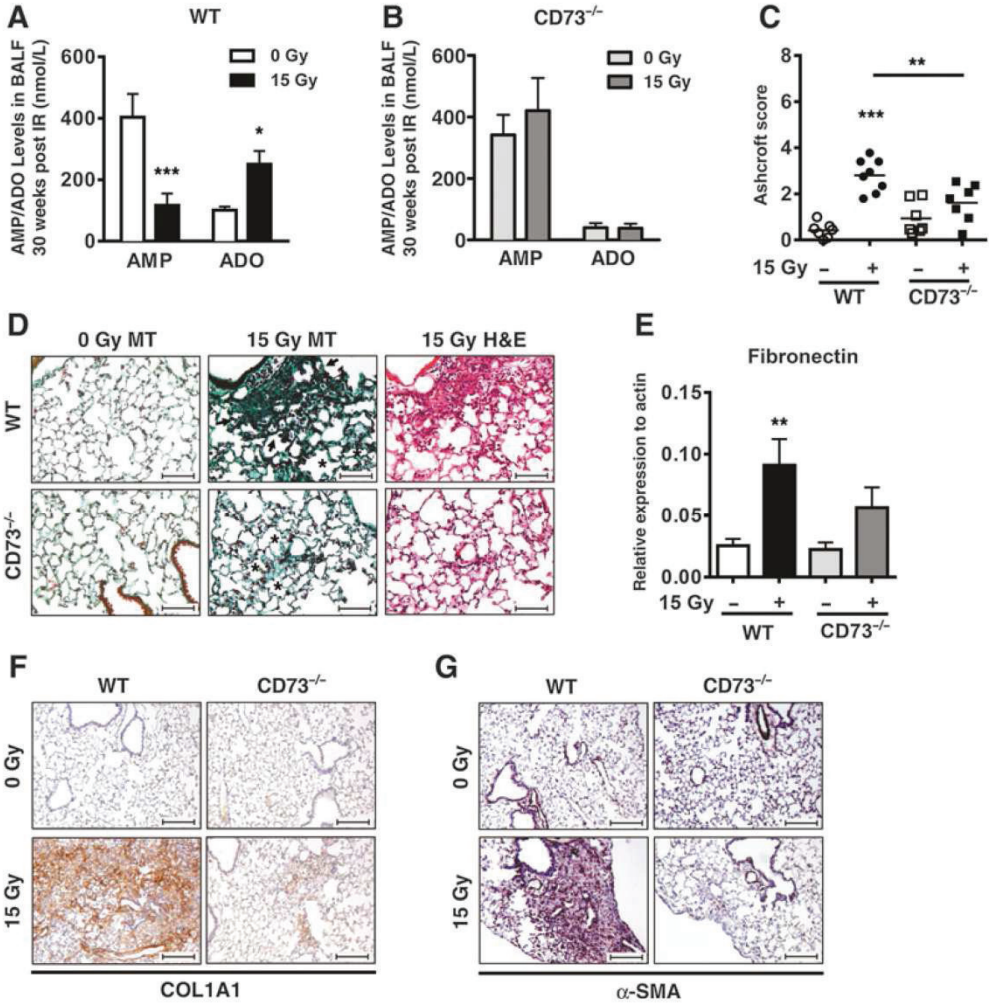

Figure 4.

Genetic deficiency of CD73 prevents radiation-induced accumulation of adenosine and attenuates radiation-induced lung fibrosis. CD73$^{-/-}$ and WT mice received 0 or 15 Gy WTI and were sacrificed at ≥25 weeks postirradiation. Adenosine and AMP levels in BALF for C57BL/6 WT (A) and CD73$^{-/-}$ (B) mice [mean ± SEM, n = 16/9, 23/14 (A); n = 7/4, 8/6 (B)]. C, quantification of fibrosis in WT (n = 7/8) and CD73$^{-/-}$ (n = 7/7) mice by Ashcroft scores; horizontal lines represent mean values. D, MT and H&E-stained lung sections. Asterisks emphasize thickening of alveolar wall structures and arrowheads fibrotic regions (scale bar, 100 μm). E, qPCR analysis of fibronectin expression normalized to actin (n = 9/10/7/8). Immunohistochemical stainings of paraffin-embedded lung sections for collagen type 1 (COL1A1; F) and α-SMA expression (G). Scale bar, 200 μm. Data show means ± SEM. *, $P \leq 0.05$; **, $P \leq 0.01$; ***, $P \leq 0.001$ by two-way ANOVA followed by *post hoc* Bonferroni test (A and B), one-way ANOVA followed by *post hoc* Newman–Keuls test (C and E), or representative pictures (D, F, and G).

treated mice by more than 25% ($P < 0.05$; Fig. 6D and E). These findings suggest that local concentrations of adenosine in the vicinity of relevant adenosine receptors may have been decreased. The above observations demonstrate that therapies aimed at reducing local adenosine concentrations in lung tissue through increasing its catabolism or through targeting CD73 can protect the lung from the adverse effects of thorax irradiation.

Discussion

Here we demonstrate for the first time that CD73-generated adenosine plays a crucial role in the pathogenesis of radiation-induced lung fibrosis, a dose-limiting side effect of thorax irradiation, and show that CD73 and adenosine are new targets for therapeutic intervention. Thoracic irradiation triggered upregulation of CD73 in lung tissue, progressive accumulation of adenosine in the BALF, increased expression of profibrotic mediators such as OPN and TGFβ, and lung fibrosis. CD73$^{-/-}$ mice were protected from early damage to resident lung cells, the progressive increase of BALF adenosine, the accumulation of OPN and TGFβ, and exhibited attenuated lung fibrosis. Importantly, treatment with a CD73 antibody or inhibition of adenosine accumulation with PEG-ADA beginning at 16 weeks postirradiation significantly reduced the severity of radiation-induced fibrosis. We hypothesize that upregulation of CD73 in response to thoracic irradiation leads to a sustained increase in pulmonary adenosine promoting

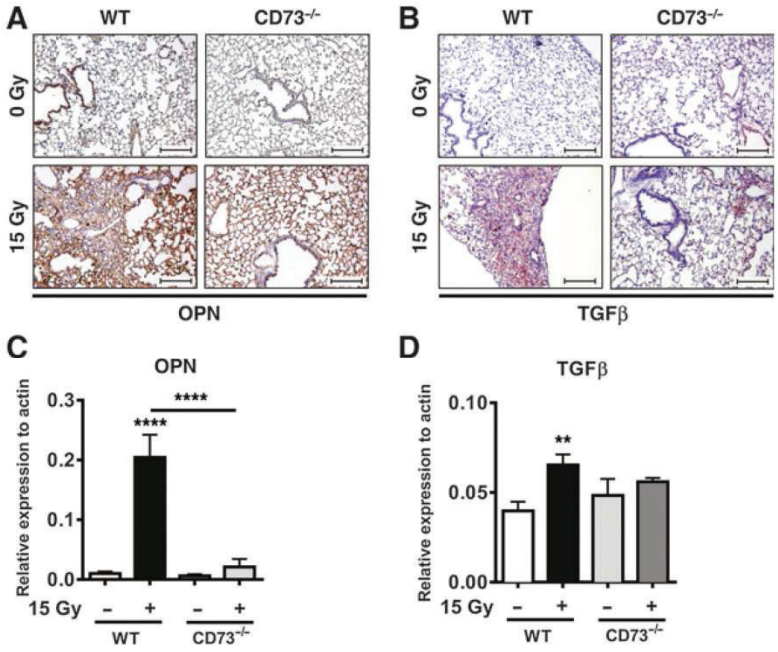

Figure 5.
Genetic deficiency of CD73 prevents radiation-induced accumulation of the profibrotic markers osteopontin and TGFβ. WT and CD73$^{-/-}$ mice received 0 or 15 Gy WTI and were sacrificed at ≥25 weeks post IR. Immunohistochemical staining of paraffin-embedded lung sections for osteopontin (A) or TGFβ expression (B). Scale bar, 200 μm. qPCR analysis for osteopontin (OPN; $n = 7/7, 4/4$; C) and TGFβ ($n = 14/11, 7/8$; D) expression normalized to actin. Shown are means ± SD (CD73$^{-/-}$) or SEM (WT). $^{**}P \leq 0.01$; ****, $P \leq 0.0001$ by one-way ANOVA followed by *post hoc* Newman–Keuls test.

pathologic tissue remodeling and progression of chronic lung inflammation to fibrosis.

Our findings corroborate earlier reports of reduced liver and skin fibrosis in CD73$^{-/-}$ mice induced by CCl_4 and thioacetamide or bleomycin, respectively (33, 34). In contrast, acute bleomycin-induced pulmonary fibrosis was exacerbated in CD73$^{-/-}$ mice (18). Later work revealed that inhibition of the low-affinity ADORA2B attenuates bleomycin-induced pulmonary fibrosis in chronic disease models (19, 35). Thus, the beneficial or disease-promoting effects of adenosine vary depending on the tissue, the type of injury and acute versus chronic disease stages and may be dictated by the local expression of specific adenosine receptors (19, 36, 37).

Lung injury induced by ionizing radiation resulted in delayed acute inflammation after 3 to 6 weeks that developed into chronic inflammation and progressed to fibrosis after 25 to 30 weeks (6, 21). Chronic inflammation was associated with a constant increase in CD73$^+$CD45$^+$ leukocytes in the lung as of 12 weeks and an accumulation of CD73$^+$CD4$^+$ T cells including CD4$^+$ FoxP3$^+$ Tregs, during the fibrotic phase. We therefore postulate that thorax irradiation induces a chronic disease state where the tissue-destructive and profibrotic effects of adenosine prevail so that abrogation of CD73 activity or adenosine accumulation has a net benefit.

Convincing evidence that chronically elevated adenosine causes pulmonary injury and fibrosis comes from studies of ADA-deficient mice; these have markedly elevated adenosine levels and die from respiratory distress caused by lung inflammation and progressive airway remodeling (23, 38). Thus, the increased CD73 activity and pulmonary adenosine levels in irradiated WT mice likely amplify profibrotic signaling. In other published studies, adenosine promoted progression of skin, liver, and peritoneal fibrosis, mainly via the ADORA2A (36, 39), and fibrotic lung disease mainly by activation of the ADORA2B (35, 40).

Interestingly, thorax irradiation triggered upregulation of OPN during the fibrotic phase in WT mice, but not in CD73$^{-/-}$ mice, suggesting that the CD73/adenosine axis is a major inducer of OPN in irradiated lung tissue. OPN is also elevated in alveolar macrophages of ADA-deficient mice by activation of the ADORA2B, suggesting that adenosine and OPN contribute to the pathogenesis of the COPD-like syndrome in these mice (40). OPN is produced by diverse resident and immune cells and is associated with fibroblast -activation, wound healing, inflammation and fibrosis in multiple organs, including lung fibrosis induced by bleomycin (41–43). Importantly, it constitutes a valid serum biomarker of lung fibrosis in idiopathic pulmonary fibrosis patients (30). Therefore, we speculate that radiation-induced accumulation of adenosine may promote fibrosis by amplifying profibrotic signaling through induction of OPN and that OPN may represent a biomarker for adverse late effects after lung irradiation.

OPN$^{-/-}$ mice show reduced expression of profibrotic TGFβ, particularly in macrophages, and reduced TGFβ-dependent fibroblast activation (43). Therefore, the reduced TGFβ levels observed in irradiated CD73$^{-/-}$ mice may result from a missing adenosine/OPN-amplification loop. However, TGFβ levels were not altered in OPN$^{-/-}$ ADA$^{-/-}$ mice, suggesting that high adenosine levels are sufficient to induce TGFβ expression (40). Tregs may also contribute to TGFβ accumulation under pathologic conditions (44). As TGFβ induces Tregs and CD73 expression (45), the accumulation of CD73$^+$CD4$^+$FoxP3$^+$ Tregs in fibrotic lungs of irradiated mice could be caused by pathologic adenosine accumulation, high TGFβ levels, or both, and subsequently contribute to additional TGFβ secretion and CD73-dependent adenosine generation (14, 44). We therefore hypothesize that adenosine-induced accumulation of TGFβ and Tregs provides a feed-forward

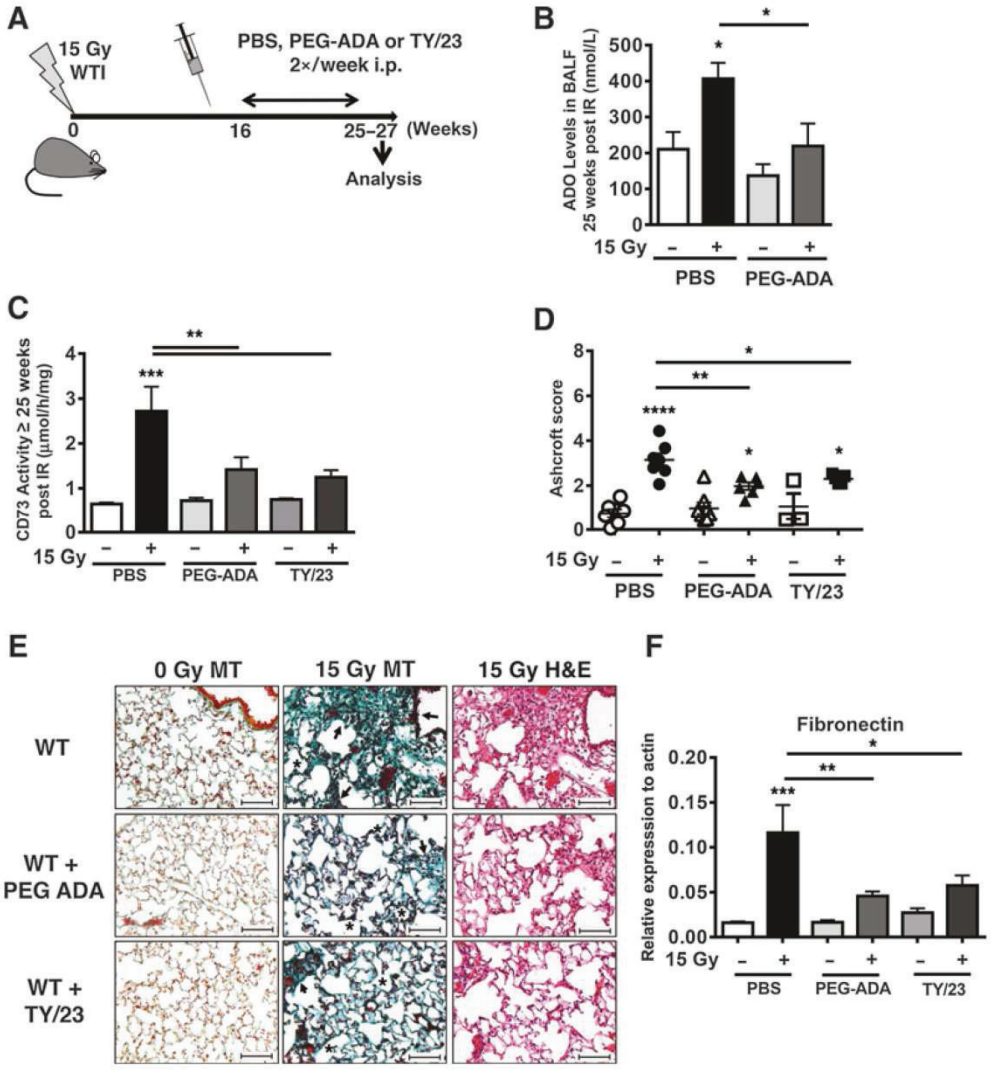

Figure 6.

PEG-ADA or mAb TY/23 reduce radiation-induced lung fibrosis. C57BL/6 mice irradiated with 0 or 15 Gy WTI were treated with PBS, PEG-ADA (5 units), or mAb TY/23 (100 μg) twice weekly i.p. beginning at week 16. A, schematic depiction of the experimental setup. B, adenosine levels (nmol/L) in BALF from WT mice at 25 weeks postirradiation ± treatment with PEG-ADA ($n = 6/6, 5/6$). C, CD73 enzyme activity in lungs of WT mice ≥ 25 weeks postirradiation ± treatment with PEG-ADA or TY/23 ($n = 9/9, 8/9, 3/6$). IR, irradiation. D, Ashcroft scores of WT mice ± PEG-ADA or TY/23 at 25 weeks postirradiation ($n = 7/7, 7/6, 3/5$). Horizontal lines represent means. E, MT or H&E–stained lung sections from WT mice with PBS, PEG-ADA, or TY/23 treatment at ≥ 25 weeks postirradiation. Asterisks emphasize thickening of alveolar wall structures and arrowheads fibrotic regions (scale bar, 100 μm). F, qPCR analysis of fibronectin expression normalized to actin ($n = 8/9, 7/9, 3/6$) at ≥ 25 weeks postirradiation (mean ± SEM, B–D and F). *, $P \leq 0.05$; **, $P \leq 0.01$; ***, $P \leq 0.001$; ****, $P \leq 0.0001$ by one-way ANOVA followed by *post hoc* Newman–Keuls test (B, C, D, and F).

mechanism for progressive accumulation of adenosine and TGFβ. Consistent with this concept, preliminary data indicate that irradiated $CD73^{-/-}$ mice do not accumulate Tregs during the fibrotic phase (unpublished observations).

As ADA-deficient mice can be rescued by enzyme replacement therapy with PEG-ADA to decrease tissue adenosine levels (38), we tried PEG-ADA as well as targeting CD73 with mAb TY/23 to treat irradiated mice. Both treatments significantly reduced radiation-induced lung fibrosis. Although TY/23 did not decrease adenosine accumulation in the BALF as much as PEG-ADA, it was nearly as effective in reducing radiation-induced lung fibrosis. TY/23 may impact local adenosine receptor signaling, yet not cause a measurable decrease in BALF adenosine levels. It is not surprising that PEG-ADA is more effective at reducing BALF adenosine levels, as it should degrade all extracellular adenosine including that generated by CD73-independent mechanisms such as release from cells damaged during lavage.

Surprisingly, CD73 loss also reduced the damaging effects of thorax irradiation on resident lung cells and the blood–air barrier at 3 weeks, a time when increased numbers of $CD73^{+}CD45^{-}$ resident cells and $CD73^{+}CD45^{+}CD4^{+}$ T cells are observed in WT mice. As the magnitude of radiation-induced early damage to resident lung cells correlates with adverse late effects (2, 4), these

findings suggest that $CD73^{-/-}$ mice are protected from lung fibrosis in part due to attenuation of CD73-dependent early damage to resident cells. We therefore postulate that the benefit of radiotherapy may be further improved when CD73 inhibition is initiated at earlier time points.

Despite the obvious benefits of CD73 deficiency after WTI, targeting of CD73 or adenosine with TY/23 or PEG-ADA did not provide complete protection. The beneficial effects of adenosine in other models of lung inflammation and fibrosis make it highly likely that therapeutic inhibition of CD73 may blunt protective effects of CD73-dependent adenosine signaling that limit radiation-induced tissue damage and the resulting inflammation particularly during acute disease stages. For example, ADORA2A signaling via CD73-generated adenosine may suppress inflammatory functions of the innate and adaptive immune systems, modulate angiogenesis and matrix-induced proinflammatory and profibrotic signaling, and induce Tregs, which are known to contribute to adenosine-mediated resolution of acute lung injury (17, 46). Intriguingly, we observed pulmonary accumulation of $CD73^{+}CD4^{+}FoxP3^{+}$ Tregs during the pneumonitic and fibrotic phases upon WTI. However, the specific roles played by Tregs, additional CD73-expressing immune cells, resident endothelial and epithelial cells or fibroblasts and specific adenosine receptors in radiation-induced fibrosis remain to be explored.

Certainly, the tissue-, injury- and disease stage–dependent beneficial or adverse effects of adenosine demand further investigation to define the optimal therapeutic target and treatment schedule. Moreover, any pharmacologic strategies targeting the CD73/adenosine pathway for protection against radiation-induced fibrosis will require careful testing as they may bring complications such as excessive inflammation or autoimmunity by abrogating protective signals mediated by various adenosine receptors, particularly during acute disease stages (47–50). Nevertheless, therapeutic inhibition of CD73 activity or adenosine accumulation provided a significant protection of mice against radiation-induced lung fibrosis offering new opportunities for therapeutic intervention.

In tumor-bearing mice, CD73 and adenosine promote tumor immune escape (51, 52). Intriguingly, radio(chemo)therapy triggers upregulation of CD73 and CD39 in circulating immune cells of cancer patients and may thereby dampen antitumor immune responses (53). It is therefore likely that pharmacologic modulation of the CD73/adenosine pathway may provide a clear therapeutic gain in cancer treatment through multiple mechanisms including immune enhancement (10, 32) and protection of normal tissues against the adverse effects of radio(chemo)therapy by abrogating profibrotic adenosine signals.

Multiple approaches for pharmacologic modulation of adenosine levels exist and some (TY/23, APCP, PEG-ADA) have already been used successfully in preclinical models (17, 32, 54) and PEG-ADA has been given to ADA-deficient patients for decades. Thus, there is every reason for optimism that targeting the CD73/adenosine pathway offers new strategies to limit lung toxicity during therapeutic whole-body or thorax irradiation.

Disclosure of Potential Conflicts of Interest

No potential conflicts of interest were disclosed.

Authors' Contributions

Conception and design: F. Wirsdörfer, T. Eldh, V. Jendrossek
Development of methodology: F. Wirsdörfer, S. de Leve, F. Cappuccini, T. Eldh, M. Kasper, V. Jendrossek
Acquisition of data (provided animals, acquired and managed patients, provided facilities, etc.): F. Wirsdörfer, S. de Leve, F. Cappuccini, T. Eldh, A.V. Meyer, E. Gau, L.F. Thompson, H. Karmouty-Quintana, U. Fischer, D. Klein, J.W. Ritchey, A.M. Westendorf, M. Stuschke, V. Jendrossek
Analysis and interpretation of data (e.g., statistical analysis, biostatistics, computational analysis): F. Wirsdörfer, S. de Leve, F. Cappuccini, T. Eldh, E. Gau, L.F. Thompson, H. Karmouty-Quintana, M. Kasper, D. Klein, J.W. Ritchey, M.R. Blackburn, V. Jendrossek
Writing, review, and/or revision of the manuscript: F. Wirsdörfer, S. de Leve, F. Cappuccini, A.V. Meyer, L.F. Thompson, H. Karmouty-Quintana, U. Fischer, M. Kasper, J.W. Ritchey, M. Stuschke, V. Jendrossek
Administrative, technical, or material support (i.e., reporting or organizing data, constructing databases): A.V. Meyer, E. Gau, N.-Y. Chen, U. Fischer, D. Klein, J.W. Ritchey, M.R. Blackburn,
Study supervision: V. Jendrossek
Other (performed the ecto-5′-nucleotidase enzyme assays): L.F. Thompson
Other (pathology support): J.W. Ritchey,

Acknowledgments

The authors thank Gabriele von Kürthy, Michael Groneberg, Fayong Luo, and Stephanie McGee for excellent technical support.

Grant Support

This work was supported by grants of the Doctoral Programs of the Deutsche Forschungsgemeinschaft (DFG) grant numbers GRK1739/1 and JE275/4-1 (V. Jendrossek), the Bundesministerium für Bildung und Forschung (BMBF) grant number 02NUK024D (V. Jendrossek), and the NIH grant AI18220 (L.F. Thompson).

The costs of publication of this article were defrayed in part by the payment of page charges. This article must therefore be hereby marked *advertisement* in accordance with 18 U.S.C. Section 1734 solely to indicate this fact.

Received August 25, 2015; revised February 19, 2016; accepted February 21, 2016; published OnlineFirst February 26, 2016.

References

1. Ding NH, Li JJ, Sun LQ. Molecular mechanisms and treatment of radiation-induced lung fibrosis. Curr Drug Targets 2013;14:1347–56.
2. Graves PR, Siddiqui F, Anscher MS, Movsas B. Radiation pulmonary toxicity: from mechanisms to management. Semin Radiat Oncol 2010; 20:201–7.
3. Kelsey CR, Horwitz ME, Chino JP, Craciunescu O, Steffey B, Folz RJ, et al. Severe pulmonary toxicity after myeloablative conditioning using total body irradiation: an assessment of risk factors. Int J Radiat Oncol Biol Phy 2011;81:812–8.
4. Kasper M, Haroske G. Alterations in the alveolar epithelium after injury leading to pulmonary fibrosis. Histol Histopathol 1996;11: 463–83.
5. Tsoutsou PG, Koukourakis MI. Radiation pneumonitis and fibrosis: mechanisms underlying its pathogenesis and implications for future research. Int J Radiat Oncol Biol Phy 2006;66:1281–93.
6. Heinzelmann F, Jendrossek V, Lauber K, Nowak K, Eldh T, Boras R, et al. Irradiation-induced pneumonitis mediated by the CD95/CD95-ligand system. J Natl Cancer Inst 2006;98:1248–51.

7. Koukourakis MI. Radiation damage and radioprotectants: new concepts in the era of molecular medicine. Br J Radiol 2012;85:313–30.
8. Bentzen SM. Preventing or reducing late side effects of radiation therapy: radiobiology meets molecular pathology. Nature Rev Cancer 2006;6: 702–13.
9. Eltzschig HK, Sitkovsky MV, Robson SC. Purinergic signaling during inflammation. N Engl J Med 2012;367:2322–33.
10. Antonioli L, Blandizzi C, Pacher P, Hasko G. Immunity, inflammation and cancer: a leading role for adenosine. Nature Rev Cancer 2013;13:842–57.
11. Linden J. Regulation of leukocyte function by adenosine receptors. Adv Pharmacol 2011;61:95–114.
12. Thompson LF, Eltzschig HK, Ibla JC, Van De Wiele CJ, Resta R, Morote-Garcia JC, et al. Crucial role for ecto-5′-nucleotidase (CD73) in vascular leakage during hypoxia. J Exp Med 2004;200:1395–405.
13. Thompson LF, Takedachi M, Ebisuno Y, Tanaka T, Miyasaka M, Mills JH, et al. Regulation of leukocyte migration across endothelial barriers by ECTO-5′-nucleotidase-generated adenosine. Nucleosides, Nucleotides Nucleic Acids 2008;27:755–60.
14. Deaglio S, Dwyer KM, Gao W, Friedman D, Usheva A, Erat A, et al. Adenosine generation catalyzed by CD39 and CD73 expressed on regulatory T cells mediates immune suppression. J Exp Med 2007;204: 1257–65.
15. Kaku H, Cheng KF, Al-Abed Y, Rothstein TL. A novel mechanism of B cell-mediated immune suppression through CD73 expression and adenosine production. J Immunol 2014;193:5904–13.
16. Mikhailov A, Sokolovskaya A, Yegutkin GG, Amdahl H, West A, Yagita H, et al. CD73 participates in cellular multiresistance program and protects against TRAIL-induced apoptosis. J Immunol 2008;181:464–75.
17. Hasko G, Linden J, Cronstein B, Pacher P. Adenosine receptors: therapeutic aspects for inflammatory and immune diseases. Nature Rev Drug Discov 2008;7:759–70.
18. Volmer JB, Thompson LF, Blackburn MR. Ecto-5′-nucleotidase (CD73)-mediated adenosine production is tissue protective in a model of bleomycin-induced lung injury. J Immunol 2006;176:4449–58.
19. Zhou Y, Schneider DJ, Morschl E, Song L, Pedroza M, Karmouty-Quintana H, et al. Distinct roles for the A2B adenosine receptor in acute and chronic stages of bleomycin-induced lung injury. J Immunol 2011;186:1097–106.
20. Chunn JL, Molina JG, Mi T, Xia Y, Kellems RE, Blackburn MR. Adenosine-dependent pulmonary fibrosis in adenosine deaminase-deficient mice. J Immunol 2005;175:1937–46.
21. Eldh T, Heinzelmann F, Velalakan A, Budach W, Belka C, Jendrossek V. Radiation-induced changes in breathing frequency and lung histology of C57BL/6J mice are time- and dose-dependent. Strahlenther Onkol 2012;188:274–81.
22. Wirsdorfer F, Cappuccini F, Niazman M, de Leve S, Westendorf AM, Ludemann L, et al. Thorax irradiation triggers a local and systemic accumulation of immunosuppressive CD4+ FoxP3+ regulatory T cells. Radiat Oncol 2014;9:98.
23. Blackburn MR, Aldrich M, Volmer JB, Chen W, Zhong H, Kelly S, et al. The use of enzyme therapy to regulate the metabolic and phenotypic consequences of adenosine deaminase deficiency in mice. Differential impact on pulmonary and immunologic abnormalities. J Biol Chem 2000; 275:32114–21.
24. Yamashita Y, Hooker SW, Jiang H, Laurent AB, Resta R, Khare K, et al. CD73 expression and fyn-dependent signaling on murine lymphocytes. Eur J Immunol 1998;28:2981–90.
25. Thompson LF, Boss GR, Spiegelberg HL, Jansen IV, O'Connor RD, Waldmann TA, et al. Ecto-5′-nucleotidase activity in T and B lymphocytes from normal subjects and patients with congenital X-linked agammaglobulinemia. J Immunol 1979;123:2475–8.
26. Cappuccini F, Eldh T, Bruder D, Gereke M, Jastrow H, Schulze-Osthoff K, et al. New insights into the molecular pathology of radiation-induced pneumopathy. Radiother oncol 2011;101:86–92.
27. Wakamiya M, Blackburn MR, Jurecic R, McArthur MJ, Geske RS, Cartwright JJr, et al. Disruption of the adenosine deaminase gene causes hepatocellular impairment and perinatal lethality in mice. Proc Natl Acad Sci U S A 1995;92:3673–7.
28. Ashcroft T, Simpson JM, Timbrell V. Simple method of estimating severity of pulmonary fibrosis on a numerical scale. J Clin Pathol 1988;41:467–70.
29. Silber R, Conklyn M, Grusky G, Zucker-Franklin D. Human lymphocytes: 5′-nucleotidase-positive and -negative subpopulations. J Clin Invest 1975;56:1324–7.
30. Pardo A, Gibson K, Cisneros J, Richards TJ, Yang Y, Becerril C, et al. Up-regulation and profibrotic role of osteopontin in human idiopathic pulmonary fibrosis. PLoS Med 2005;2:e251.
31. Khalil N, O'Connor RN, Unruh HW, Warren PW, Flanders KC, Kemp A, et al. Increased production and immunohistochemical localization of transforming growth factor-beta in idiopathic pulmonary fibrosis. Am J Respir Cell Mol Biol 1991;5:155–62.
32. Wang L, Fan J, Thompson LF, Zhang Y, Shin T, Curiel TJ, et al. CD73 has distinct roles in nonhematopoietic and hematopoietic cells to promote tumor growth in mice. J Clin Invest 2011;121:2371–82.
33. Peng Z, Fernandez P, Wilder T, Yee H, Chiriboga L, Chan ES, et al. Ecto-5′-nucleotidase (CD73)-mediated extracellular adenosine production plays a critical role in hepatic fibrosis. FASEB J 2008;22:2263–72.
34. Fernandez P, Perez-Aso M, Smith G, Wilder T, Trzaska S, Chiriboga L, et al. Extracellular generation of adenosine by the ectonucleotidases CD39 and CD73 promotes dermal fibrosis. Am J Pathol 2013; 183:1740–6.
35. Karmouty-Quintana H, Zhong H, Acero L, Weng T, Melicoff E, West JD, et al. The A2B adenosine receptor modulates pulmonary hypertension associated with interstitial lung disease. FASEB J 2012;26: 2546–57.
36. Cronstein BN. Adenosine receptors and fibrosis: a translational review. F1000 Biol Rep 2011;3:21.
37. Roberts VS, Cowan PJ, Alexander SI, Robson SC, Dwyer KM. The role of adenosine receptors A2A and A2B signaling in renal fibrosis. Kidney int 2014;86:685–92.
38. Chunn JL, Mohsenin A, Young HW, Lee CG, Elias JA, Kellems RE, et al. Partially adenosine deaminase-deficient mice develop pulmonary fibrosis in association with adenosine elevations. Am J Physiol Lung Cell Mol Physiol 2006;290:L579–87.
39. Burnstock G, Vaughn B, Robson SC. Purinergic signalling in the liver in health and disease. Purinergic Signal 2014;10:51–70.
40. Schneider DJ, Lindsay JC, Zhou Y, Molina JG, Blackburn MR. Adenosine and osteopontin contribute to the development of chronic obstructive pulmonary disease. FASEB J 2010;24:70–80.
41. Takahashi F, Takahashi K, Okazaki T, Maeda K, Ienaga H, Maeda M, et al. Role of osteopontin in the pathogenesis of bleomycin-induced pulmonary fibrosis. Am J Respira Cell Mol Biol 2001;24:264–71.
42. Berman JS, Serlin D, Li X, Whitley G, Hayes J, Rishikof DC, et al. Altered bleomycin-induced lung fibrosis in osteopontin-deficient mice. Am J Physiol Lung cell Mol Physiol 2004;286:L1311–8.
43. Wu M, Schneider DJ, Mayes MD, Assassi S, Arnett FC, Tan FK, et al. Osteopontin in systemic sclerosis and its role in dermal fibrosis. J Invest Dermatol 2012;132:1605–14.
44. Wan YY, Flavell RA. Yin-Yang' functions of transforming growth factor-beta and T regulatory cells in immune regulation. Immunol Rev 2007;220:199–213.
45. Regateiro FS, Howie D, Nolan KF, Agorogiannis EI, Greaves DR, Cobbold SP, et al. Generation of anti-inflammatory adenosine by leukocytes is regulated by TGF-beta. Eur J Immunol 2011;41:2955–65.
46. Chan ES, Cronstein BN. Adenosine in fibrosis. Mod Rheumatol 2010; 20:114–22.
47. Sun CX, Young HW, Molina JG, Volmer JB, Schnermann J, Blackburn MR. A protective role for the A1 adenosine receptor in adenosine-dependent pulmonary injury. J Clin Invest 2005;115:35–43.
48. Eckle T, Grenz A, Laucher S, Eltzschig HK. A2B adenosine receptor signaling attenuates acute lung injury by enhancing alveolar fluid clearance in mice. J Clin Invest 2008;118:3301–15.
49. Ehrentraut H, Clambey ET, McNamee EN, Brodsky KS, Ehrentraut SF, Poth JM, et al. CD73+ regulatory T cells contribute to adenosine-mediated resolution of acute lung injury. FASEB J 2013;27:2207–19.
50. Morschl E, Molina JG, Volmer JB, Mohsenin A, Pero RS, Hong JS, et al. A3 adenosine receptor signaling influences pulmonary inflammation and fibrosis. Am J Respir Cell Mol Biol 2008;39:697–705.
51. Sitkovsky MV. T regulatory cells: hypoxia-adenosinergic suppression and re-direction of the immune response. Trends Immunol 2009;30: 102–8.

52. Stagg J, Divisekera U, Duret H, Sparwasser T, Teng MW, Darcy PK, et al. CD73-deficient mice have increased antitumor immunity and are resistant to experimental metastasis. Cancer Res 2011;71:2892–900.
53. Mandapathil M, Szczepanski MJ, Szajnik M, Ren J, Lenzner DE, Jackson EK, et al. Increased ectonucleotidase expression and activity in regulatory T cells of patients with head and neck cancer. Clin Cancer Res 2009;15:6348–57.
54. Stagg J, Divisekera U, McLaughlin N, Sharkey J, Pommey S, Denoyer D, et al. Anti-CD73 antibody therapy inhibits breast tumor growth and metastasis. Proc Natl Acad Sci U S A 2010;107:1547–52.
55. Vermaelen K, Pauwels R. Accurate and simple discrimination of mouse pulmonary dendritic cell and macrophage populations by flow cytometry: methodology and new insights. Cytometry A 2004; 61:170–77.

3.4 Loss of CD73 prevents accumulation of alternatively activated macrophages and the formation of pre-fibrotic macrophage clusters in irradiated lungs

Contribution to present publication:

- Writing and critical reviewing of the whole manuscript, literature research
- Data collection for flow cytometry (together with Wirsdörfer)
    - Isolation of lung
    - Isolation of immune cells lung (tissue digestion, filtration steps, erythrocyte lysis)
    - Staining of isolated immune cells for flow cytometric analysis: surface staining as well as intracellular staining
    - Measurement of stained immune cells
    - Data analysis (of the data, Fig. 1, 2, 3, 5); established new gating strategy for alveolar macrophages for these measurements (Fig. 1A)
- Isolation of lung tissue for histological analysis (WT samples except for 24 weeks after IR, with Wirsdörfer)
    - IHC stainings and evaluations, Fig. 4A+B, 6A
    - IF staining Fig. 4B
- RNA isolation and QPCR analyses
    - Isolation of RNA from all tissue samples
    - primer design and optimization for QPCR
    - Performed QPCR for iNOS, ARG1 and IL-10Rα, Fig. 4D, 5D

The above listed contributions of Simone de Leve to the publication are correct.

Essen, den _____ _____

Unterschrift der Doktorandin

Essen, den _____ _____

Unterschrift des wissenschaftl. Betreuers/
Mitglieds der Universität Duisburg-Essen

Loss of CD73 prevents accumulation of alternatively activated macrophages and the formation of pre-fibrotic macrophage clusters in irradiated lungs

Simone de Leve[1*], Florian Wirsdörfer[1*], Federica Cappuccini[1], Alexandra Schütze[2], Alina V. Meyer[1], Katharina Röck[2], Linda F. Thompson[3], Jens W. Fischer[2], Martin Stuschke[4], Verena Jendrossek[1]

[1]Institute of Cell Biology (Cancer Research), University Hospital Essen, Essen, Germany; [2]Pharmacology and Clinical Pharmacology, University Hospital, Heinrich-Heine-University, Düsseldorf, Germany; [3]Immunobiology and Cancer Program, Oklahoma Medical Research Foundation, 825 N.E. 13th Street, Oklahoma City, Oklahoma, USA; [4]Department of Radiation Oncology, University Hospital Essen, Hufelandstrasse 55, Essen, Germany

* equal contribution

Correspondence: Verena Jendrossek, Institute of Cell Biology (Cancer Research), University Hospital Essen, Virchowstrasse 173, 45122 Essen, Germany; Phone: +49-201-7233380; Fax: +49-201-7235904; E-mail: verena.jendrossek@uni-due.de.

Total word count: 3990

Total number of figures: 6

Key words: radiation-induced lung fibrosis, alternative activated macrophages, thorax irradiation, pneumonitis, CD73, adenosine

Conflict of interest notification:

No conflict of interest does exist for any of the authors.

Abstract

Alternatively activated macrophages play a pathogenic role in idiopathic pulmonary fibrosis but their contribution to radiation-induced lung fibrosis remains elusive. We aimed to define alterations in the numbers and phenotypes of total and alveolar macrophages (AM) upon whole thorax irradiation (WTI) and to explore a potential role of radiation-induced environmental lung changes for driving AM polarization in a murine model with a focus on CD73 and adenosine. For this, wild type C57BL/6 (WT) mice and CD73 knockout mice ($CD73^{-/-}$) received a single dose whole thorax irradiation (15 Gray). Lung tissue was collected at defined time points post-irradiation for isolation and phenotyping of myeloid cells (monocytes/macrophages) and complementary histological, immunohistochemical and RNA analyses. We observed a dramatic loss of AM at 3 weeks post-irradiation in WT and $CD73^{-/-}$ mice. Myeloid cells repopulated the lung tissue of WT mice within 6 weeks after irradiation, whereas $CD73^{-/-}$ mice showed a trend to delayed macrophage repopulation. Total macrophages and AM displayed increased surface-expression of pro-inflammatory markers such as MHCII throughout the observation period in both strains but particularly in $CD73^{-/-}$ mice. In contrast, we detected a significant up-regulation of the anti-inflammatory macrophage mannose receptor 1 (MMR) during the fibrotic stage only on AM of WT mice. Interestingly, the development of radiation-induced pulmonary fibrosis in WT mice was accompanied by the accumulation of macrophages within organized clusters expressing pro-fibrotic marker proteins such as transforming growth factor beta (TGFβ), alpha-smooth muscle actin (α-SMA) and arginase-1 (ARG1). In contrast reduced fibrosis development in $CD73^{-/-}$ mice was associated with a failure to develop clusters of alternatively activated macrophages. We speculate that accumulation of alternatively activated macrophages in organized clusters represents the origin of fibrotic foci in the irradiated lung and is driven by the

cross-talk of chronic accumulation of adenosine, the hyaluronic acid system and potentially TGFβ.

Introduction

Radiation is a major treatment option for cancer patients. However, the normal lung tissue is highly sensitive to radiation-induced damage and has only little repair capacity. As a consequence, radiation-induced pneumonitis and pulmonary fibrosis may develop in patients upon thoracic or total body irradiation (TBI), thereby reducing survival rates and quality of life [1, 2]. So far no effective treatment is available for clinical use, so that these dose-limiting side effects are still a major barrier to successful radiotherapy of thorax-associated neoplasms [3, 4].

Deregulated cytokine production without or with aseptic lung inflammation is a frequent pathologic finding in patients after thoracic irradiation or TBI [4, 5] and is observed in murine models [4, 6-10]. In own investigations, the time-dependent recruitment of immune cells to the lung tissue after hemithorax irradiation of C57BL/6 mice with 15 Gray (Gy) was associated with a significant increase in the levels of various monocyte/macrophage associated cytokines and chemokines, for example macrophage-colony stimulating factor (M-CSF), macrophage chemoattractant protein-1 (MCP-1; CCL-2), macrophage inflammatory proteins (MIP)-1β and MIP-2 in the bronchoalveolar lavage fluid (BALF) of irradiated mice compared to sham controls [11].

M-CSF and MCP-1 promote the influx, proliferation or differentiation of monocytes/macrophages and have been associated with increased macrophage accumulation, production of connective tissue growth factor (CTGF) and fibrosis in bleomycin-induced lung fibrosis [12]. A pathogenic role of macrophages has also been postulated for idiopathic pulmonary fibrosis (IPF) [13, 14]. The influx of myeloid

cells has also been observed in murine models of radiation-induced pneumopathy during both, the pneumonitic phase and the fibrotic phase [15-17]. Importantly, several reports including our own studies suggested a potential role of foamy macrophages or alternatively activated macrophages in radiation-induced adverse late effects though the responses may depend on the mouse strain [11, 16, 18-20].

Generally, mononuclear phagocytes participate in orchestrating innate and adaptive immune responses and thereby play essential roles in inflammation and host defense against infections. But they also exert homeostatic functions in diverse tissues, coordinate tissue remodeling in injured tissues or within the tumor environment, and even impact host metabolism [21, 22]. Their high plasticity allows macrophages to adapt quickly to various environmental signals such as those from lymphocyte subsets or danger signals in injured tissues [23]. Macrophages have initially been classified into classically activated (M1) and alternatively activated (M2) populations executing predominantly pro-inflammatory or anti-inflammatory actions, respectively [24]. However, it is now clear that macrophages can adopt various phenotypes as a continuum in between the M1/M2 extremes, including mixed M1/M2 phenotypes under pathological conditions [25], and that the various phenotypes have tissue- and context-dependent functions [26, 27].

We recently showed that activation of ecto-5′-nucleotidase (NT5E, CD73) and chronic accumulation of adenosine participate in radiation-induced lung fibrosis and that genetic deficiency or pharmacologic inhibition of CD73/adenosine signaling reduces extracellular adenosine thereby significantly decreasing radiation-induced fibrosis in mice [17]. CD73 and adenosine play critical roles in balancing tissue inflammation and repair processes regulating, amongst others, leukocyte extravasation and function [28-32]. But depending on the disease model (acute or chronic) extracellular accumulation of adenosine has either tissue protective or

adverse effects in pulmonary fibrosis [17, 33-35].

Fibrosis is characterized by excessive deposition of extracellular matrix (ECM) molecules [36]. These include mainly collagens and fibronectin but the glycosaminoglycan hyaluronan (hyaluronic acid, HA) can also participates in the regulation of chronic lung inflammation and fibrosis, at least in the preclinical bleomycin model [37-39]. Cell stress triggers the fragmentation of high molecular weight (HMW) HA to low molecular weight (LMW) HA and interactions between LMW HA and macrophages [38, 40, 41], as well as between the HA system and adenosine signaling through two (ADORA2A, ADORA2B) of its four receptors are well documented [39, 42]. Our own previous work revealed that HA accumulates in murine lungs during the fibrotic phase [43]. However, not much is known about the regulation of macrophage phenotype and functions in the changing environment of irradiated lungs and their impact on the development of radiation-induced lung fibrosis. Here, we aimed to gain further insight into radiation-induced immune changes in the lung tissue. In particular, we aimed to characterize radiation-induced changes in macrophage recruitment, differentiation and function, and to define their role for fibrosis development in a murine model with a focus on suspected regulatory molecules identified in our previous work such as adenosine as well as HA.

Materials and Methods

Mice

C57BL/6 wild-type (WT; $CD73^{+/+}$; Harlan) and $CD73^{-/-}$ mice (C57BL/6 background) [29] were bred and housed under specific pathogen-free conditions in the Laboratory Animal Facilities of the University Hospital Essen. Food and drinking water were provided ad libitum. The animal facility and all protocols were approved by the Universities Animal Protection Boards in conjunction with the Landesamt für Natur, Umwelt und Verbraucherschutz Nordrhein-Westfalen (LANUV) according to the German animal welfare regulations (AZ.8.87-51.04.20.09.333, AZ.84-02.04.2011.A407).

Irradiation

Mice (8-12 weeks) were anesthetized with 3% isoflurane and irradiated in 0.8% isoflurane with either a single dose of 0 Gy (sham control) or with 15 Gy over their whole thorax (WTI) using a Cobalt-60 source (Philips, Hamburg, Germany) [44]. Mice were sacrificed at 3, 6, 12, 24, or 25-30 weeks post-irradiation and lung tissue was collected.

Lung leukocyte phenotyping

Total lung cells were isolated as described previously [44]. Isolated cells were stained with anti-mouse CD45 PacificBlue (30-F11) for total leukocytes. Within lung leukocytes, myeloid cells were defined with anti-CD11b PerCP-Cy5.5 (M1/70), macrophages were defined with anti-F4/80 PE-Cy7 (BM8), and AMs were defined with anti-CD11c BV (N418) and increased FL-1 autofluorescence as recently published [45]. Populations were further characterized with anti-MHCII APC (M5/114.15.2) and anti-MMR PE (C068C2). Antibodies were obtained from BD

Biosciences (Heidelberg, Germany), BioLegend (Fell, Germany) or eBioscience (Frankfurt, Germany). Data acquisition and analysis were performed on a LSRII using FACS DIVA (BD Bioscience, USA) and FlowJo (Tree Star, Ashland, USA).

RNA isolation

Tissue RNA: Fresh frozen lung tissue was pulverized, lysed in RLT buffer (Qiagen, Hilden, Germany) and sonicated with an Ultraturrax IKA T10 (IKA, Staufen, Germany) for 30 seconds. RNA was further isolated using the homogenizer QIAshredder and RNeasy Mini Kits (Qiagen) according to the manufacturer's instructions.

Quantitative real-time PCR (QPCR)

RNA was reversely transcribed with the QuantiTect Reverse Transcription Kit (Qiagen). QPCR expression levels were normalized to the reference gene (β-actin; set as 1). Quantitative real-time PCR was carried out using specific oligonucleotide primers (β-Actin (*Actb*): fw, CCAGAGCAAGAGAGGTATCC; rev, CTGTGGTGGTGAAGCTGTAG; iNOS (*Nos2*): fw, AGCTCCTCCCAGGACCACAC; rev, ACGCTGAGTACCTCATTGGC; ARG1 (*Arg1*): fw, GTGAAGAACCCACGGTCTGT; rev, CTCGCAAGCCAATGTACACG; IL-10Rα (*Il10ra*): fw, AGGCAGAGGCAGCAGGCCCAGCAGAATG; rev, TGGAGCCTGGCTAGCTGGTCACAGTAGG; Has3 (*Has3*): fw, GATGTCCAAATCCTCAACAAG; rev, CCCACTAATACATTGCACAC; CD44 (*Cd44*): fw, AGGATGACTCCTTCTTTATCCG; rev, CTTGAGTGTCCAGCTAATTCG; RHAMM (*Hmmr*): fw, GAATATGAGAGCTCTAAGCCTG; rev

CCATCATACTCCTCATCTTTGTC, using QPCR MasterMix for SYBR® Assay ROX (Eurogentec, Cologne, Germany) according to the manufacturer's instructions.

Histopathology

Paraffin embedded tissue: Lungs were perfused (with PBS) and then fixed overnight with 4% (wt/vol) paraformaldehyde in PBS (pH 7.2). Upon dehydration, lungs were embedded in paraffin and sectioned into 5 µm slices.

Immunohistochemistry:

iNOS *(NOS2),* **ARG1** *(ARG1)* ***TGF-β*** *(TGFB1),* ***α-SMA*** *(ACTA2)**:*** Immunohistochemical (IHC) staining of paraffin-embedded lung tissue slides was performed using the Mouse on Mouse (M.O.M.™) ImmPRESS™ HRP (horseradish peroxidase) Polymer Kit (Vector Laboratories, Burlingame, USA) according to the manufacturer's instructions. Anti-inducible nitric oxid synthase (iNOS) (BD Biosciences, Heidelberg, Germany), anti-ARG1 (Santa Cruz Biotechnology, Heidelberg, Germany), anti-TGFβ (R&D Systems, Wiesbaden, Germany) and anti-α-SMA (Merck Millipore, Darmstadt, Germany) were used as mouse primary antibodies. The ImmPACT™ VIP Peroxidase (HRP) Substrate Kit (Vector Laboratories) was used to detect TGFβ and α-SMA according to the manufacturer's instructions. Stained sections were counterstained with hematoxylin.

Mac-3 (LAMP2)**:** Tissue slides were deparaffinised, rehydrated and steam boiled in citrate buffer pH 6. After blocking endogenous peroxidase with 3% H_2O_2, sections were blocked for 20 min with 2% normal goat serum (NGS) and subsequently incubated with anti-Mac-3 antibody (BioLegend, Fell, Germany) overnight at 4°C. Mac-3 was detected by secondary antibody linked to HRP and subsequent Diaminobenzidine (DAB) staining.

Affinity histochemistry:

bHABP (HA binding protein): Tissue slides were deparaffinised, rehydrated and endogenous peroxidase activity was blocked with 3% H_2O_2. Affinity histochemistry of HA was performed incubating biotinylated bHABP overnight (ON) (Seikagaku, Tokyo, Japan) and further detection using HRP-labeled streptavidin (Calbiochem, Bad Soden, Germany) and subsequent DAB staining.

Immunofluorescence:

ARG1/Mac-3 double staining: Immunofluorescence staining of paraffin-embedded lung tissue slides was performed using the Mouse on Mouse (M.O.M.™) Immunodetection Kit BASIC (Vector Laboratories) according to the manufacturer's instructions. Tissue sections were incubated with anti-ARG1 antibodies ON at 4°C. Anti-ARG1 was detected using Alexa Fluor® 555 conjugate (Invitrogen, Thermo Fisher Scientific, Waltham, USA). Slides were the blocked with 2% NGS and incubated with anti-Mac-3 antibody ON at 4°C. Anti-Mac-3 was detected using Alexa Fluor® 488 conjugate (Invitrogen).

Statistics

Statistical analyses were performed using Prism 5.0 (GraphPad). For normalization, sham control values were set to 100% or 1 and values for irradiated animals were depicted as % of sham controls or relative to controls. Student's two-tailed unpaired t tests were used to compare differences between two groups. Two-way ANOVA with post-hoc Sidak's multiple comparisons test was used to compare groups split on two independent variables. Statistical significance was set at $P < 0.05$.

Results

Thorax irradiation triggers an early loss of pulmonary macrophages, influx of CD11b$^+$ cells, and upregulation of pro- and anti-inflammatory macrophage markers

To study the macrophage response in irradiated lungs, we exposed mice to WTI with a single dose of 15 Gy or 0 Gy (sham control) and dissected the lung tissue for flow cytometric analysis at different time-points. Total macrophages were gated based on CD45 and F4/80 staining (Fig. 1A upper panel). In non-irradiated mice the proportion of F4/80$^+$ pulmonary macrophages from leukocytes (CD45$^+$) was 20.9±0.6%. Irradiation led to a significant reduction in the percentage of F4/80$^+$ macrophages at 3 weeks after IR (Fig 1B). We identified AM among living leukocytes by a gating strategy recently developed by Vermaelen and colleagues for distinguishing AM (CD45$^+$CD11c^{high} autofluorescent cells) from pulmonary dendritic cells [45]. This strategy is depicted in Fig. 1A middle panel and revealed a percentage of AMs in total living CD45$^+$ leukocytes in control mice of 6.8±0.6% (Fig. 1A). Exposure to ionizing radiation (IR) caused a reduction in AM levels of almost 90% after 3 weeks (Fig. 1C) and was accompanied by significantly enhanced levels of CD11b$^+$ monocytic cells within the leukocyte population (Fig. 1A lower panel + 1D). The level of CD45$^+$CD11b$^+$ cells in non-irradiated mice was on average 36.2 ±1.1%.

To analyze the phenotype of macrophages we used major histocompatibility complex II (MHCII) as marker for a pro-inflammatory phenotype and macrophage mannose receptor (MMR) as marker for alternative activation, respectively. Fig. 2A shows the strategy for determination of the mean fluorescence intensity (MFI) for MHCII and MMR on F4/80$^+$ macrophages as well as AM. The flow cytometric analyses revealed that macrophages present in irradiated lung tissue 3 weeks after IR express MHCII and MMR (Fig. 2B).

When analyzing the proportions of macrophages and $CD11b^+$ cells at different time points after IR, percentages of macrophages recovered at 6 weeks upon radiation treatment compared to non-irradiated controls with a trend for a slight delay in complete recovery of AM (Fig. 2C).

Pulmonary macrophages undergo changes in their phenotype during the fibrotic stage

We next investigated time-dependent changes in the macrophage phenotype in fibrosis-prone WT mice after irradiation. Flow cytometric analyses revealed a trend to enhanced levels of the pro-inflammatory marker MHCII throughout the observation period in the $F4/80^+$ population whereas the anti-inflammatory marker MMR was found to be slightly but significantly enhanced only at 6 weeks after IR (Fig. 3A). AM also showed enhanced expression of MHCII throughout the observation period with a significant increase during the fibrotic phase at 25-30 weeks post irradiation (Fig. 3B). In contrast to $F4/80^+$ macrophages we detected a significant up-regulation of MMR expression on AM at 25-30 weeks after IR.

Alternatively activated macrophages form clusters in the lung tissue and express pro-fibrotic markers

Our earlier work revealed that histologic signs of fibrosis can be detected at 25-30 weeks after IR [17, 43]. We therefore performed a detailed immunohistochemical analysis of macrophages for this time-point and found that macrophages accumulating in the lung tissue during the fibrotic phase formed organized clusters (Fig. 4A) and showed pronounced expression of ARG1, a marker for alternatively activated macrophages [18], and of the pro-fibrotic markers TGFβ and α-SMA (Fig. 4B+C), respectively. In contrast, expression of the pro-inflammatory iNOS could be

detected in only a few clusters. Double staining of tissue sections with Mac-3 and ARG1 confirmed a specific co-localization of ARG1 on macrophages (Fig. 4B). QPCR analyses of whole lung tissue RNA samples from 12 and 25-30 weeks after IR confirmed the enhanced expression of ARG1, whereas iNOS and the receptor of interleukin 10 (subunit alpha) (IL-10Rα) showed slightly enhanced but not significantly different values (Fig. 4D).

CD73 deficiency prevents the accumulation of alternatively activated macrophages

Our previous work revealed that genetic deficiency of ecto-5'-nucleotidase (CD73) attenuates radiation-induced pulmonary fibrosis in $CD73^{-/-}$ mice [17]. We were therefore interested in whether loss of CD73 would affect accumulation and phenotype of pulmonary macrophages. Indeed, genetic loss of CD73 was associated with a failure of pulmonary macrophages to develop organized macrophage clusters at 25-30 weeks post-IR (Fig. 5A).

Furthermore, comparable to the results obtained in WT mice we found that $F4/80^{+}$ lung macrophages isolated from irradiated $CD73^{-/-}$ mice displayed up-regulated expression of the pro-inflammatory marker MHCII throughout the observation period (Fig. 5B left panel) whereas the anti-inflammatory marker MMR was not enhanced at any time point (Fig. 5B right panel). MHCII was also significantly up-regulated on $CD73^{-/-}$ AM at 3 and 25-30 weeks after irradiation (Fig. 5C left panel). However, in contrast to the observations in WT mice MMR was found to be up-regulated on $CD73^{-/-}$ AM only at the 3 weeks time but not during the fibrotic phase (Fig. 5C right panel). QPCR analyses from whole lung tissue RNA samples (Fig. 5D) revealed that neither ARG1 nor IL-10Rα or iNOS were enhanced in CD73 deficient mice upon IR, confirming the failure to initiate alternative activation in

macrophages. Taken together the results suggest that the pathogenesis of radiation-induced lung fibrosis involves an accumulation of AM in organized clusters and a CD73-dependent shift of these AM towards an alternatively activated phenotype.

CD73 deficiency impacts on the HA signaling pathway

Earlier reports pointed to a link between the HA system and adenosine signaling [39, 42]. Furthermore, our previous work revealed increased deposition of HA in WT mice during the fibrotic phase [43]. Affinity histochemical staining for HA binding protein (HABP) corroborated the accumulation of HA within the fibrotic areas (Fig. 6A). A detailed analysis of the time course of HA accumulation revealed that HA deposition became visible already at 16-20 weeks (Fig. 6A). Interestingly, HA staining seemed to be more diffuse at the late time-point (30 weeks). Of note, no histologically detectable formation of HA positive fibrotic foci could be observed in the $CD73^{-/-}$ mice (Fig. 6A right panels).

Next we examined whether the time-dependent changes in HA abundance in irradiated lungs of WT mice and the differences between WT and $CD73^{-/-}$ mice could be attributed to radiation-induced differences in the regulation of genes of the HA pathway (Fig. 6B and C). For this we compared relative mRNA expression levels of irradiated whole lung tissue samples and sham controls from WT and $CD73^{-/-}$ mice. Has1 and Has2 underwent reciprocal changes in expression after IR in both, WT and $CD73^{-/-}$ animals (Fig. 6B). While Has1 levels declined over time until the fibrotic phase Has2 underwent a time-dependent up-regulation after irradiation with highest levels observed in the fibrotic phase. Interestingly, at the 12 week time-point and thus just before the onset of visible HA deposition in WT mice, Has1 and Has2 expression was increased in WT compared to $CD73^{-/-}$ mice (Fig. 6B).

Instead, Has3 was found to be up-regulated at the 3 week time point in the lungs of irradiated WT animals and declined throughout the observation period; in contrast, in $CD73^{-/-}$ mice Has3 expression was low at the 3 week time point but showed a significant increase during the fibrotic phase (Fig. 6C). This was paralleled by a comparable time-course in the expression of the HA receptors CD44 and hyaluronan-mediated motility receptor (Hmmr, RHAMM) in $CD73^{-/-}$ mice (Fig 6C). In contrast, the expression of CD44 remained almost unchanged in WT mice whereas the expression of RHAMM displayed a dual increase at the 3 week and the 30 week time-points in these mice, respectively (Fig 6C).

Discussion

Here we demonstrate for the first time that thorax-irradiation of fibrosis-prone C57BL/6 mice triggers a switch of AM towards an alternatively activated phenotype and their accumulation in organized clusters expressing fibrotic marker proteins during the fibrotic phase. Genetic deficiency of CD73 abrogated both, the phenotypic switch of AM and the formation of organized macrophage clusters in the irradiated lung tissue. Reduced deposition of ECM molecules in $CD73^{-/-}$ mice was accompanied by specific differences in the expression of genes of the HA system and reduced HA deposition. We conclude that radiation-induced activation of the CD73/adenosine and HA pathways cooperate in promoting radiation-induced pulmonary fibrosis by driving the formation of macrophage clusters and a phenotypic switch of AM towards alternatively activated, pro-fibrotic phenotypes in the context of further radiation-induced changes in the pulmonary environment.

In detail, while the percentage of pulmonary macrophages, particularly AMs, declined during the first weeks after WTI, which is consistent with findings by others [20], we detected an increased influx of $CD11b^{+}$ myeloid cells. As this myeloid cell population is known to contain macrophage precursors we speculate that radiation-induced tissue damage and subsequent up-regulation of monocyte-chemoattractants trigger the influx of myeloid cells into the lung tissue to replace eradicated tissue resident macrophages [11, 46]. Accordingly, we observed a reconstitution of $F4/80^{+}$ macrophages at 6 weeks and of AMs at 12 weeks post-irradiation that was accompanied by a normalization of $CD11b^{+}$ cell levels. In line with our observations, bone-marrow-derived cells replaced eradicated AMs in unshielded murine lungs around 6 weeks after TBI [47] whereas under homeostatic conditions AMs expand via self-renewal [48].

Macrophage-phenotyping in WT mice revealed that pro-inflammatory markers like MHCII were significantly up-regulated in F4/80$^+$ macrophages and in remaining AM at the 3 week time-point. The anti-inflammatory marker MMR was also significantly up-regulated at early time points on F4/80$^+$ macrophages (6 weeks post-irradiation) and AMs (3 weeks post-irradiation). While MHCII levels remained elevated during the observation period in both macrophage populations, expression levels of MMR declined during the transition phase but were up-regulated during the fibrotic phase specifically on AM. Our findings corroborate earlier reports on the generation of alternatively activated macrophages in murine lungs upon thoracic irradiation [18, 20], though the murine studies differ in radiation doses, investigated time points, as well as markers and gating-strategies used to identify pulmonary macrophages. A contribution of alternatively activated macrophages to bleomycine-induced lung fibrosis in mice has also been suggested [49].

The generation of alternatively activated macrophages in irradiated lungs was associated with their accumulation in organized clusters. This is reminiscent of findings in the rat model of bleomycin-induced pulmonary fibrosis where organized macrophage clusters were observed at day 7 and 14 after intratracheal bleomycin injection [50]. Furthermore, focal lesions containing numerous macrophages were observed in lungs of irradiated C57L/J mice, but already at 8 weeks post-irradiation [51]. A strong association between organized macrophage clusters in the lung and fibrosis development was also reported in a model of targeted type II alveolar epithelial cell injury [52]. Instead, Franko and coworkers described the formation of focal lesions containing TGFβ positive fibroblasts upon single dose thoracic irradiation (15 Gy) in fibrosis-prone C57BL/6 mice but not in fibrosis-resistant C3HeB/FeJ mice [53]. In the present study we now demonstrate that organized macrophage clusters are exclusively present during the fibrotic phase and strongly

express pro-fibrotic mediators, suggesting a role for cluster-forming alternatively activated macrophages, presumably AMs, in radiation-induced pulmonary fibrosis.

So far, the role of macrophages in radiation-induced pneumopathy and the molecular networks involved in their regulation remained elusive. Here we show for the first time that in irradiated CD73$^{-/-}$ mice, macrophages fail to organize into clusters and AMs do not up-regulate markers for alternative activation such as MMR and ARG1. Our findings suggest a role for chronic CD73-dependent adenosine accumulation in driving the phenotypic switch in macrophages and a potential contribution of these alternatively activated alveolar macrophages in promoting radiation-induced fibrosis. This assumption is supported by earlier reports demonstratinga role of adenosine in driving and modulating alternative activation of macrophages [54-57]. Moreover, adenosine signaling has also been identified as contributor to fibrotic disease in other murine models in a tissue-dependent and injury-dependent manner [33, 58]. In this context, signaling via ADORA2B and ADORA3 seem to be particularly important in pulmonary fibrotic disease [14, 39, 59].

Suggested mechanisms of the pro-fibrotic actions of pulmonary macrophages involve overproduction of reactive oxygen species as well as generation and activation of pro-fibrotic cytokines such as TGFβ [24, 60]. Comparative transcriptome analysis of lung tissue from fibrosis-prone and fibrosis-resistant mice exposed to thoracic irradiation revealed differences in the expression of signaling molecules associated with immune activation [61, 62]. Accordingly, we observed up-regulated mRNA and protein levels of TGFβ and osteopontin (OPN) upon WTI only in the lung tissue of C57BL/6 mice whereas the levels of these clinically relevant fibrotic markers were lower in the lungs of CD73$^{-/-}$ mice [17]. As the pro-fibrotic mediator TGFβ can induce alternative macrophage activation [63, 64] we speculate that the accumulation of TGFβ in irradiated lungs may cooperate with adenosine in driving the phenotypic

switch in macrophages during the fibrotic phase. Furthermore, macrophages can produce OPN induced downstream of ADORA2B signaling [65].

Interestingly, the specific knockout of ADORA2B on myeloid cells ($LysM^{Cre}$) reduced adenosine levels in the BALF, the numbers of alternatively activated macrophages and of α-SMA^{+} fibroblasts, and fibrosis development in the chronic bleomycin model [14]. Moreover, CD73 and ADORA2B were up-regulated in lung biopsies from patients with chronic obstructive pulmonary disease (COPD) Stage 4 or severe IPF, respectively, with their expression particularly confined to alternatively activated pulmonary macrophages [49]. These findings highlight a role of CD73-activation, adenosine accumulation, and ADORA2B activation in driving the accumulation of alternatively activated macrophages and fibrotic pulmonary disease also in patients.

We also identified the HA pathway as another important modulator of radiation-induced pulmonary fibrosis, presumably through an interaction with the CD73/adenosine-pathway: We observed increased HA-deposition only in irradiated WT but not in $CD73^{-/-}$ mice. Furthermore, HA-deposition in WT lungs was observed at 16-20 weeks post-irradiation, and thus in parallel to the chronic accumulation of adenosine but prior to the occurrence of histologically detectable fibrosis described in our recent study [17]. Interestingly, the differences in HA deposition between irradiated WT and $CD73^{-/-}$ mice were associated with differences in the expression of HA synthases. At the critical 12 week time-point that represents the onset of adenosine accumulation [17] Has1 and Has2 displayed increased expression in WT compared to $CD73^{-/-}$ mice. These observations corroborate the suggested link between the adenosine and hyaluronan pathways in regulating tissue inflammation and fibrosis in other murine models and for patients with COPD [39, 42, 66]. In contrast, Has3 was up-regulated during the fibrotic phase only in the $CD73^{-/-}$ mice.

Unlike Has1 and Has2, Has3 mainly synthesizes LMW HA with reported pro-inflammatory actions [67, 68]. Activation of the pro-inflammatory arm of the HA pathway during the fibrotic phase may thus help the $CD73^{-/-}$ mice to limit fibrosis development, e.g. through activating ECM-degrading enzymes [69].

Taken together our results point to a pathogenic role of the accumulation of alternatively activated macrophages in pre-fibrotic clusters in radiation-induced lung fibrosis. Reduced extracellular adenosine accumulation in $CD73^{-/-}$ mice prevented macrophage from accumulation in organized clusters, to undergo a phenotypic switch, and to express pro-fibrotic markers in irradiated lungs. Thus, radiation-induced increases in adenosine, TGFβ, and HA may cooperate in driving macrophage recruitment, activation and organization in pre-fibrotic clusters and fibrosis progression. Our findings contribute to a better understanding of the signaling networks driving polarized macrophage activation and fibrosis in the irradiated lung and may allow us to define new diagnostic biomarkers and therapeutic strategies for this dose-limiting adverse effect of thorax irradiation.

Authors contributions

SDL and FW designed research, performed experiments, analyzed data and wrote manuscript; FC designed research, performed experiments and evaluated data; AVM, AS and KR, performed experiments; LFT, wrote and critical reviewed manuscript; JWF and MS discussed data and critically reviewed manuscript; VJ designed research, wrote and critically reviewed manuscript,

Acknowledgements

We thank Michael Groneberg and Eva Gau for excellent technical support. The work was supported by grants of the Deutsche Forschungsgemeinschaft (DFG) grant numbers GRK1739/1 and JE275/4-1 (V. Jendrossek), and the Bundesministerium für Bildung und Forschung (BMBF) grant number 02NUK024D (V. Jendrossek).

Abbreviations: adenosine receptor A1, A2A, A2B, A3: ADORA1,2A,2B,3; alpha smooth muscle actin: α-SMA; alveolar macrophage: AM; arginase-1: ARG1; bronchoalveolar lavage (fluid): BAL(F); C57BL/6 mice: WT, $CD73^{+/+}$; CD73 knockout mice: $CD73^{-/-}$; connective tissue growth factor: CTGF; Diaminobenzidine (DAB); ecto-5′-nucelotidase: CD73; extracellular matrix: ECM; Gray: Gy; HA binding protein: HABP; high molecular weight: HMW; hyaluronan: HA; hyaluronan synthase 1-3: Has1-3; hyaluronan-mediated motility receptor: Hmmr, RHAMM; hyaluronidase 1+2: Hyal1+2; idiopathic pulmonary fibrosis: IPF; inducible nitric oxid synthase: iNOS; interleukin 10 receptor (subunit alpha): IL-10Rα; low molecular weight: LMW; macrophage chemoattractant protein-1: MCP-1; macrophage inflammatory protein-1 beta: MIP-1β; macrophage inflammatory protein-2: MIP-2; macrophage mannose receptor: MMR; macrophage-3 antigen: Mac-3; macrophage-colony stimulating factor: M-CSF; major histocompatibility complex II: MHCII; mean fluorescence intensity: MFI; normal goat serum: NGS; osteopontin: OPN; post ionizing radiation: post IR; quantitative real-time PCR: QPCR; reactive oxygen species: ROS; transforming growth factor beta: TGFβ; whole thorax irradiation: WTI

References

1. Begg AC, Stewart FA, Vens C. Strategies to improve radiotherapy with targeted drugs. *Nat Rev Cancer* 2011; **11**: 239-253.
2. Kong FM, Ten Haken R, Eisbruch A*, et al.* Non-small cell lung cancer therapy-related pulmonary toxicity: an update on radiation pneumonitis and fibrosis. *Semin Oncol* 2005; **32**: S42-54.
3. Kelsey CR, Horwitz ME, Chino JP*, et al.* Severe pulmonary toxicity after myeloablative conditioning using total body irradiation: an assessment of risk factors. *Int J Radiat Oncol Biol Phys* 2011; **81**: 812-818.
4. Graves PR, Siddiqui F, Anscher MS*, et al.* Radiation pulmonary toxicity: from mechanisms to management. *Semin Radiat Oncol* 2010; **20**: 201-207.
5. Arpin D, Perol D, Blay JY*, et al.* Early variations of circulating interleukin-6 and interleukin-10 levels during thoracic radiotherapy are predictive for radiation pneumonitis. *J Clin Oncol* 2005; **23**: 8748-8756.
6. Rubin P, Johnston CJ, Williams JP*, et al.* A perpetual cascade of cytokines postirradiation leads to pulmonary fibrosis. *Int J Radiat Oncol Biol Phys* 1995; **33**: 99-109.
7. Johnston CJ, Wright TW, Rubin P*, et al.* Alterations in the expression of chemokine mRNA levels in fibrosis-resistant and -sensitive mice after thoracic irradiation. *Exp Lung Res* 1998; **24**: 321-337.
8. Buttner C, Skupin A, Rieber EP. Transcriptional activation of the type I collagen genes COL1A1 and COL1A2 in fibroblasts by interleukin-4: analysis of the functional collagen promoter sequences. *J Cell Physiol* 2004; **198**: 248-258.
9. Rube CE, Uthe D, Wilfert F*, et al.* The bronchiolar epithelium as a prominent source of pro-inflammatory cytokines after lung irradiation. *Int J Radiat Oncol Biol Phys* 2005; **61**: 1482-1492.
10. Hong ZY, Song KH, Yoon JH*, et al.* An experimental model-based exploration of cytokines in ablative radiation-induced lung injury in vivo and in vitro. *Lung* 2015; **193**: 409-419.
11. Cappuccini F, Eldh T, Bruder D*, et al.* New insights into the molecular pathology of radiation-induced pneumopathy. *Radiother Oncol* 2011; **101**: 86-92.
12. Baran CP, Opalek JM, McMaken S*, et al.* Important roles for macrophage colony-stimulating factor, CC chemokine ligand 2, and mononuclear phagocytes in the pathogenesis of pulmonary fibrosis. *Am J Respir Crit Care Med* 2007; **176**: 78-89.
13. Zhang-Hoover J, Sutton A, van Rooijen N*, et al.* A critical role for alveolar macrophages in elicitation of pulmonary immune fibrosis. *Immunology* 2000; **101**: 501-511.
14. Karmouty-Quintana H, Philip K, Acero LF*, et al.* Deletion of ADORA2B from myeloid cells dampens lung fibrosis and pulmonary hypertension. *FASEB J* 2015; **29**: 50-60.
15. Johnston CJ, Williams JP, Elder A*, et al.* Inflammatory cell recruitment following thoracic irradiation. *Exp Lung Res* 2004; **30**: 369-382.
16. Chiang CS, Liu WC, Jung SM*, et al.* Compartmental responses after thoracic irradiation of mice: strain differences. *Int J Radiat Oncol Biol Phys* 2005; **62**: 862-871.
17. Wirsdorfer F, de Leve S, Cappuccini F*, et al.* Extracellular Adenosine Production by ecto-5'-Nucleotidase (CD73) Enhances Radiation-Induced Lung Fibrosis. *Cancer Res* 2016; **76**: 3045-3056.
18. Zhang H, Han G, Liu H*, et al.* The development of classically and alternatively activated macrophages has different effects on the varied stages of radiation-induced pulmonary injury in mice. *J Radiat Res* 2011; **52**: 717-726.
19. Abernathy LM, Fountain MD, Rothstein SE*, et al.* Soy Isoflavones Promote Radioprotection of Normal Lung Tissue by Inhibition of Radiation-Induced Activation of Macrophages and Neutrophils. *J Thorac Oncol* 2015; **10**: 1703-1712.

20. Groves AM, Johnston CJ, Misra RS*, et al.* Whole-Lung Irradiation Results in Pulmonary Macrophage Alterations that are Subpopulation and Strain Specific. *Radiat Res* 2015; **184**: 639-649.
21. Sica A, Mantovani A. Macrophage plasticity and polarization: in vivo veritas. *J Clin Invest* 2012; **122**: 787-795.
22. Biswas SK, Mantovani A. Orchestration of metabolism by macrophages. *Cell Metab* 2012; **15**: 432-437.
23. Biswas SK, Mantovani A. Macrophage plasticity and interaction with lymphocyte subsets: cancer as a paradigm. *Nat Immunol* 2010; **11**: 889-896.
24. Gordon S. Alternative activation of macrophages. *Nat Rev Immunol* 2003; **3**: 23-35.
25. Martinez FO, Gordon S. The M1 and M2 paradigm of macrophage activation: time for reassessment. *F1000Prime Rep* 2014; **6**: 13.
26. Murray PJ, Allen JE, Biswas SK*, et al.* Macrophage activation and polarization: nomenclature and experimental guidelines. *Immunity* 2014; **41**: 14-20.
27. Mosser DM, Edwards JP. Exploring the full spectrum of macrophage activation. *Nat Rev Immunol* 2008; **8**: 958-969.
28. Linden J. Regulation of leukocyte function by adenosine receptors. *Adv Pharmacol* 2011; **61**: 95-114.
29. Thompson LF, Eltzschig HK, Ibla JC*, et al.* Crucial role for ecto-5'-nucleotidase (CD73) in vascular leakage during hypoxia. *J Exp Med* 2004; **200**: 1395-1405.
30. Thompson LF, Takedachi M, Ebisuno Y*, et al.* Regulation of leukocyte migration across endothelial barriers by ECTO-5'-nucleotidase-generated adenosine. *Nucleosides Nucleotides Nucleic Acids* 2008; **27**: 755-760.
31. Deaglio S, Dwyer KM, Gao W*, et al.* Adenosine generation catalyzed by CD39 and CD73 expressed on regulatory T cells mediates immune suppression. *J Exp Med* 2007; **204**: 1257-1265.
32. Kaku H, Cheng KF, Al-Abed Y*, et al.* A novel mechanism of B cell-mediated immune suppression through CD73 expression and adenosine production. *J Immunol* 2014; **193**: 5904-5913.
33. Chunn JL, Molina JG, Mi T*, et al.* Adenosine-dependent pulmonary fibrosis in adenosine deaminase-deficient mice. *J Immunol* 2005; **175**: 1937-1946.
34. Volmer JB, Thompson LF, Blackburn MR. Ecto-5'-nucleotidase (CD73)-mediated adenosine production is tissue protective in a model of bleomycin-induced lung injury. *J Immunol* 2006; **176**: 4449-4458.
35. Zhou Y, Schneider DJ, Morschl E*, et al.* Distinct roles for the A2B adenosine receptor in acute and chronic stages of bleomycin-induced lung injury. *J Immunol* 2011; **186**: 1097-1106.
36. Wynn TA. Common and unique mechanisms regulate fibrosis in various fibroproliferative diseases. *J Clin Invest* 2007; **117**: 524-529.
37. Nettelbladt O, Hallgren R. Hyaluronan (hyaluronic acid) in bronchoalveolar lavage fluid during the development of bleomycin-induced alveolitis in the rat. *Am Rev Respir Dis* 1989; **140**: 1028-1032.
38. Savani RC, Hou G, Liu P*, et al.* A role for hyaluronan in macrophage accumulation and collagen deposition after bleomycin-induced lung injury. *Am J Respir Cell Mol Biol* 2000; **23**: 475-484.
39. Karmouty-Quintana H, Weng T, Garcia-Morales LJ*, et al.* Adenosine A2B receptor and hyaluronan modulate pulmonary hypertension associated with chronic obstructive pulmonary disease. *Am J Respir Cell Mol Biol* 2013; **49**: 1038-1047.
40. McKee CM, Lowenstein CJ, Horton MR*, et al.* Hyaluronan fragments induce nitric-oxide synthase in murine macrophages through a nuclear factor kappaB-dependent mechanism. *J Biol Chem* 1997; **272**: 8013-8018.
41. McKee CM, Penno MB, Cowman M*, et al.* Hyaluronan (HA) fragments induce chemokine gene expression in alveolar macrophages. The role of HA size and CD44. *J Clin Invest* 1996; **98**: 2403-2413.

42. Scheibner KA, Boodoo S, Collins S*, et al.* The adenosine a2a receptor inhibits matrix-induced inflammation in a novel fashion. *Am J Respir Cell Mol Biol* 2009; **40**: 251-259.
43. Klein D, Steens J, Wiesemann A*, et al.* Mesenchymal stem cell therapy protects lungs from radiation-induced endothelial cell loss by restoring superoxide dismutase 1 expression. *Antioxid Redox Signal* 2016.
44. Wirsdorfer F, Cappuccini F, Niazman M*, et al.* Thorax irradiation triggers a local and systemic accumulation of immunosuppressive CD4+ FoxP3+ regulatory T cells. *Radiat Oncol* 2014; **9**: 98.
45. Vermaelen K, Pauwels R. Accurate and simple discrimination of mouse pulmonary dendritic cell and macrophage populations by flow cytometry: methodology and new insights. *Cytometry A* 2004; **61**: 170-177.
46. Groves AM, Johnston CJ, Misra RS*, et al.* Effects of IL-4 on Pulmonary Fibrosis and the Accumulation and Phenotype of Macrophage Subpopulations Following Thoracic Irradiation. *Int J Radiat Biol* 2016: 1-36.
47. Matute-Bello G, Lee JS, Frevert CW*, et al.* Optimal timing to repopulation of resident alveolar macrophages with donor cells following total body irradiation and bone marrow transplantation in mice. *J Immunol Methods* 2004; **292**: 25-34.
48. Tarling JD, Lin HS, Hsu S. Self-renewal of pulmonary alveolar macrophages: evidence from radiation chimera studies. *J Leukoc Biol* 1987; **42**: 443-446.
49. Zhou Y, Murthy JN, Zeng D*, et al.* Alterations in adenosine metabolism and signaling in patients with chronic obstructive pulmonary disease and idiopathic pulmonary fibrosis. *PLoS One* 2010; **5**: e9224.
50. Khalil N, Bereznay O, Sporn M*, et al.* Macrophage production of transforming growth factor beta and fibroblast collagen synthesis in chronic pulmonary inflammation. *J Exp Med* 1989; **170**: 727-737.
51. Franko AJ, Sharplin J. Development of fibrosis after lung irradiation in relation to inflammation and lung function in a mouse strain prone to fibrosis. *Radiat Res* 1994; **140**: 347-355.
52. Osterholzer JJ, Christensen PJ, Lama V*, et al.* PAI-1 promotes the accumulation of exudate macrophages and worsens pulmonary fibrosis following type II alveolar epithelial cell injury. *J Pathol* 2012; **228**: 170-180.
53. Franko AJ, Sharplin J, Ghahary A*, et al.* Immunohistochemical localization of transforming growth factor beta and tumor necrosis factor alpha in the lungs of fibrosis-prone and "non-fibrosing" mice during the latent period and early phase after irradiation. *Radiat Res* 1997; **147**: 245-256.
54. Ferrante CJ, Pinhal-Enfield G, Elson G*, et al.* The adenosine-dependent angiogenic switch of macrophages to an M2-like phenotype is independent of interleukin-4 receptor alpha (IL-4Ralpha) signaling. *Inflammation* 2013; **36**: 921-931.
55. Csoka B, Selmeczy Z, Koscso B*, et al.* Adenosine promotes alternative macrophage activation via A2A and A2B receptors. *FASEB J* 2012; **26**: 376-386.
56. Hasko G, Pacher P. Regulation of macrophage function by adenosine. *Arterioscler Thromb Vasc Biol* 2012; **32**: 865-869.
57. Koscso B, Csoka B, Kokai E*, et al.* Adenosine augments IL-10-induced STAT3 signaling in M2c macrophages. *J Leukoc Biol* 2013; **94**: 1309-1315.
58. Chan ES, Cronstein BN. Adenosine in fibrosis. *Mod Rheumatol* 2010; **20**: 114-122.
59. Morschl E, Molina JG, Volmer JB*, et al.* A3 adenosine receptor signaling influences pulmonary inflammation and fibrosis. *Am J Respir Cell Mol Biol* 2008; **39**: 697-705.
60. Todd NW, Luzina IG, Atamas SP. Molecular and cellular mechanisms of pulmonary fibrosis. *Fibrogenesis Tissue Repair* 2012; **5**: 11.
61. Paun A, Lemay AM, Haston CK. Gene expression profiling distinguishes radiation-induced fibrosing alveolitis from alveolitis in mice. *Radiat Res* 2010; **173**: 512-521.

62. Kalash R, Berhane H, Au J*, et al.* Differences in irradiated lung gene transcription between fibrosis-prone C57BL/6NHsd and fibrosis-resistant C3H/HeNHsd mice. *In Vivo* 2014; **28**: 147-171.
63. Zhang F, Wang H, Wang X*, et al.* TGF-beta induces M2-like macrophage polarization via SNAIL-mediated suppression of a pro-inflammatory phenotype. *Oncotarget* 2016.
64. Mantovani A, Biswas SK, Galdiero MR*, et al.* Macrophage plasticity and polarization in tissue repair and remodelling. *J Pathol* 2013; **229**: 176-185.
65. Schneider DJ, Lindsay JC, Zhou Y*, et al.* Adenosine and osteopontin contribute to the development of chronic obstructive pulmonary disease. *FASEB J* 2010; **24**: 70-80.
66. Nettelbladt O, Bergh J, Schenholm M*, et al.* Accumulation of hyaluronic acid in the alveolar interstitial tissue in bleomycin-induced alveolitis. *Am Rev Respir Dis* 1989; **139**: 759-762.
67. Itano N, Sawai T, Yoshida M*, et al.* Three isoforms of mammalian hyaluronan synthases have distinct enzymatic properties. *J Biol Chem* 1999; **274**: 25085-25092.
68. Weigel PH, Hascall VC, Tammi M. Hyaluronan synthases. *J Biol Chem* 1997; **272**: 13997-14000.
69. Bot PT, Pasterkamp G, Goumans MJ*, et al.* Hyaluronic acid metabolism is increased in unstable plaques. *Eur J Clin Invest* 2010; **40**: 818-827.

Figures and Figure Legends

Figure 1

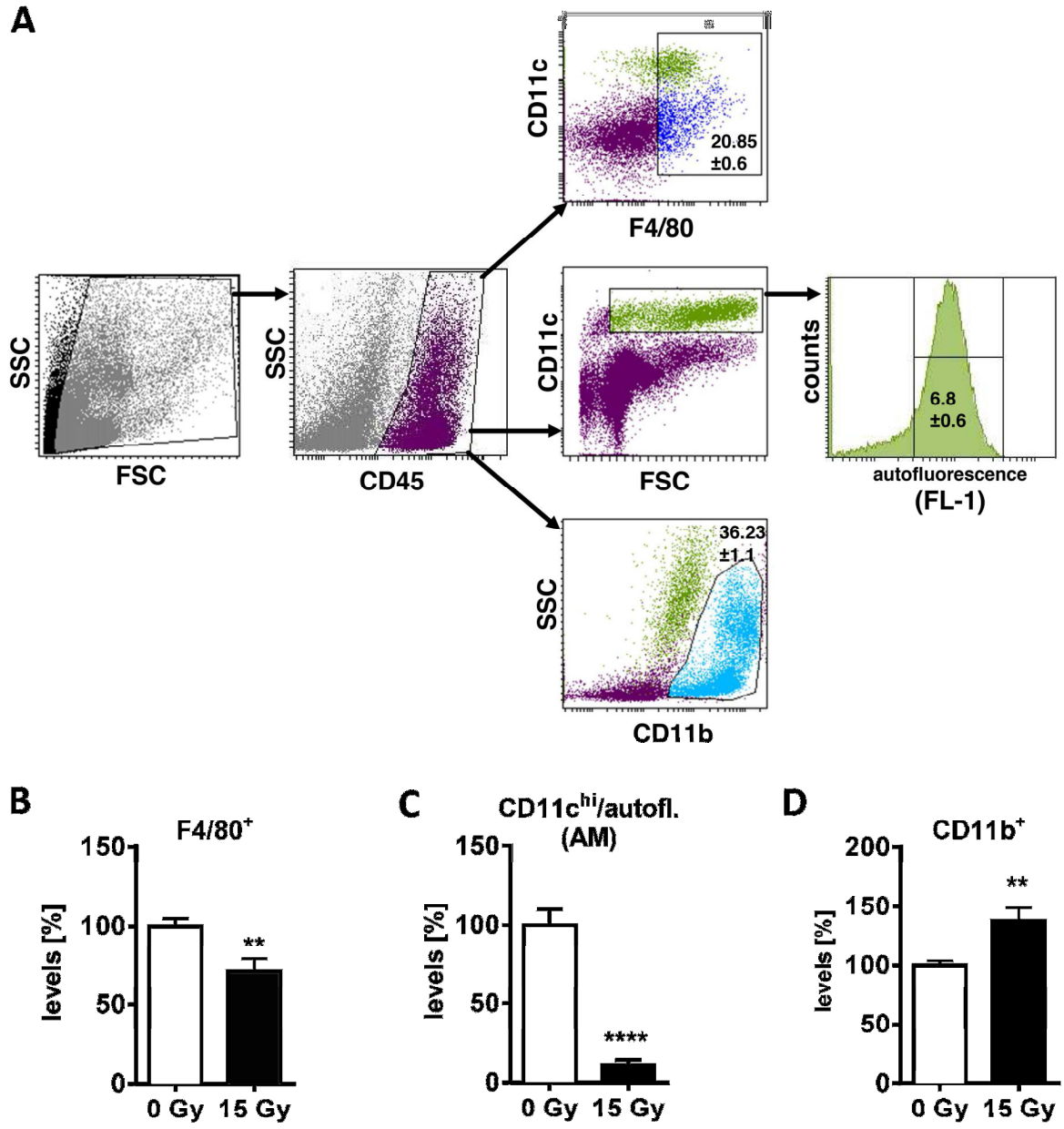

Radiation treatment triggers early loss of pulmonary macrophages and an early influx of CD11b$^+$ cells. C57BL/6 WT mice received 0 or 15 Gy WTI and were sacrificed at 3 weeks post-irradiation. Whole lung cells were stained and further analyzed by flow cytometry. (**A**) Gating strategy for F4/80$^+$ macrophages, alveolar macrophages (AM, via the expression of CD11c and autofluorescent property of AM [45]) and CD11b$^+$ cells from all living CD45$^+$ cells in the lung, shown for a 0 Gy

irradiated sample. Relative percentages of F4/80$^+$ cells (**B**), AM (**C**) and CD11b$^+$ cells (**D**) normalized to non-irradiated controls (n = 7). Shown are mean values ± SEM (B, C, D), $^{**}P \leq 0.01$, $^{****}P \leq 0.0001$ by unpaired two-tailed t-test.

Figure 2

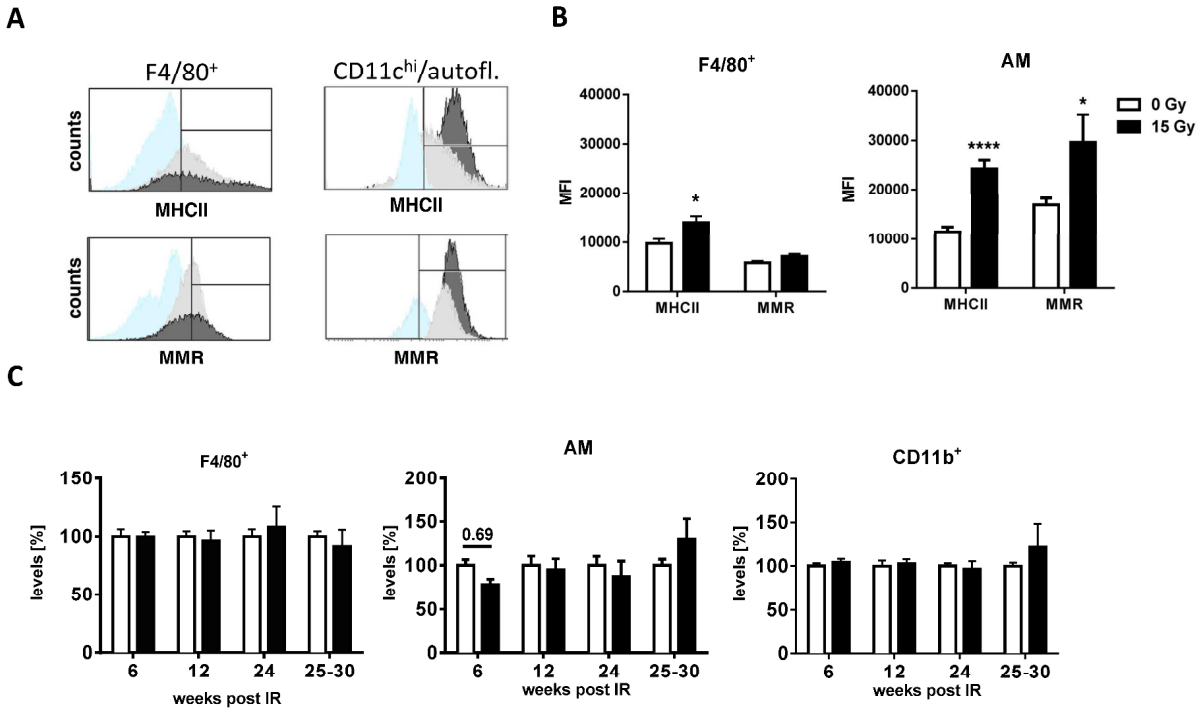

Whole thorax irradiation leads to upregulation of pro- and anti-inflammatory markers predominantly in alveolar macrophages. C57BL/6 WT mice received 0 or 15 Gy WTI and were sacrificed at the indicated time points upon irradiation. Whole lung cells were stained and further analyzed by flow cytometry. (**A**) Histograms show representative samples (isotype control in light blue, 0 Gy in light grey and 15 Gy dark grey) for the surface markers major histocompatibility complex (MHCII) and macrophage mannose receptor (MMR) for F4/80$^+$ macrophages (3 week time point) and AM (30 week time point). Indicated area was used for quantification. (**B**) At 3 weeks post-irradiation, lung macrophages (F4/80$^+$ macrophages or AM) were characterized for their expression of MHCII or MMR. Shown are mean fluorescent

intensities (MFI) per cell (n = 7). (**C**) At the indicated time points leukocytes ($CD45^+$) were stained with F4/80, CD11c or CD11b to define percentages of lung macrophages (n = 6/7, 6/6, 6/5, and 8/2 at the indicated time points), AMs (n = 6/7, 6/6, 6/5 and 11/8 at the indicated time points) or monocytic cells (n= 6/7, 6/6, 6/6 and 8/2 at the indicated time points) respectively. Shown are mean values ± SEM, $*P \leq 0.05$, $****P \leq 0.0001$ by unpaired two-tailed t-test (B) or by two-way ANOVA followed by Sidak's multiple comparisons test (C).

Figure 3

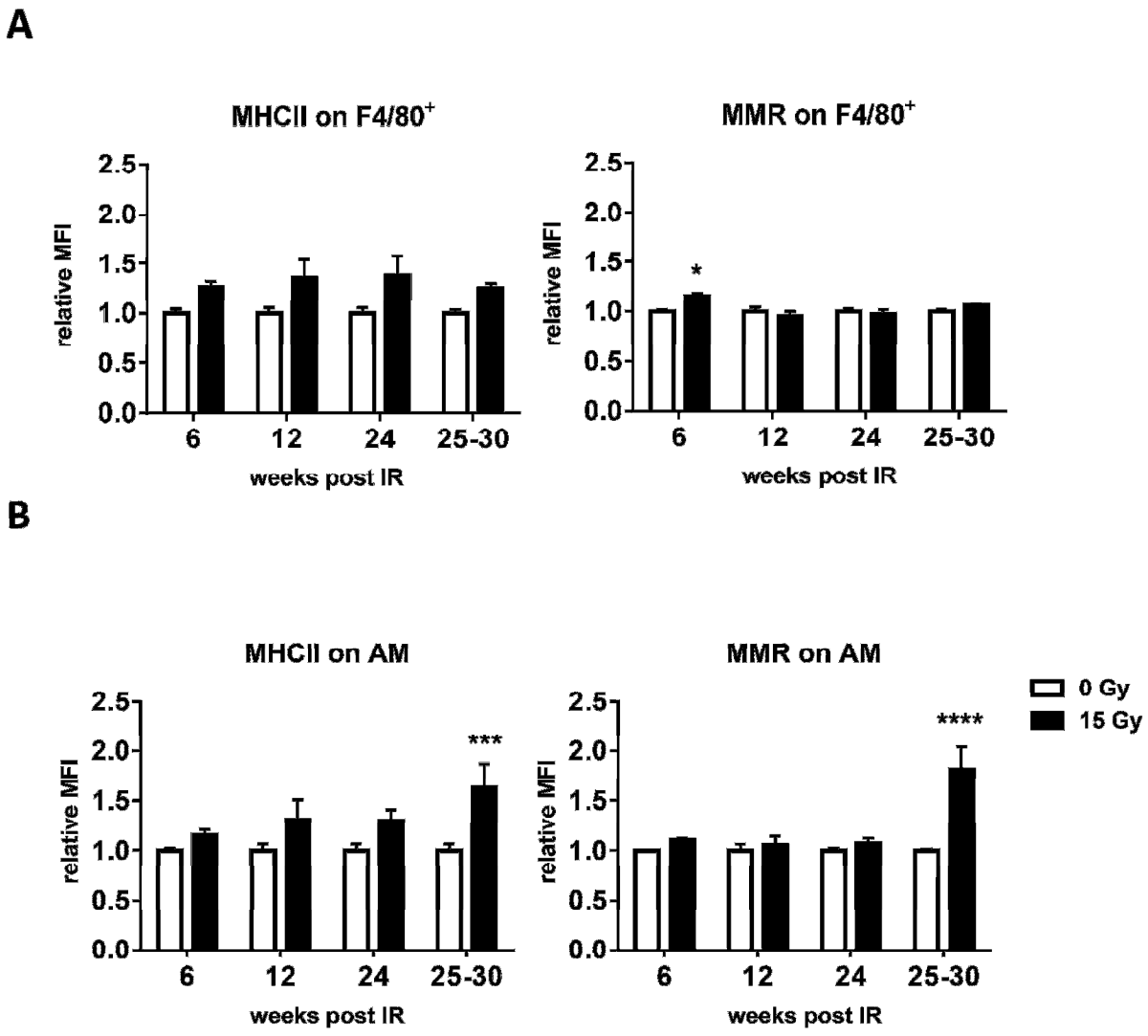

Macrophages in the irradiated lung tissue undergo changes in their phenotype in the fibrotic state. C57BL/6 WT mice received 0 or 15 Gy WTI and were sacrificed at the indicated time points after irradiation. Bar diagrams (**A**) show the relative MFI of MHCII and MMR for F4/80^{+} macrophages (n = 6/7, 6/6, 6/5 and 8/2 at the indicated time points) or AMs (**B**, n = 6/7, 6/6, 6/5 and 12/6 at the indicated time points) at the indicated time points. Shown are mean values ± SEM, **P* ≤ 0.05, ****P* ≤ 0.001, *****P* ≤ 0.0001 by two-way ANOVA followed by Sidak's multiple comparisons test.

Figure 4

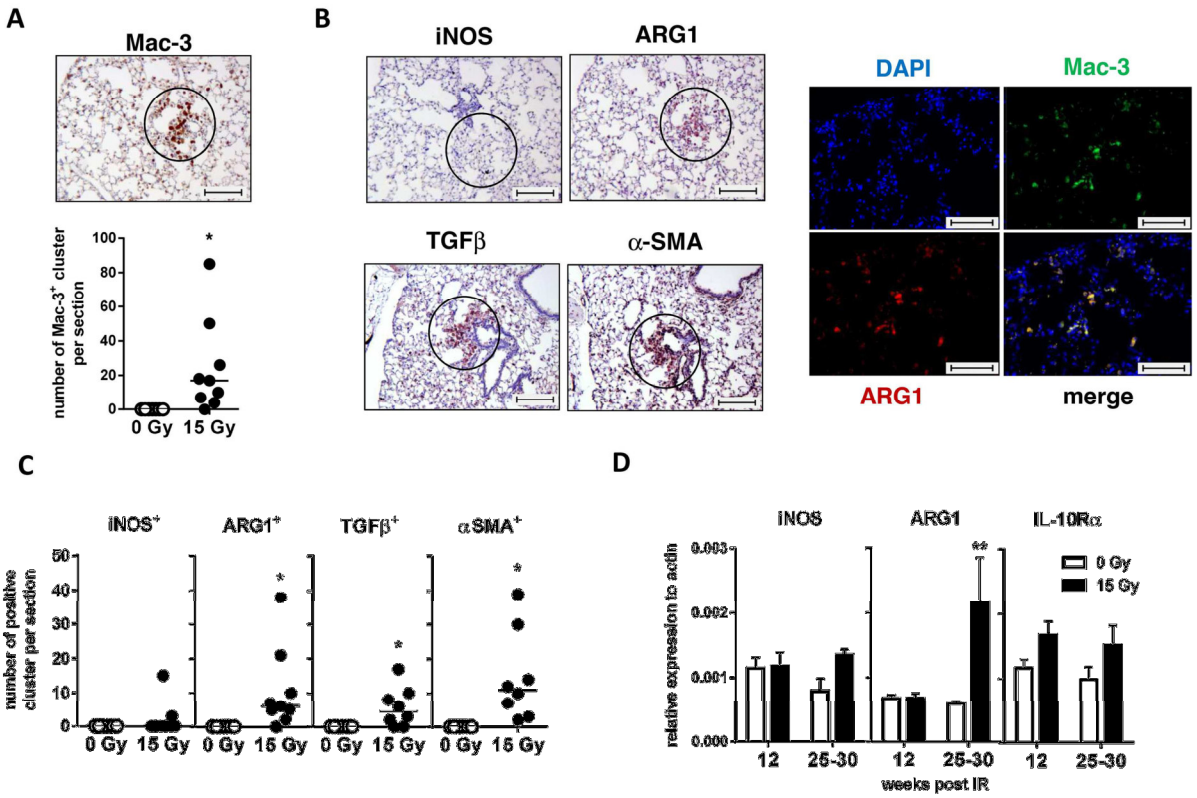

Alternatively activated macrophages form clusters in the lung tissue and have a pro-fibrotic phenotype. C57BL/6 WT mice received 0 or 15 Gy WTI and were sacrificed at 25-30 weeks upon irradiation. (**A**) IHC staining of paraffin-embedded lung tissue with primary antibody for Mac-3 was performed to identify macrophages

and macrophage clusters per section. Scale bar = 100µm. Numbers of clusters are shown in scatter plot (horizontal line indicates median). (**B**) Representative IHC pictures (from 15 Gy irradiated samples) for macrophage clusters stained with iNOS, ARG1, TGFβ or α-SMA primary antibody are shown (left panels). Scale bar = 100µm. The right panels show an immunofluorescence double staining for Mac-3 and ARG1. Double staining results in a yellow signal. Scale bar = 100 µm. (**C**) Quantification of evaluated macrophage clusters from IHC stainings for indicated markers in scatter plots (horizontal line indicates median). (**D**) QPCR analysis for iNOS (n = 8/7 and 8/7 at the indicated time points), ARG1 (n = 8/8 and 7/7 at the indicated time points) and IL-10Rα (n = 8/8 and 8/8 for both time points) from whole tissue RNA samples for indicated time points after irradiation, shown are mean values ± SEM. **P* ≤ 0.05, ***P* ≤ 0.01, by unpaired two-tailed t-test (A+C) or by two-way ANOVA followed by Sidak's multiple comparisons test (D).

Figure 5

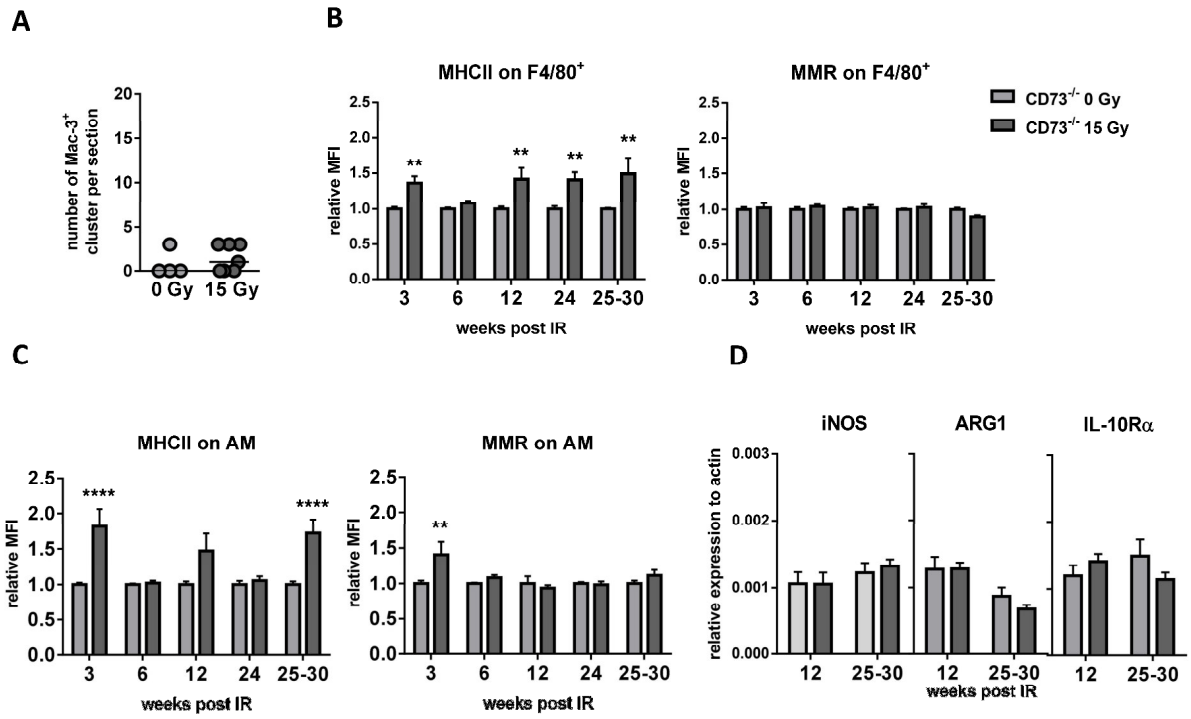

CD73 deficiency prevents the accumulation of alternatively activated macrophages. $CD73^{-/-}$ mice received 0 or 15 Gy WTI and were sacrificed at indicated time points. (**A**) IHC staining of paraffin-embedded lung tissue with primary antibody for Mac-3 was performed and macrophage clusters per section were counted. Numbers of clusters are shown in scatter plot (horizontal line indicates median). Bar diagrams show the relative MFI of MHCII and MMR for $F4/80^{+}$ macrophages (**B,** n = 7/7, 7/7, 6/5, 6/6 and 7/3 at the indicated time points) or AMs (**C**, n = 7/7, 6/7, 6/5, 6/6 and 10/7 at the indicated time points) at indicated time points. (**D**) QPCR analysis for iNOS (n = 9/10 and 10/10), ARG1 (n = 9/10 and 10/10) and IL-10Rα (n = 10/9 and 10/10 at the indicated time points) from whole tissue RNA samples for indicated time points upon irradiation. Shown are mean values ± SEM, $^{**}P \leq 0.01$, $^{***}P \leq 0.001$, by unpaired two-tailed t-test (A) or by two-way ANOVA followed by Sidak's multiple comparisons test (B-D).

Figure 6

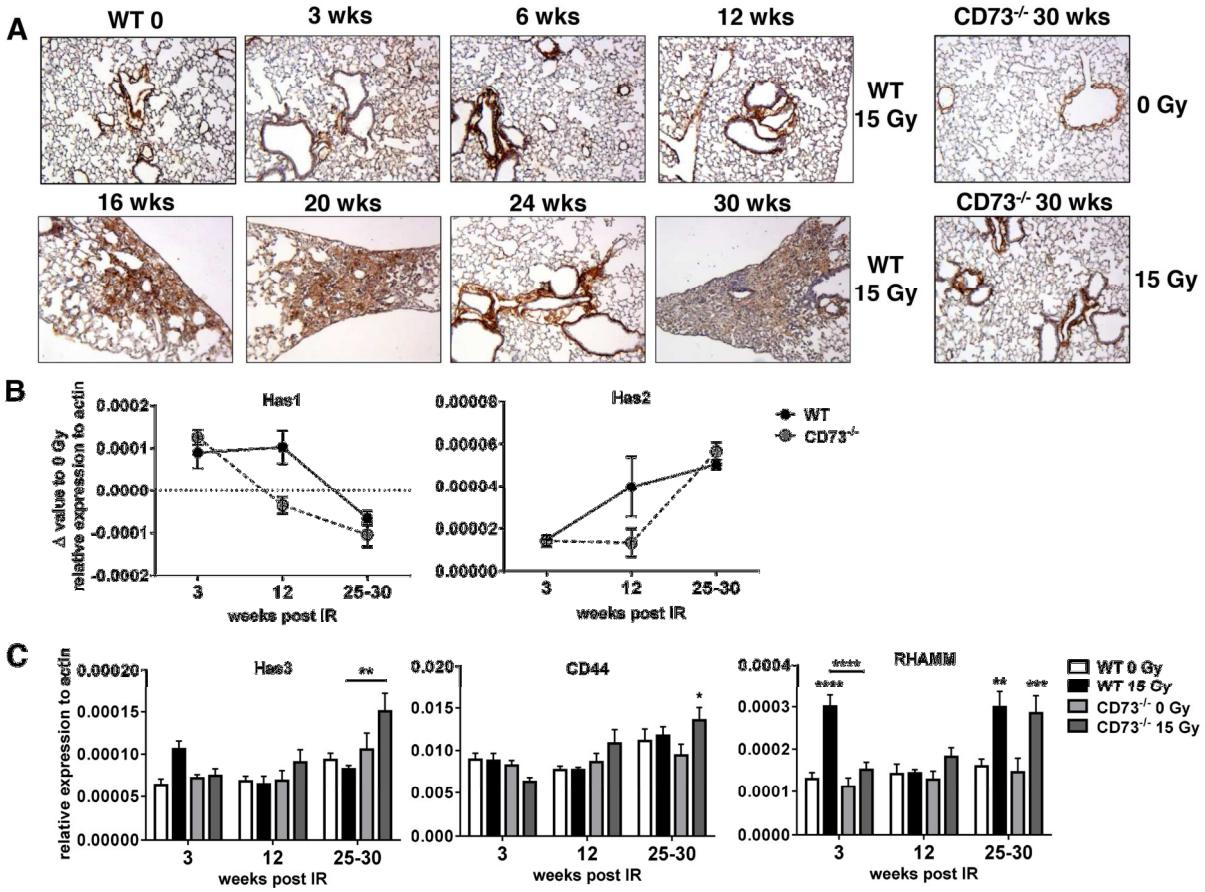

RT induced pattern of hyaluronic signaling induction varies between WT and CD73$^{-/-}$ mice. C57BL/6 or CD73$^{-/-}$ mice received 0 or 15 Gy WTI and were sacrificed at indicated time points and lung tissue was dissected. (**A**) Shown are representative IHC stainings with hyaluronan binding protein (HABP) of 0 Gy or 15 Gy irradiated WT and CD73 knockout animals at the indicated time points. (**B**) QPCR analyses for Has1 and Has2 from whole tissue RNA samples at the indicated time points after irradiation. Shown are 2 technical replicates from pooled samples per time point as Δvalues from 15 Gy value compared to 0 Gy value (shown as mean ± SD). (**C**) QPCR analyses for Has3 (n = 10/9/6/6; 7/8/9/10; 7/8/10/10), CD44 (n = 10/9/6/6; 7/7/8/10; 8/8/10/10) and RHAMM (n = 10/9/6/6; 7/8/9/10; 8/8/10/10) from whole tissue RNA samples at the indicated time points after irradiation (shown as mean ±

SEM)). *$P \leq 0.05$, **$P \leq 0.01$, ***$P \leq 0.001$, ****$P \leq 0.0001$, by two-way ANOVA followed by Sidak's multiple comparisons test.

4 Discussion

In the present PhD project, new findings on the contribution of innate and adaptive immune cells as well as the purinergic and hyaluronic system to radiation-induced pneumopathy in a murine model have been revealed. Irradiation of the thoracic region in C57BL/6 wildtype mice led to an initial reduction of $CD3^+$ T cells in the lung as well as in the spleen and cervical lymph nodes of the treated animals. While the levels of $CD3^+$ T cells stayed reduced in spleen and lymph nodes, $CD3^+$ as well as $CD4^+$ T cell populations were increased in the lung at 6 and 12 weeks post RT. Furthermore, our data showed for the first time enhanced levels of immunosuppressive regulatory $CD4^+FoxP3^+$ T cells (Treg) at 3 and 25-30 weeks after IR.

Enhanced expression of CD73 was not only found on T cells but also on alveolar macrophages and $CD45^-$ cells within the lung tissue beyond the pneumonitic phase up to 30 weeks post IR. We showed for the first time, that the enzymatic product of CD73, adenosine, accumulates in BAL as of week 16 in irradiated mice. Between 25 and 30 weeks after WTI, the pro-fibrotic mediators OPN and TGFβ were elevated and pronounced fibrosis was visible in the lung tissue. Interestingly, genetically (use of $CD73^{-/-}$ mice) or pharmacological targeting (with the monoclonal CD73 antibody TY/23) of CD73 or its product adenosine (with PEG-ADA) resulted in reduced levels of BAL adenosine, reduced expression of OPN and TGFβ, and attenuated fibrosis development.

Another difference we observed between wildtype and $CD73^{-/-}$ mice upon irradiation was the formation of organized macrophage clusters in the fibrotic tissue, which was restricted to wildtype animals. The formation of organized macrophage clusters in a murine model of RILF was described for the first time in the present project. Characterization of the macrophages from wildtype mice by flow cytometric and histologic approaches showed enhanced expression of anti-inflammatory markers on alveolar macrophages. These cells are presumably also the ones organized in clusters in the fibrotic lung tissue. In contrast, the macrophages from $CD73^{-/-}$ mice failed to express anti-inflammatory markers during the fibrotic phase, suggesting a connection between chronic enhanced levels of adenosine, the upregulation of anti-inflammatory markers on alveolar macrophages, the formation of organized macrophage clusters and fibrosis development.

The hyaluronic system was identified as an additional potential contributor to RILF that was differentially regulated after irradiation of the whole thorax in CD73 wildtype and knockout mice.

In the following, the findings of the project will be discussed in detail in the context of newest research findings and conclusions regarding the underlying mechanisms of radiation-induced pneumopathy will be drawn.

4.1 The role of CD73 and adenosine

The purinergic signaling plays an important role in the orchestration of inflammation and repair in the lung. CD39 and CD73 as well as their receptors are expressed on various pulmonary cells including cells of the innate and adaptive immune system [33]. In response to WTI, we found that CD73 was elevated on Treg and alveolar macrophages but also on other cells of leukocyte and non-leukocyte origin. The expression and activity of CD73 in the lung tissue raised time-dependently upon irradiation and led to high levels of extracellular adenosine measured in the BAL fluid. Enhanced CD73 activity and high extracellular adenosine concentrations were also observed in patients with asthma, COPD and IPF and could also been shown for BLM-induced lung injury (i.t.) [67, 152]. After WTI, adenosine was accumulating in the lung tissue before the detection of fibrotic lesions and foci, suggesting that high extracellular adenosine levels triggers fibrosis development.

To prove the functional relevance of adenosine in our model we performed the experiments also in CD73 deficient mice. In our chronic lung injury model the loss of CD73/adenosine during the initial damage response upon lung injury protected mice from RT-induced barrier dysfunction without affecting the infiltration of leukocytes. The inhibition of chronic enhanced adenosine levels led to strongly reduced fibrosis development. This is in contrast to earlier findings from the BLM i.t. model in $CD73^{-/-}$ mice, where BLM administration led to enhanced inflammation and fibrosis development, indicating a protective role for CD73/adenosine in this acute model of lung injury [152]. These conflicting data indicate different roles for adenosine in acute versus chronic disease models as described later in more detail.

Irradiation of $CD73^{-/-}$ mice led moreover to reduced expressions of the fibrotic mediators OPN and TGFβ, as well as the ECM molecules collagen and fibronectin in contrast to irradiated wildtype mice. TGFβ is a well-known and studied pro-fibrotic mediator and was shown to be upregulated initially after thorax irradiation of mice and during the fibrotic phase [124]. Inhibition of TGFβ resulted in attenuated fibrosis development in irradiated mice and reduced levels of OPN compared to untreated controls [29, 39]. OPN plays essential roles in the regulation of the recruitment and differentiation of fibroblasts and myofibroblasts [74]. The genetic loss of OPN in mice resulted in reduced levels of collagen type I, fibronectin and TGFβ [100]. Taken together the results indicate that the expression of CD73 and chronic accumulating adenosine after WTI triggers the expression and secretion of TGFβ and OPN, which can mutually influence each other. Subsequently TGFβ and OPN trigger fibroblast recruitment, myofibroblast differentiation, EMT and secretion of ECM molecules [154].

Moreover, we could show that treatment with PEG-ADA, to convert the extracellular adenosine further to inosine, or use of the CD73 antibody TY/23, to inhibit the enzymatic

conversion from AMP to adenosine, also effectively reduced fibrosis development and the expression of fibronectin. These findings support the hypothesis that the chronic accumulating adenosine, and not CD73 itself, is the main driver of RILF.

These data give new possibilities in the prevention of late adverse effects of radiation treatment in the thoracic region. Of special interest is in this sense PEG-ADA as it is already successfully used since years in the treatment of ADA deficiency in patients [42]. The integration of CD73 antibodies into the clinics is another promising approach to widen the therapeutic window of tumor treatment with radiation. It has been shown that various tumor types express CD73 on their surface (reviewed in [1]). Like on Treg, CD73 expression on tumor cells is also associated with immunosuppressive capacities, thereby helping the tumor cells to escape the host immune system and in worst case reeducate the host immune cells to support tumor growth and invasiveness [5, 136]. Consequently, the treatment of patients with CD73 antibodies could help on the one hand, to protect from early and late adverse side effects of irradiation as shown by us, and on the other hand, blocking CD73 on tumor cells could potentially help to sensitize the immune cells to the tumor cells and increase their eradication [53]. Furthermore, own preliminary data and data from other groups showed that genetic loss of CD73 reduces the metastatic potential of tumor cells [135, 136, 168]. Patient studies confirmed, that in metastatic tumors CD73 levels are increased [76].

Extracellular adenosine can either be transported via ENTs into target cells, undergo conversion into inosine or it can signal via four different adenosine receptors (for details see section 1.4.1). Current knowledge about the role of the different receptors in fibrotic diseases is mainly based on studies using BLM-induced lung injury models and ADA deficient mice. Like already mentioned in the introduction the i.t. BLM model triggers acute injury whereas the i.p. BLM and $ADA^{-/-}$ model cause chronic tissue injury and enhanced levels of adenosine [23]. The project now reveals differences in the results obtained from acute and chronic injury models. The i.t. BLM model in $CD73^{-/-}$ mice caused exaggerated lung inflammation and fibrosis [152], whereas loss of CD73 in the radiation model protected from early damage and reduced fibrosis establishment. The differential results from the acute and chronic disease models of $CD73^{-/-}$ mice suggest also distinct contributions of the adenosine receptors in the respective disease model. Therefore, the role of the adenosine receptors in the radiation-induced lung injury model is under current investigation in our lab.

It was shown that a double knockout of ADA and ADORA1 resulted in enhanced inflammation and damage of the lung, thereby attributing anti-inflammatory functions to the A1 receptor [141].

In a study with ADA and ADORA2A double knockout mice it was shown that deletion of the A2A receptor resulted in elevated inflammation and chemokine expression in the corresponding lungs [98]. Challenging ADORA2A knockout ($ADORA2A^{-/-}$) mice with i.t. BLM

resulted in a high mortality rate of the mice during the initial inflammatory phase, led to elevated numbers of inflammatory cells in the BAL and enhanced tissue damage [130]. Both studies suggest a protective role for adenosine signaling via ADORA2A upon acute and chronic tissue damage.

The functions of adenosine signaling through the low affinity receptor ADORA2B are reported to be controversial. As the receptor has a rather low affinity for adenosine it is suggested that binding of adenosine to ADORA2B takes mainly place during chronic inflammatory phases where long lasting high levels of adenosine exist [130]. ADORA2B expression was shown to be enhanced in $ADA^{-/-}$ mice and pharmacological targeting of ADORA2B resulted in reduced lung inflammation and fibrosis. Moreover, the expression of the pro-fibrotic mediators TGFβ and OPN was reduced [142]. Another study compared the role of ADORA2B in acute and chronic lung injury BLM models. While genetic deficiency of the ADORA2B in the BLM i.t. model led to an elevated acute lung injury and slightly reduction of fibrosis development, $ADORA2B^{-/-}$ mice that were exposed to BLM by i.p.-injections showed a mild inflammatory phase and a significant reduction in fibrosis development [174]. On the other hand, pharmacological inhibition of ADORA2B in a BLM i.t. model dampened levels of lung fibrosis and pulmonary inflammation, indicating that adenosine had not only protective roles [142]. In conclusion, signaling via the ADORA2B receptor seems to vary substantially between acute and chronic injury of the lung tissue.

Genetical or pharmacological targeting of the ADORA3 receptor in $ADA^{-/-}$ mice could dampen pneumopathy, indicating a pro-inflammatory role for the A3 receptor in pathogenesis [169]. In the acute injury model ADORA3 knockout ($ADORA3^{-/-}$) mice showed enhanced inflammation after BLM administration. Although ADORA3 seems to have an anti-inflammatory role during the acute injury no change in fibrosis development was observed [101].

From what is known from chronic disease models it can be speculated that radiation-induced pneumopathy might be exaggerated in ADORA1 and ADORA2A deficient mice. In contrast ADORA2B or ADORA3 deficiency might reduce disease development after WTI. In line with this speculation, unpublished microarray data from irradiated versus non-irradiated wildtype mice revealed elevated expression of ADORA3. Furthermore, preliminary quantitative real-time PCR (QPCR) data from whole tissue RNA samples confirmed enhanced levels of ADORA3 but also slightly enhanced levels of ADORA2B. First data from an own study with $ADORA2A^{-/-}$ mice indicate that loss of ADORA2A leads to high numbers of infiltrating immune cells to the lung tissue and a worsened fibrosis after WTI. Preliminary histologic data of irradiated $ADORA2B^{-/-}$ mice indicate reduced fibrosis development compared to wildtype mice, supporting our hypothesis and results from the chronic disease models.

4.2 The role of lymphocytes

WTI triggered an initial loss of T cells in the irradiated lung tissue but also systemically in the spleen and lymph nodes. Subsequently, potentially through cytokine/chemokine-induced recruitment by resident cells and activated innate immune cells, $CD4^+$ T cells infiltrated into the lung tissue at 6 weeks post-irradiation. The infiltration of $CD4^+$ T cells was also observed in patients with symptomatic pneumonitis and in other murine studies [63, 105, 121]. It has been suggested that the early infiltration of T cells is linked to late adverse side effects of WTI. In an experimental study with depletion of $CD4^+$ T cells in rats early upon IR resulted in decreased fibrosis development, indicating a disease promoting role for CD4+ T cells [107]. In contrast, previous data from our lab showed that the absence of mature T and B cells in in $RAG2^{-/-}$ mice worsened fibrosis, indicating also protective effects of lymphocytes in normal tissue toxicity [17, 157].

As the infiltration of $CD4^+$ T cells seemed to be a pathologic feature of radiation-induced pneumonitis we characterized these cells in more detail. Treg are characterized by their high CD25 expression and at least in mice, by the transcription factor Forkhead-Box-Protein P3 (FoxP3). Treg are known to be immunosuppressive and execute important roles in the regulation and dampening of inflammatory responses [126, 162]. We found elevated levels of Treg 3 weeks upon IR in the lung but also in lymph nodes and spleen of irradiated mice. The Treg seem to dampen the inflammatory response of $CD4^+$ effector cells at the very early time point after irradiation resulting in a delayed onset of pneumonitis. Enhanced levels of Treg were additionally found during the fibrotic phase 24 to 30 weeks post irradiation.

Besides TGFβ and CTLA-4, the expression of CD73 on Treg is associated with their immunosuppressive capacity [30, 109]. Furthermore, adenosine signaling via ADORA2A was shown to drive Treg induction and proliferation, so that the elevated levels of Treg during the pneumonitic and fibrotic phase might be due to high extracellular adenosine concentrations [109]. As Treg can also be induced by TGFβ [118], which is found initially after lung injury and during the fibrotic phase, their appearance could be related to the pro-fibrotic mediator TGFβ [70, 72, 124]. Treg were shown to secrete TGFβ, a mechanism by which they could drive fibrotic actions [79, 80]. A recent study showed that the presence of Treg in a murine model of BLM-induced lung injury aggravated lung fibrosis [8]. In a radiation-induced lung injury model depletion of Tregs with an anti-CD25 antibody inhibited fibrocyte recruitment and reduced fibrosis development [166].

Since we found elevated levels of $B220^+$ cells, presumably B lymphocytes, at 12 weeks after RT there might be an important role also for B cells in disease progression which needs to be further addressed but was not investigated in the present project.

The data on T-lymphocytes strongly suggest important roles for effector T cells as well as Treg in the pathology of radiation-induced pneumonitis and fibrosis. Therefore,

studies to define their roles for radiation-induced pneumopathy are under current investigation in our lab. Nevertheless, the focus of my project was the myeloid compartment of immune cells and their impact especially on RILF.

4.3 The role of myeloid cells

It has been shown that WTI triggers the secretion of pro-inflammatory cytokines and chemokines that lead to the infiltration of monocytes and macrophages in patients as well as murine studies [17, 63, 85, 125]. Our present results confirm a repopulation of pulmonary macrophages after a drastic reduction especially of alveolar macrophages initially after radiation treatment. Moreover, during the pneumonitic phase lung macrophages showed enhanced expression of the pro-inflammatory marker major histocompatibility complex class II (MHCII). As pulmonary macrophages are the first line of defense and one of their main tasks upon damage is to phagocyte cell debris and apoptotic cells, it is more than reasonable to find activation markers upregulated [12]. Interestingly, MHCII remained (slightly) enhanced throughout the observed period up to 30 weeks in the irradiated wildtype mice, indicating a chronically inflamed micromilieu upon thorax irradiation. In contrast to MHCII, the anti-inflammatory marker macrophage mannose receptor (MMR) was elevated during the early pneumonitic phase on alveolar macrophages and pulmonary macrophages, but exclusively upregulated on alveolar macrophages during the fibrotic phase 25-30 weeks after IR. These observations suggested an important role for the alveolar macrophages in orchestrating pro-fibrotic actions. The presence of alternatively activated macrophages has already been reported in patients with IPF and COPD [51, 173], in the model of i.t. BLM [62], and recently also in RILF in mice [49, 171]. But so far the contribution of alternatively activated macrophages, particularly to RILF, remains poorly understood.

Although our results show that total numbers of pulmonary macrophages were not altered in late stages of pneumopathy upon irradiation, histological analysis revealed an accumulation of lung macrophages in organized clusters. The organization of macrophages into clusters has so far only been described in a rat model of i.t. BLM [70]. Interestingly, the clustered macrophages expressed pro-fibrotic markers like TGFβ and α-SMA as well as the anti-inflammatory marker ARG1 but not the pro-inflammatory marker iNOS, corroborating our flow cytometry data. As already mentioned in the introduction, the enzymes iNOS and ARG1 compete for the same substrate (L-Arginine). Activity of ARG1 results in cell growth and collagen synthesis [171]. Through the expression of TGFβ and potentially further fibrotic mediators, the clustered macrophages may participate in fibrosis development by mediating recruitment and activation of fibroblasts and fibrocytes [165]. Taken together, the results suggest that the organized macrophages in the fibrotic lung tissue consist mainly of alveolar

macrophages as those were the ones that upregulated MMR at late stages of the disease and that they might contribute to fibrosis development.

As $CD73^{-/-}$ mice showed attenuated fibrosis development upon WTI and alveolar macrophages showed enhanced expression of CD73 in wildtype mice 6-12 weeks after irradiation we were curious about the phenotype of macrophages in the $CD73^{-/-}$ mice. Interestingly, lung tissue analyses revealed that macrophages in $CD73^{-/-}$ mice were not organized in clusters. Besides its enzymatic function, CD73 has been shown to be important in lymphocyte binding to endothelial cells during extravasation as well as in the interaction with ECM molecules like fibronectin [3, 131]. Therefore it could be discussed whether the lack of macrophage clusters in $CD73^{-/-}$ mice might be due to reduced infiltration of macrophages or an up to now not proved loss of cell-to-cell interaction. However, numbers of pulmonary macrophages depicted by flow cytometry were not different from those of wildtype mice (data not shown). Thus, the infiltration of macrophages in $CD73^{-/-}$ mice seems not to be inhibited in our model. Nevertheless, we cannot exclude that CD73 itself might impact on macrophage clustering, although also reduced numbers of macrophage clusters were also found in TY/23 and PEG-ADA treated wildtype mice after WTI (data not shown).

Phenotype analysis of lung macrophages showed that MHCII was also upregulated in $CD73^{-/-}$ mice upon irradiation. However, in $CD73^{-/-}$ mice the anti-inflammatory marker MMR was only upregulated in alveolar macrophages initially upon WTI (3 weeks), but importantly not during the fibrotic disease stages. These data suggest that adenosine might be an important driver of alternative macrophage activation and organization into clusters. In line with our finding, results from an *in vitro* study demonstrated that adenosine could promote alternative macrophage polarization [28]. Since macrophages can recruit fibroblasts and myofibroblasts, the main producers of fibrosis-associated ECM molecules like collagens and fibronectins [73], prevention of the switch of the macrophage phenotype may be a promising treatment strategy and is under current investigation in the lab.

Our data strongly suggest that the accumulation of extracellular adenosine impacts either on the organization of macrophages into cluster, on their phenotype switch from pro- to anti-inflammatory or to both processes. Up to now it is still unclear whether adenosine can also *in vivo* directly act on the macrophages to manipulate their phenotype and the clustering or whether adenosine exerts its function via action on other cells in the microenvironment. As already mentioned above, adenosine is known to exert its functions through four different adenosine receptors. Identifying and targeting the involved adenosine receptor(s) might therefore be another option to attenuate pro-fibrotic actions of chronically accumulating adenosine and is under current investigation in our lab.

From what has been discussed about adenosine receptors before it can be suggested, that ADORA1 and ADORA2A deficient mice undergoing WTI show an enhanced

pneumonitis, possibly leading to enhanced recruitment of macrophages and finally elevated fibrosis development or earlier onset of fibrotic actions. In line with this, own preliminary data indicate that loss of ADORA2A leads to high numbers of infiltrating immune cells to the lung tissue and a worsened fibrosis. Furthermore, it can be speculated that targeting signaling of adenosine via ADORA2B and ADORA3 in our radiation-induced model of pneumopathy might lead to mild pneumonitis and attenuated fibrosis development without the formation of alternatively activated macrophage clusters. Indeed, preliminary histologic data of irradiated ADORA2B$^{-/-}$ mice indicate reduced fibrosis development compared to wildtype mice.

So far our studies with the adenosine receptor knockout mice are still ongoing and lack the characterization of macrophages. But a recent study wherein mice, deficient for ABORA2B on their myeloid cell compartment (Adora2B(f/f)-LysM(Cre)), were treated with BLM i.p., resulted in reduced fibrosis development, improved lung functions and reduced numbers of macrophages expressing alternative activation markers [66]. The study suggests a direct action of adenosine on macrophages via ADORA2B that results in a phenotypic switch of macrophages. Furthermore, the development of fibrosis is suggested to be linked to macrophages and their phenotype. From those data ADORA2B seems to be a promising candidate for the prevention of lung fibrosis development also in radiation-induced lung disease.

But besides a direct action of adenosine on macrophages it is also possible that adenosine triggers changes in the microenvironment that lead to the polarization of macrophages towards an anti-inflammatory or pro-fibrotic phenotype. For example, the expression of the mediators TGFβ and OPN were reduced in irradiated CD73$^{-/-}$ mice compared to irradiated WT mice. The actions of TGFβ and OPN have already been explained in the previous section. In summary, both are important pro-fibrotic mediators regulating recruitment and differentiation of fibroblasts and myofibroblasts, driving EMT and secretion of ECM molecules. These processes are all associated with fibrosis development. Importantly TGFβ was shown to drive alternative activation of bone-marrow derived macrophages [46].

4.4 The role of hyaluronan

Our data suggest that the presence of adenosine affects the HA pathway, as we could detect less HA in the lung tissue of CD73$^{-/-}$ mice and QPCR analyses showed differential expression of HA synthases in response to irradiation. So far it remains unclear whether this is a direct effect of adenosine or whether this is a secondary effect initiated by e.g. TGFβ or OPN and can for now only be speculated. Interestingly, we found a slight, but time dependent upregulation of CD44 in the CD73 deficient animals. CD44 is not only the receptor for HA but can also bind OPN which was dramatically reduced in CD73$^{-/-}$ compared

to WT mice upon irradiation. The upregulation of CD44 might therefore be a response to low levels of HA as well as OPN, a potential feedback loop mechanism. Has3 is described to produce HA molecules of LMW that are known to act pro-inflammatory [58, 155]. Our results showed an initial upregulation of Has3 in the WT mice, potentially as a mechanism to recruit immune cells to the injury site as it has been shown that LMW HA induces the expression of MIP-1α, MIP-1β, RANTES (regulated on activation, normal T cell expressed and secreted) and MCP-1 in alveolar macrophages [92]. At the same time point also the receptor RHAMM was upregulated. RHAMM is essential for recruitment of macrophages upon stimulation with LMW fragments [107, 127, 148]. Interestingly it has been shown that inhibition of RHAMM in rats, that were challenged i.t. with BLM, reduced the number of recruited macrophages to the lung tissue as well as fibrosis development [170]. These data indicate that the early recruitment of macrophages after lung injury impacts on fibrosis development.

During the chronic accumulation of adenosine, no enhanced expression of Has3 was found in wildtype animals, instead at later time points Has3 was upregulated in $CD73^{-/-}$ mice. This observation was paralleled by the upregulation of RHAMM. It would be of interest to follow up the $CD73^{-/-}$ mice longer than 30 weeks in terms of macrophage numbers, the formation of macrophage clusters and their phenotype. It is postulated that signaling of adenosine via ADORA2A, in the early response to damage, can inhibit the upregulation of pro-inflammatory mediators (e.g. TNF-α) that are induced by LMW HA [130]. The same group further showed, that upon chronic lung inflammation LMW HA could down-regulate the expression of ADORA2A and that this regulation was CD44-dependent [26]. In a study with ADA deficient mice, signaling of adenosine through ADORA2B was linked to an increased expression of Has1 and Has2 [67]. In line with this observation, our data showed at 12 weeks after RT reduced expression of Has1 and Has2 in irradiated $CD73^{-/-}$ mice compared to irradiated wildtype mice. The data indicate a connection between accumulating extracellular adenosine and the expression of HA synthases. In this regard our results strengthen the hypothesis that the extracellular adenosine might, at least in parts, influence HA-dependent processes. But these regulatory functions seem to be of high complexity and need further investigations.

Finally, a schematic overview (depicted in Figure 5) will summarize my conclusion regarding the underlying mechanisms of radiation-induced pneumopathy with respect to CD73/adenosine, HA, macrophages and T-lymphocytes.

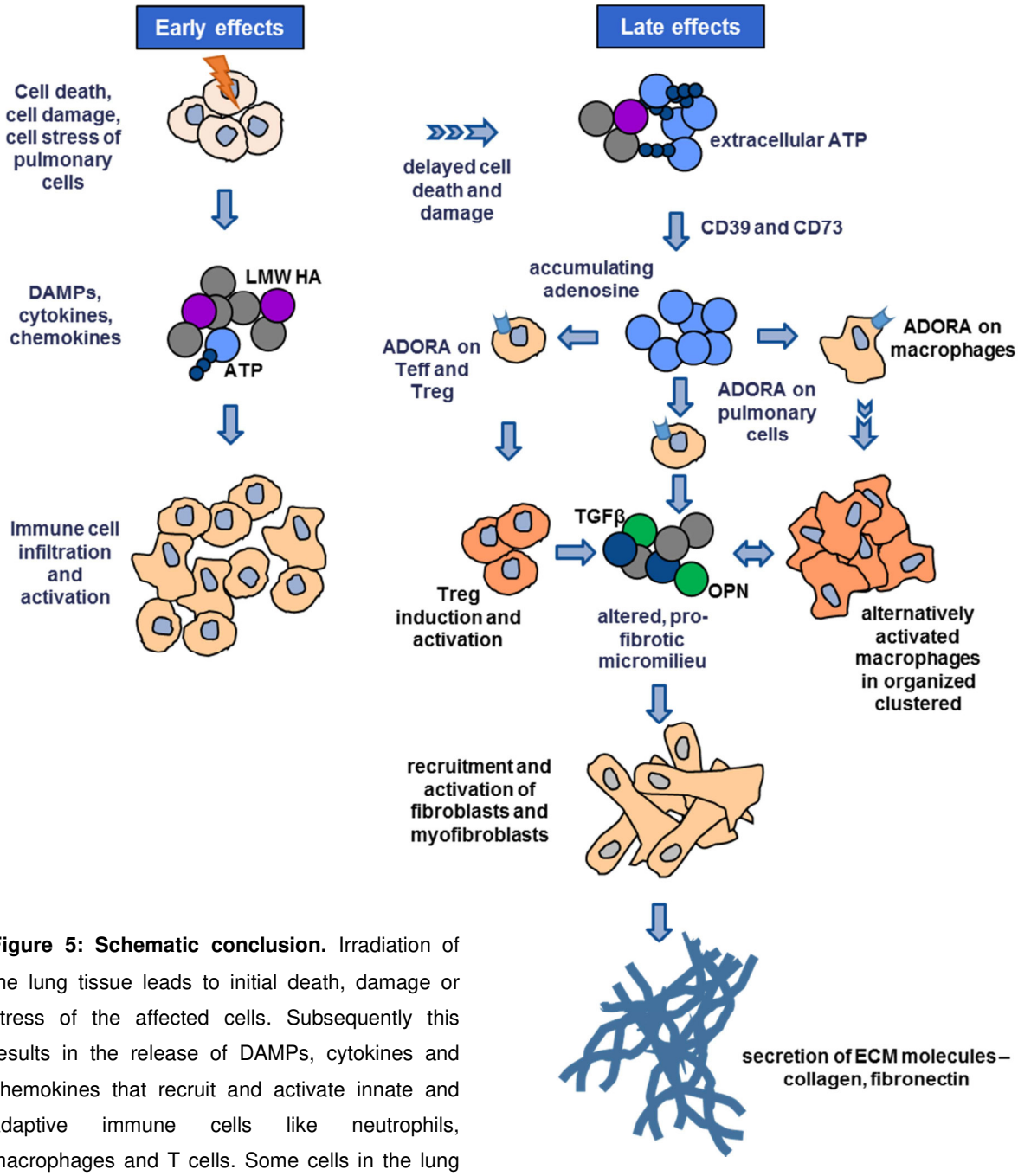

Figure 5: Schematic conclusion. Irradiation of the lung tissue leads to initial death, damage or stress of the affected cells. Subsequently this results in the release of DAMPs, cytokines and chemokines that recruit and activate innate and adaptive immune cells like neutrophils, macrophages and T cells. Some cells in the lung tissue undergo delayed damage and cell death and chronic release of soluble mediators like ATP takes place. Via CD39 and CD73 on the surface of various cells in the lung adenosine accumulates in the extracellular space. Accumulating adenosine in the irradiated lung tissue can act on multiple targets. It can either bind to adenosine receptors on the macrophages, T cells or to other lung cells. Signaling through e.g. ADORA2B on macrophages might lead to alternative activation of macrophages. Whether cluster building is necessary for alternative activation, alternative activation is necessary for cluster building or whether both processes are independent of each other remains elusive. Signaling of adenosine via ADORA2A can induce and activate Treg that are known to secrete TGFβ. Signaling of adenosine via other pulmonary cells might lead to changes in the micromilieu which could also drive alternative polarization of macrophages. The alternative activated macrophages are known to drive a pro-fibrotic and anti-inflammatory micromilieu that leads to the recruitment and activation of fibroblasts and fibrocytes, which are finally responsible for secretion of ECM molecules and development of lung fibrosis. ADORA = adenosine receptor, Teff = T effector cells.

5 Summary and Outlook

Radiotherapy is an integral part of cancer treatment for patients suffering from a neoplasm in the thoracic region. Unfortunately, life-threatening early and late side effects of the healthy lung tissue limit the applied radiation dose thereby enhancing the risk of tumor relapses. One goal of research is the widening of the therapeutic window by protection of the normal tissue without protecting the tumor from irradiation or by sensitizing the tumor cells to radiation-induced cell death without sensitizing the normal tissue. Taken together, the results obtained during my PhD project provide new insights into normal tissue toxicity upon irradiation within the thoracic region. The data suggest new treatment options for patients receiving RT by immunomodulation or modulation of adenosine signaling.

WTI in wildtype mice led to an initial loss of alveolar macrophages and elevated numbers of Treg at 3 weeks after IR. Fibrosis was detected 25-30 weeks after IR and was accompanied by the appearance of alternatively activated macrophages, which were organized in clusters, and increased numbers of Treg. Moreover, the data showed that extracellular adenosine accumulated progressively after RT in the lung tissue, which could be attributed to elevated CD73 activity. Targeting CD73 genetically ($CD73^{-/-}$) or pharmacological (TY/23), or by reducing adenosine levels with PEG-ADA treatment led in all cases to significantly reduced expression of fibrotic markers (OPN, TGFβ, fibronectin, α-SMA) and fibrosis levels. Moreover, the loss of CD73 led to an altered organization and phenotype of macrophages during the fibrotic phase. Alternatively activated macrophages that were organized in clusters were not found in in $CD73^{-/-}$ mice. Furthermore, $CD73^{-/-}$ mice showed a modified HA signaling, that has an impact on the recruitment of macrophages upon tissue damage. In conclusion, the data indicate that Treg, high levels of extracellular adenosine and alternatively activated and in clusters organized macrophages drive fibrosis development after WTI. The organization and phenotypic switch of macrophages is presumably triggered by high extracellular adenosine levels and potentially through HA signaling.

Interestingly, alternatively activated macrophages share many characteristics with tumor-associated macrophages that are known to drive tumor growth. Moreover, it has been shown that various types of tumors highly express CD73/adenosine thus having the capability to escape the immune system. Therefore, immunomodulation as well as the modulation of adenosine signaling by inhibiting CD73 are good options for an optimal widening of the therapeutic window in both directions, protection of the normal tissue and sensitization of the tumor cells.

To gain a better insight into the underlying mechanism that trigger the phenotypic switch of macrophages in wildtype mice and the role of alternative activated macrophages for disease progression and development, several aspects can be addressed in the future. One

interesting aspect is the targeting (genetic and pharmacologic) of the different adenosine receptors to uncover whether signaling through one specific receptor triggers alternative macrophage activation and fibrosis development. Moreover, a repolarization of the macrophage phenotype to a more pro-inflammatory subtype might attenuate fibrosis development. Treatment experiments with a macrophage inhibitor in our model of RILF are still ongoing, but first preliminary results indicate attenuated fibrosis development in the treated mice. Another option to interfere with the pathologic effects driven by organized and alternatively activated macrophages offers the HA system. Preventing exaggerated production of LMW HA fragments after initial damage or blocking of the HA receptor RHAMM could reduce the number of recruited macrophages. On the other hand, enhanced production of HMW HA molecules at the end of the pneumonitic phase could also be a critical step for fibrosis development. Inhibition of HA syntheses and reduction of mRNA expression could be addressed by treatment with 4-Methylumbelliferone [103].

6 References

1. Allard, B., M. Turcotte, and J. Stagg, *CD73-generated adenosine: orchestrating the tumor-stroma interplay to promote cancer growth.* J Biomed Biotechnol, 2012. 2012: p. 485156.
2. Arpin, D., D. Perol, J.Y. Blay, L. Falchero, et al., *Early variations of circulating interleukin-6 and interleukin-10 levels during thoracic radiotherapy are predictive for radiation pneumonitis.* J Clin Oncol, 2005. 23(34): p. 8748-56.
3. Arvilommi, A.M., M. Salmi, L. Airas, K. Kalimo, and S. Jalkanen, *CD73 mediates lymphocyte binding to vascular endothelium in inflamed human skin.* Eur J Immunol, 1997. 27(1): p. 248-54.
4. Barankiewicz, J., H.M. Dosch, and A. Cohen, *Extracellular nucleotide catabolism in human B and T lymphocytes. The source of adenosine production.* J Biol Chem, 1988. 263(15): p. 7094-8.
5. Beavis, P.A., J. Stagg, P.K. Darcy, and M.J. Smyth, *CD73: a potent suppressor of antitumor immune responses.* Trends Immunol, 2012. 33(5): p. 231-7.
6. Begg, A.C., F.A. Stewart, and C. Vens, *Strategies to improve radiotherapy with targeted drugs.* Nat Rev Cancer, 2011. 11(4): p. 239-53.
7. Berchtold, S., A.L. Ogilvie, C. Bogdan, P. Muhl-Zurbes, A. Ogilvie, G. Schuler, and A. Steinkasserer, *Human monocyte derived dendritic cells express functional P2X and P2Y receptors as well as ecto-nucleotidases.* FEBS Lett, 1999. 458(3): p. 424-8.
8. Birjandi, S.Z., V. Palchevskiy, Y.Y. Xue, S. Nunez, R. Kern, S.S. Weigt, J.P. Lynch, 3rd, T.A. Chatila, and J.A. Belperio, *CD4(+)CD25(hi)Foxp3(+) Cells Exacerbate Bleomycin-Induced Pulmonary Fibrosis.* Am J Pathol, 2016. 186(8): p. 2008-20.
9. Bjermer, L., R. Hallgren, K. Nilsson, L. Franzen, T. Sandstrom, B. Sarnstrand, and R. Henriksson, *Radiation-induced increase in hyaluronan and fibronectin in bronchoalveolar lavage fluid from breast cancer patients is suppressed by smoking.* Eur Respir J, 1992. 5(7): p. 785-90.
10. Bjermer, L., R. Lundgren, and R. Hallgren, *Hyaluronan and type III procollagen peptide concentrations in bronchoalveolar lavage fluid in idiopathic pulmonary fibrosis.* Thorax, 1989. 44(2): p. 126-31.
11. Blackburn, M.R., S.K. Datta, and R.E. Kellems, *Adenosine deaminase-deficient mice generated using a two-stage genetic engineering strategy exhibit a combined immunodeficiency.* J Biol Chem, 1998. 273(9): p. 5093-100.
12. Boorsma, C.E., C. Draijer, and B.N. Melgert, *Macrophage heterogeneity in respiratory diseases.* Mediators Inflamm, 2013. 2013: p. 769214.
13. Bubici, C., S. Papa, K. Dean, and G. Franzoso, *Mutual cross-talk between reactive oxygen species and nuclear factor-kappa B: molecular basis and biological significance.* Oncogene, 2006. 25(51): p. 6731-48.
14. Buenestado, A., S. Grassin Delyle, I. Arnould, F. Besnard, E. Naline, S. Blouquit-Laye, A. Chapelier, J.F. Bellamy, and P. Devillier, *The role of adenosine receptors in regulating production of tumour necrosis factor-alpha and chemokines by human lung macrophages.* Br J Pharmacol, 2010. 159(6): p. 1304-11.
15. Burnstock, G. and J.M. Boeynaems, *Purinergic signalling and immune cells.* Purinergic Signal, 2014. 10(4): p. 529-64.
16. Camus, P., A. Fanton, P. Bonniaud, C. Camus, and P. Foucher, *Interstitial lung disease induced by drugs and radiation.* Respiration, 2004. 71(4): p. 301-26.
17. Cappuccini, F., T. Eldh, D. Bruder, M. Gereke, et al., *New insights into the molecular pathology of radiation-induced pneumopathy.* Radiother Oncol, 2011. 101(1): p. 86-92.
18. Carre, P.C., R.L. Mortenson, T.E. King, Jr., P.W. Noble, C.L. Sable, and D.W. Riches, *Increased expression of the interleukin-8 gene by alveolar macrophages in idiopathic pulmonary fibrosis. A potential mechanism for the recruitment and activation of neutrophils in lung fibrosis.* J Clin Invest, 1991. 88(6): p. 1802-10.

19. Chang, B.K. and R.D. Timmerman, *Stereotactic body radiation therapy: a comprehensive review.* Am J Clin Oncol, 2007. 30(6): p. 637-44.
20. Chargari, C., F. Riet, M. Mazevet, E. Morel, C. Lepechoux, and E. Deutsch, *Complications of thoracic radiotherapy.* Presse Med, 2013. 42(9 Pt 2): p. e342-51.
21. Chen, Y., A. Shukla, S. Namiki, P.A. Insel, and W.G. Junger, *A putative osmoreceptor system that controls neutrophil function through the release of ATP, its conversion to adenosine, and activation of A2 adenosine and P2 receptors.* J Leukoc Biol, 2004. 76(1): p. 245-53.
22. Chiang, C.S., W.C. Liu, S.M. Jung, F.H. Chen, C.R. Wu, W.H. McBride, C.C. Lee, and J.H. Hong, *Compartmental responses after thoracic irradiation of mice: strain differences.* Int J Radiat Oncol Biol Phys, 2005. 62(3): p. 862-71.
23. Chua, F., J. Gauldie, and G.J. Laurent, *Pulmonary fibrosis: searching for model answers.* Am J Respir Cell Mol Biol, 2005. 33(1): p. 9-13.
24. Chunn, J.L., A. Mohsenin, H.W. Young, C.G. Lee, J.A. Elias, R.E. Kellems, and M.R. Blackburn, *Partially adenosine deaminase-deficient mice develop pulmonary fibrosis in association with adenosine elevations.* Am J Physiol Lung Cell Mol Physiol, 2006. 290(3): p. L579-87.
25. Chunn, J.L., H.W. Young, S.K. Banerjee, G.N. Colasurdo, and M.R. Blackburn, *Adenosine-dependent airway inflammation and hyperresponsiveness in partially adenosine deaminase-deficient mice.* J Immunol, 2001. 167(8): p. 4676-85.
26. Collins, S.L., K.E. Black, Y. Chan-Li, Y.H. Ahn, P.A. Cole, J.D. Powell, and M.R. Horton, *Hyaluronan fragments promote inflammation by down-regulating the anti-inflammatory A2a receptor.* Am J Respir Cell Mol Biol, 2011. 45(4): p. 675-83.
27. Csoka, A.B., G.I. Frost, and R. Stern, *The six hyaluronidase-like genes in the human and mouse genomes.* Matrix Biol, 2001. 20(8): p. 499-508.
28. Csoka, B., Z. Selmeczy, B. Koscso, Z.H. Nemeth, et al., *Adenosine promotes alternative macrophage activation via A2A and A2B receptors.* FASEB J, 2012. 26(1): p. 376-86.
29. Dadrich, M., N.H. Nicolay, P. Flechsig, S. Bickelhaupt, et al., *Combined inhibition of TGFbeta and PDGF signaling attenuates radiation-induced pulmonary fibrosis.* Oncoimmunology, 2016. 5(5): p. e1123366.
30. Deaglio, S., K.M. Dwyer, W. Gao, D. Friedman, et al., *Adenosine generation catalyzed by CD39 and CD73 expressed on regulatory T cells mediates immune suppression.* J Exp Med, 2007. 204(6): p. 1257-65.
31. Degryse, A.L., H. Tanjore, X.C. Xu, V.V. Polosukhin, B.R. Jones, F.B. McMahon, L.A. Gleaves, T.S. Blackwell, and W.E. Lawson, *Repetitive intratracheal bleomycin models several features of idiopathic pulmonary fibrosis.* Am J Physiol Lung Cell Mol Physiol, 2010. 299(4): p. L442-52.
32. Delaney, G., S. Jacob, C. Featherstone, and M. Barton, *The role of radiotherapy in cancer treatment: estimating optimal utilization from a review of evidence-based clinical guidelines.* Cancer, 2005. 104(6): p. 1129-37.
33. Della Latta, V., M. Cabiati, S. Rocchiccioli, S. Del Ry, and M.A. Morales, *The role of the adenosinergic system in lung fibrosis.* Pharmacol Res, 2013. 76: p. 182-9.
34. Ding, N.H., J.J. Li, and L.Q. Sun, *Molecular mechanisms and treatment of radiation-induced lung fibrosis.* Curr Drug Targets, 2013. 14(11): p. 1347-56.
35. Eldh, T., F. Heinzelmann, A. Velalakan, W. Budach, C. Belka, and V. Jendrossek, *Radiation-induced changes in breathing frequency and lung histology of C57BL/6J mice are time- and dose-dependent.* Strahlenther Onkol, 2012. 188(3): p. 274-81.
36. Eltzschig, H.K., M.V. Sitkovsky, and S.C. Robson, *Purinergic signaling during inflammation.* N Engl J Med, 2012. 367(24): p. 2322-33.
37. Eltzschig, H.K., T. Weissmuller, A. Mager, and T. Eckle, *Nucleotide metabolism and cell-cell interactions.* Methods Mol Biol, 2006. 341: p. 73-87.
38. Eriksson, D. and T. Stigbrand, *Radiation-induced cell death mechanisms.* Tumour Biol, 2010. 31(4): p. 363-72.
39. Flechsig, P., M. Dadrich, S. Bickelhaupt, J. Jenne, et al., *LY2109761 attenuates radiation-induced pulmonary murine fibrosis via reversal of TGF-beta and BMP-*

associated proinflammatory and proangiogenic signals. Clin Cancer Res, 2012. 18(13): p. 3616-27.
40. Fox, S.B., J. Fawcett, D.G. Jackson, I. Collins, K.C. Gatter, A.L. Harris, A. Gearing, and D.L. Simmons, *Normal human tissues, in addition to some tumors, express multiple different CD44 isoforms.* Cancer Res, 1994. 54(16): p. 4539-46.
41. Fredholm, B.B., I.J. AP, K.A. Jacobson, J. Linden, and C.E. Muller, *International Union of Basic and Clinical Pharmacology. LXXXI. Nomenclature and classification of adenosine receptors--an update.* Pharmacol Rev, 2011. 63(1): p. 1-34.
42. Gaspar, H.B., A. Aiuti, F. Porta, F. Candotti, M.S. Hershfield, and L.D. Notarangelo, *How I treat ADA deficiency.* Blood, 2009. 114(17): p. 3524-32.
43. Gessi, S., K. Varani, S. Merighi, E. Cattabriga, et al., *Expression of A3 adenosine receptors in human lymphocytes: up-regulation in T cell activation.* Mol Pharmacol, 2004. 65(3): p. 711-9.
44. Giap, H. and B. Giap, *Historical perspective and evolution of charged particle beam therapy.* Translational Cancer Research, 2012. 1(3): p. 127-136.
45. Giorgio, S., *Macrophages: plastic solutions to environmental heterogeneity.* Inflamm Res, 2013. 62(9): p. 835-43.
46. Gong, D., W. Shi, S.J. Yi, H. Chen, J. Groffen, and N. Heisterkamp, *TGFbeta signaling plays a critical role in promoting alternative macrophage activation.* BMC Immunol, 2012. 13: p. 31.
47. Graves, P.R., F. Siddiqui, M.S. Anscher, and B. Movsas, *Radiation pulmonary toxicity: from mechanisms to management.* Semin Radiat Oncol, 2010. 20(3): p. 201-7.
48. Gross, N.J., K.R. Narine, and R. Wade, *Protective effect of corticosteroids on radiation pneumonitis in mice.* Radiat Res, 1988. 113(1): p. 112-9.
49. Groves, A.M., C.J. Johnston, R.S. Misra, J.P. Williams, and J.N. Finkelstein, *Whole-Lung Irradiation Results in Pulmonary Macrophage Alterations that are Subpopulation and Strain Specific.* Radiat Res, 2015. 184(6): p. 639-49.
50. Guilliams, M., I. De Kleer, S. Henri, S. Post, et al., *Alveolar macrophages develop from fetal monocytes that differentiate into long-lived cells in the first week of life via GM-CSF.* J Exp Med, 2013. 210(10): p. 1977-92.
51. Hancock, A., L. Armstrong, R. Gama, and A. Millar, *Production of interleukin 13 by alveolar macrophages from normal and fibrotic lung.* Am J Respir Cell Mol Biol, 1998. 18(1): p. 60-5.
52. Hashimoto, D., A. Chow, C. Noizat, P. Teo, et al., *Tissue-resident macrophages self-maintain locally throughout adult life with minimal contribution from circulating monocytes.* Immunity, 2013. 38(4): p. 792-804.
53. Hay, C.M., E. Sult, Q. Huang, K. Mulgrew, et al., *Targeting CD73 in the tumor microenvironment with MEDI9447.* Oncoimmunology, 2016. 5(8): p. e1208875.
54. Hay, J., S. Shahzeidi, and G. Laurent, *Mechanisms of bleomycin-induced lung damage.* Arch Toxicol, 1991. 65(2): p. 81-94.
55. Hernnas, J., O. Nettelbladt, L. Bjermer, B. Sarnstrand, A. Malmstrom, and R. Hallgren, *Alveolar accumulation of fibronectin and hyaluronan precedes bleomycin-induced pulmonary fibrosis in the rat.* Eur Respir J, 1992. 5(4): p. 404-10.
56. Herold, S., K. Mayer, and J. Lohmeyer, *Acute lung injury: how macrophages orchestrate resolution of inflammation and tissue repair.* Front Immunol, 2011. 2: p. 65.
57. Huang, S., S. Apasov, M. Koshiba, and M. Sitkovsky, *Role of A2a extracellular adenosine receptor-mediated signaling in adenosine-mediated inhibition of T-cell activation and expansion.* Blood, 1997. 90(4): p. 1600-10.
58. Itano, N., T. Sawai, M. Yoshida, P. Lenas, et al., *Three isoforms of mammalian hyaluronan synthases have distinct enzymatic properties.* J Biol Chem, 1999. 274(35): p. 25085-92.
59. Iwakawa, M., S. Noda, T. Ohta, C. Oohira, H. Tanaka, A. Tsuji, A. Ishikawa, and T. Imai, *Strain dependent differences in a histological study of CD44 and collagen fibers*

with an expression analysis of inflammatory response-related genes in irradiated murine lung. J Radiat Res, 2004. 45(3): p. 423-33.
60. Jackson, I.L., Z. Vujaskovic, and J.D. Down, *Revisiting strain-related differences in radiation sensitivity of the mouse lung: recognizing and avoiding the confounding effects of pleural effusions.* Radiat Res, 2010. 173(1): p. 10-20.
61. Jackson, I.L., Z. Vujaskovic, and J.D. Down, *A further comparison of pathologies after thoracic irradiation among different mouse strains: finding the best preclinical model for evaluating therapies directed against radiation-induced lung damage.* Radiat Res, 2011. 175(4): p. 510-18.
62. Jakubzick, C., E.S. Choi, B.H. Joshi, M.P. Keane, S.L. Kunkel, R.K. Puri, and C.M. Hogaboam, *Therapeutic attenuation of pulmonary fibrosis via targeting of IL-4- and IL-13-responsive cells.* J Immunol, 2003. 171(5): p. 2684-93.
63. Johnston, C.J., J.P. Williams, A. Elder, E. Hernady, and J.N. Finkelstein, *Inflammatory cell recruitment following thoracic irradiation.* Exp Lung Res, 2004. 30(5): p. 369-82.
64. Johnston, C.J., J.P. Williams, P. Okunieff, and J.N. Finkelstein, *Radiation-induced pulmonary fibrosis: examination of chemokine and chemokine receptor families.* Radiat Res, 2002. 157(3): p. 256-65.
65. Johnston, C.J., T.W. Wright, P. Rubin, and J.N. Finkelstein, *Alterations in the expression of chemokine mRNA levels in fibrosis-resistant and -sensitive mice after thoracic irradiation.* Exp Lung Res, 1998. 24(3): p. 321-37.
66. Karmouty-Quintana, H., K. Philip, L.F. Acero, N.Y. Chen, et al., *Deletion of ADORA2B from myeloid cells dampens lung fibrosis and pulmonary hypertension.* FASEB J, 2015. 29(1): p. 50-60.
67. Karmouty-Quintana, H., Y. Xia, and M.R. Blackburn, *Adenosine signaling during acute and chronic disease states.* J Mol Med (Berl), 2013. 91(2): p. 173-81.
68. Kaufmann, A., B. Musset, S.H. Limberg, V. Renigunta, R. Sus, A.H. Dalpke, K.M. Heeg, B. Robaye, and P.J. Hanley, *"Host tissue damage" signal ATP promotes non-directional migration and negatively regulates toll-like receptor signaling in human monocytes.* J Biol Chem, 2005. 280(37): p. 32459-67.
69. Kelsey, C.R., M.E. Horwitz, J.P. Chino, O. Craciunescu, B. Steffey, R.J. Folz, N.J. Chao, D.A. Rizzieri, and L.B. Marks, *Severe pulmonary toxicity after myeloablative conditioning using total body irradiation: an assessment of risk factors.* Int J Radiat Oncol Biol Phys, 2011. 81(3): p. 812-8.
70. Khalil, N., O. Bereznay, M. Sporn, and A.H. Greenberg, *Macrophage production of transforming growth factor beta and fibroblast collagen synthesis in chronic pulmonary inflammation.* J Exp Med, 1989. 170(3): p. 727-37.
71. Koch, A.E., S.L. Kunkel, L.A. Harlow, D.D. Mazarakis, G.K. Haines, M.D. Burdick, R.M. Pope, and R.M. Strieter, *Macrophage inflammatory protein-1 alpha. A novel chemotactic cytokine for macrophages in rheumatoid arthritis.* J Clin Invest, 1994. 93(3): p. 921-8.
72. Kumar, R.K., R. O'Grady, S.E. Maronese, and M.R. Wilson, *Epithelial cell-derived transforming growth factor-beta in bleomycin-induced pulmonary injury.* Int J Exp Pathol, 1996. 77(3): p. 99-107.
73. Lekkerkerker, A.N., J. Aarbiou, T. van Es, and R.A. Janssen, *Cellular players in lung fibrosis.* Curr Pharm Des, 2012. 18(27): p. 4093-102.
74. Lenga, Y., A. Koh, A.S. Perera, C.A. McCulloch, J. Sodek, and R. Zohar, *Osteopontin expression is required for myofibroblast differentiation.* Circ Res, 2008. 102(3): p. 319-27.
75. Lesley, J., R. Hyman, N. English, J.B. Catterall, and G.A. Turner, *CD44 in inflammation and metastasis.* Glycoconj J, 1997. 14(5): p. 611-22.
76. Leth-Larsen, R., R. Lund, H.V. Hansen, A.V. Laenkholm, D. Tarin, O.N. Jensen, and H.J. Ditzel, *Metastasis-related plasma membrane proteins of human breast cancer cells identified by comparative quantitative mass spectrometry.* Mol Cell Proteomics, 2009. 8(6): p. 1436-49.

77. Li, Y., D. Jiang, J. Liang, E.B. Meltzer, A. Gray, R. Miura, L. Wogensen, Y. Yamaguchi, and P.W. Noble, *Severe lung fibrosis requires an invasive fibroblast phenotype regulated by hyaluronan and CD44.* J Exp Med, 2011. 208(7): p. 1459-71.
78. Liauw, S.L., P.P. Connell, and R.R. Weichselbaum, *New paradigms and future challenges in radiation oncology: an update of biological targets and technology.* Sci Transl Med, 2013. 5(173): p. 173sr2.
79. Liu, F., J. Liu, D. Weng, Y. Chen, L. Song, Q. He, and J. Chen, *CD4+CD25+Foxp3+ regulatory T cells depletion may attenuate the development of silica-induced lung fibrosis in mice.* PLoS One, 2010. 5(11): p. e15404.
80. Lo Re, S., M. Lecocq, F. Uwambayinema, Y. Yakoub, et al., *Platelet-derived growth factor-producing CD4+ Foxp3+ regulatory T lymphocytes promote lung fibrosis.* Am J Respir Crit Care Med, 2011. 184(11): p. 1270-81.
81. Lohmann-Matthes, M.L., C. Steinmuller, and G. Franke-Ullmann, *Pulmonary macrophages.* Eur Respir J, 1994. 7(9): p. 1678-89.
82. Luo, F., N.B. Le, T. Mills, N.Y. Chen, et al., *Extracellular adenosine levels are associated with the progression and exacerbation of pulmonary fibrosis.* FASEB J, 2016. 30(2): p. 874-83.
83. Marks, L.B., X. Yu, Z. Vujaskovic, W. Small, Jr., R. Folz, and M.S. Anscher, *Radiation-induced lung injury.* Semin Radiat Oncol, 2003. 13(3): p. 333-45.
84. Marquardt, D.L., L.L. Walker, and S. Heinemann, *Cloning of two adenosine receptor subtypes from mouse bone marrow-derived mast cells.* J Immunol, 1994. 152(9): p. 4508-15.
85. Martin, C., S. Romero, J. Sanchez-Paya, B. Massuti, J.M. Arriero, and L. Hernandez, *Bilateral lymphocytic alveolitis: a common reaction after unilateral thoracic irradiation.* Eur Respir J, 1999. 13(4): p. 727-32.
86. Matute-Bello, G., J.S. Lee, C.W. Frevert, W.C. Liles, S. Sutlief, K. Ballman, V. Wong, A. Selk, and T.R. Martin, *Optimal timing to repopulation of resident alveolar macrophages with donor cells following total body irradiation and bone marrow transplantation in mice.* J Immunol Methods, 2004. 292(1-2): p. 25-34.
87. Maus, U.A., K. Waelsch, W.A. Kuziel, T. Delbeck, et al., *Monocytes are potent facilitators of alveolar neutrophil emigration during lung inflammation: role of the CCL2-CCR2 axis.* J Immunol, 2003. 170(6): p. 3273-8.
88. Maxwell, C.A., J. McCarthy, and E. Turley, *Cell-surface and mitotic-spindle RHAMM: moonlighting or dual oncogenic functions?* J Cell Sci, 2008. 121(Pt 7): p. 925-32.
89. McBride, W.H., *Cytokine cascades in late normal tissue radiation responses.* Int J Radiat Oncol Biol Phys, 1995. 33(1): p. 233-4.
90. McDonald, S., P. Rubin, T.L. Phillips, and L.B. Marks, *Injury to the lung from cancer therapy: clinical syndromes, measurable endpoints, and potential scoring systems.* Int J Radiat Oncol Biol Phys, 1995. 31(5): p. 1187-203.
91. McKee, C.M., C.J. Lowenstein, M.R. Horton, J. Wu, C. Bao, B.Y. Chin, A.M. Choi, and P.W. Noble, *Hyaluronan fragments induce nitric-oxide synthase in murine macrophages through a nuclear factor kappaB-dependent mechanism.* J Biol Chem, 1997. 272(12): p. 8013-8.
92. McKee, C.M., M.B. Penno, M. Cowman, M.D. Burdick, R.M. Strieter, C. Bao, and P.W. Noble, *Hyaluronan (HA) fragments induce chemokine gene expression in alveolar macrophages. The role of HA size and CD44.* J Clin Invest, 1996. 98(10): p. 2403-13.
93. Midgley, A.C., M. Rogers, M.B. Hallett, A. Clayton, T. Bowen, A.O. Phillips, and R. Steadman, *Transforming growth factor-beta1 (TGF-beta1)-stimulated fibroblast to myofibroblast differentiation is mediated by hyaluronan (HA)-facilitated epidermal growth factor receptor (EGFR) and CD44 co-localization in lipid rafts.* J Biol Chem, 2013. 288(21): p. 14824-38.
94. Mirabet, M., C. Herrera, O.J. Cordero, J. Mallol, C. Lluis, and R. Franco, *Expression of A2B adenosine receptors in human lymphocytes: their role in T cell activation.* J Cell Sci, 1999. 112 (Pt 4): p. 491-502.

95. Mladenov, E., S. Magin, A. Soni, and G. Iliakis, *DNA double-strand break repair as determinant of cellular radiosensitivity to killing and target in radiation therapy.* Front Oncol, 2013. 3: p. 113.
96. Moeller, A., K. Ask, D. Warburton, J. Gauldie, and M. Kolb, *The bleomycin animal model: a useful tool to investigate treatment options for idiopathic pulmonary fibrosis?* Int J Biochem Cell Biol, 2008. 40(3): p. 362-82.
97. Moeller, B.J. and M.W. Dewhirst, *HIF-1 and tumour radiosensitivity.* Br J Cancer, 2006. 95(1): p. 1-5.
98. Mohsenin, A., T. Mi, Y. Xia, R.E. Kellems, J.F. Chen, and M.R. Blackburn, *Genetic removal of the A2A adenosine receptor enhances pulmonary inflammation, mucin production, and angiogenesis in adenosine deaminase-deficient mice.* Am J Physiol Lung Cell Mol Physiol, 2007. 293(3): p. L753-61.
99. Moore, B.B. and C.M. Hogaboam, *Murine models of pulmonary fibrosis.* Am J Physiol Lung Cell Mol Physiol, 2008. 294(2): p. L152-60.
100. Mori, R., T.J. Shaw, and P. Martin, *Molecular mechanisms linking wound inflammation and fibrosis: knockdown of osteopontin leads to rapid repair and reduced scarring.* J Exp Med, 2008. 205(1): p. 43-51.
101. Morschl, E., J.G. Molina, J.B. Volmer, A. Mohsenin, R.S. Pero, J.S. Hong, F. Kheradmand, J.J. Lee, and M.R. Blackburn, *A3 adenosine receptor signaling influences pulmonary inflammation and fibrosis.* Am J Respir Cell Mol Biol, 2008. 39(6): p. 697-705.
102. Mouratis, M.A. and V. Aidinis, *Modeling pulmonary fibrosis with bleomycin.* Curr Opin Pulm Med, 2011. 17(5): p. 355-61.
103. Nagy, N., H.F. Kuipers, A.R. Frymoyer, H.D. Ishak, J.B. Bollyky, T.N. Wight, and P.L. Bollyky, *4-methylumbelliferone treatment and hyaluronan inhibition as a therapeutic strategy in inflammation, autoimmunity, and cancer.* Front Immunol, 2015. 6: p. 123.
104. Nakamura, K., S. Yokohama, M. Yoneda, S. Okamoto, Y. Tamaki, T. Ito, M. Okada, K. Aso, and I. Makino, *High, but not low, molecular weight hyaluronan prevents T-cell-mediated liver injury by reducing proinflammatory cytokines in mice.* J Gastroenterol, 2004. 39(4): p. 346-54.
105. Nakayama, Y., S. Makino, Y. Fukuda, K.Y. Min, A. Shimizu, and N. Ohsawa, *Activation of lavage lymphocytes in lung injuries caused by radiotherapy for lung cancer.* Int J Radiat Oncol Biol Phys, 1996. 34(2): p. 459-67.
106. Naor, D., R.V. Sionov, and D. Ish-Shalom, *CD44: structure, function, and association with the malignant process.* Adv Cancer Res, 1997. 71: p. 241-319.
107. Noble, P.W., C.M. McKee, M. Cowman, and H.S. Shin, *Hyaluronan fragments activate an NF-kappa B/I-kappa B alpha autoregulatory loop in murine macrophages.* J Exp Med, 1996. 183(5): p. 2373-8.
108. Ohshima, Y., M. Tsukimoto, T. Takenouchi, H. Harada, A. Suzuki, M. Sato, H. Kitani, and S. Kojima, *gamma-Irradiation induces P2X(7) receptor-dependent ATP release from B16 melanoma cells.* Biochim Biophys Acta, 2010. 1800(1): p. 40-6.
109. Ohta, A. and M. Sitkovsky, *Extracellular adenosine-mediated modulation of regulatory T cells.* Front Immunol, 2014. 5: p. 304.
110. Ozturk, B., I. Egehan, S. Atavci, and M. Kitapci, *Pentoxifylline in prevention of radiation-induced lung toxicity in patients with breast and lung cancer: a double-blind randomized trial.* Int J Radiat Oncol Biol Phys, 2004. 58(1): p. 213-9.
111. Panther, E., M. Idzko, Y. Herouy, H. Rheinen, P.J. Gebicke-Haerter, U. Mrowietz, S. Dichmann, and J. Norgauer, *Expression and function of adenosine receptors in human dendritic cells.* FASEB J, 2001. 15(11): p. 1963-70.
112. Piccinini, A.M. and K.S. Midwood, *DAMPening inflammation by modulating TLR signalling.* Mediators Inflamm, 2010. 2010.
113. Pollard, J.W., *Trophic macrophages in development and disease.* Nat Rev Immunol, 2009. 9(4): p. 259-70.
114. Ponta, H., L. Sherman, and P.A. Herrlich, *CD44: from adhesion molecules to signalling regulators.* Nat Rev Mol Cell Biol, 2003. 4(1): p. 33-45.

115. Powell, J.D. and M.R. Horton, *Threat matrix: low-molecular-weight hyaluronan (HA) as a danger signal.* Immunol Res, 2005. 31(3): p. 207-18.
116. Price, R.D., S. Myers, I.M. Leigh, and H.A. Navsaria, *The role of hyaluronic acid in wound healing: assessment of clinical evidence.* Am J Clin Dermatol, 2005. 6(6): p. 393-402.
117. Priebe, T., C.D. Platsoucas, and J.A. Nelson, *Adenosine receptors and modulation of natural killer cell activity by purine nucleosides.* Cancer Res, 1990. 50(14): p. 4328-31.
118. Prochazkova, J., J. Fric, K. Pokorna, A. Neuwirth, M. Krulova, A. Zajicova, and V. Holan, *Distinct regulatory roles of transforming growth factor-beta and interleukin-4 in the development and maintenance of natural and induced CD4+ CD25+ Foxp3+ regulatory T cells.* Immunology, 2009. 128(1 Suppl): p. e670-8.
119. Provatopoulou, X., E. Athanasiou, and A. Gounaris, *Predictive markers of radiation pneumonitis.* Anticancer Res, 2008. 28(4C): p. 2421-32.
120. Quan, T.E., S.E. Cowper, and R. Bucala, *The role of circulating fibrocytes in fibrosis.* Curr Rheumatol Rep, 2006. 8(2): p. 145-50.
121. Roberts, C.M., E. Foulcher, J.J. Zaunders, D.H. Bryant, J. Freund, D. Cairns, R. Penny, G.W. Morgan, and S.N. Breit, *Radiation pneumonitis: a possible lymphocyte-mediated hypersensitivity reaction.* Ann Intern Med, 1993. 118(9): p. 696-700.
122. Robnett, T.J., M. Machtay, E.F. Vines, M.G. McKenna, K.M. Algazy, and W.G. McKenna, *Factors predicting severe radiation pneumonitis in patients receiving definitive chemoradiation for lung cancer.* Int J Radiat Oncol Biol Phys, 2000. 48(1): p. 89-94.
123. Rosenbaum, D., S. Peric, M. Holecek, and H.E. Ward, *Hyaluronan in radiation-induced lung disease in the rat.* Radiat Res, 1997. 147(5): p. 585-91.
124. Rube, C.E., D. Uthe, K.W. Schmid, K.D. Richter, J. Wessel, A. Schuck, N. Willich, and C. Rube, *Dose-dependent induction of transforming growth factor beta (TGF-beta) in the lung tissue of fibrosis-prone mice after thoracic irradiation.* Int J Radiat Oncol Biol Phys, 2000. 47(4): p. 1033-42.
125. Rubin, P., C.J. Johnston, J.P. Williams, S. McDonald, and J.N. Finkelstein, *A perpetual cascade of cytokines postirradiation leads to pulmonary fibrosis.* Int J Radiat Oncol Biol Phys, 1995. 33(1): p. 99-109.
126. Sakaguchi, S., T. Yamaguchi, T. Nomura, and M. Ono, *Regulatory T cells and immune tolerance.* Cell, 2008. 133(5): p. 775-87.
127. Savani, R.C., G. Hou, P. Liu, C. Wang, et al., *A role for hyaluronan in macrophage accumulation and collagen deposition after bleomycin-induced lung injury.* Am J Respir Cell Mol Biol, 2000. 23(4): p. 475-84.
128. Schaue, D., E.L. Kachikwu, and W.H. McBride, *Cytokines in radiobiological responses: a review.* Radiat Res, 2012. 178(6): p. 505-23.
129. Schaue, D. and W.H. McBride, *Links between innate immunity and normal tissue radiobiology.* Radiat Res, 2010. 173(4): p. 406-17.
130. Scheibner, K.A., S. Boodoo, S. Collins, K.E. Black, Y. Chan-Li, P. Zarek, J.D. Powell, and M.R. Horton, *The adenosine a2a receptor inhibits matrix-induced inflammation in a novel fashion.* Am J Respir Cell Mol Biol, 2009. 40(3): p. 251-9.
131. Shimizu, Y. and S. Shaw, *Lymphocyte interactions with extracellular matrix.* FASEB J, 1991. 5(9): p. 2292-9.
132. Smith, R.E., R.M. Strieter, S.H. Phan, N.W. Lukacs, et al., *Production and function of murine macrophage inflammatory protein-1 alpha in bleomycin-induced lung injury.* J Immunol, 1994. 153(10): p. 4704-12.
133. Soltes, L., R. Mendichi, G. Kogan, J. Schiller, M. Stankovska, and J. Arnhold, *Degradative action of reactive oxygen species on hyaluronan.* Biomacromolecules, 2006. 7(3): p. 659-68.
134. Sprung, C.N., H.B. Forrester, S. Siva, and O.A. Martin, *Immunological markers that predict radiation toxicity.* Cancer Lett, 2015. 368(2): p. 191-7.

135. Stagg, J., P.A. Beavis, U. Divisekera, M.C. Liu, A. Moller, P.K. Darcy, and M.J. Smyth, *CD73-deficient mice are resistant to carcinogenesis.* Cancer Res, 2012. 72(9): p. 2190-6.
136. Stagg, J., U. Divisekera, H. Duret, T. Sparwasser, M.W. Teng, P.K. Darcy, and M.J. Smyth, *CD73-deficient mice have increased antitumor immunity and are resistant to experimental metastasis.* Cancer Res, 2011. 71(8): p. 2892-900.
137. Steighner, R.J. and L.F. Povirk, *Bleomycin-induced DNA lesions at mutational hot spots: implications for the mechanism of double-strand cleavage.* Proc Natl Acad Sci U S A, 1990. 87(21): p. 8350-4.
138. Steinmuller, C., G. Franke-Ullmann, M.L. Lohmann-Matthes, and A. Emmendorffer, *Local activation of nonspecific defense against a respiratory model infection by application of interferon-gamma: comparison between rat alveolar and interstitial lung macrophages.* Am J Respir Cell Mol Biol, 2000. 22(4): p. 481-90.
139. Stern, R., A.A. Asari, and K.N. Sugahara, *Hyaluronan fragments: an information-rich system.* Eur J Cell Biol, 2006. 85(8): p. 699-715.
140. Stridh, S., F. Palm, and P. Hansell, *Renal interstitial hyaluronan: functional aspects during normal and pathological conditions.* Am J Physiol Regul Integr Comp Physiol, 2012. 302(11): p. R1235-49.
141. Sun, C.X., H.W. Young, J.G. Molina, J.B. Volmer, J. Schnermann, and M.R. Blackburn, *A protective role for the A1 adenosine receptor in adenosine-dependent pulmonary injury.* J Clin Invest, 2005. 115(1): p. 35-43.
142. Sun, C.X., H. Zhong, A. Mohsenin, E. Morschl, J.L. Chunn, J.G. Molina, L. Belardinelli, D. Zeng, and M.R. Blackburn, *Role of A2B adenosine receptor signaling in adenosine-dependent pulmonary inflammation and injury.* J Clin Invest, 2006. 116(8): p. 2173-2182.
143. Takahashi, F., K. Takahashi, T. Okazaki, K. Maeda, H. Ienaga, M. Maeda, S. Kon, T. Uede, and Y. Fukuchi, *Role of osteopontin in the pathogenesis of bleomycin-induced pulmonary fibrosis.* Am J Respir Cell Mol Biol, 2001. 24(3): p. 264-71.
144. Taniguchi, N., K. Kawahara, K. Yone, T. Hashiguchi, et al., *High mobility group box chromosomal protein 1 plays a role in the pathogenesis of rheumatoid arthritis as a novel cytokine.* Arthritis Rheum, 2003. 48(4): p. 971-81.
145. Teder, P., R.W. Vandivier, D. Jiang, J. Liang, L. Cohn, E. Pure, P.M. Henson, and P.W. Noble, *Resolution of lung inflammation by CD44.* Science, 2002. 296(5565): p. 155-8.
146. Todd, N.W., I.G. Luzina, and S.P. Atamas, *Molecular and cellular mechanisms of pulmonary fibrosis.* Fibrogenesis Tissue Repair, 2012. 5(1): p. 11.
147. Tolg, C., S.R. Hamilton, E. Zalinska, L. McCulloch, et al., *A RHAMM mimetic peptide blocks hyaluronan signaling and reduces inflammation and fibrogenesis in excisional skin wounds.* Am J Pathol, 2012. 181(4): p. 1250-70.
148. Tolg, C., J.B. McCarthy, A. Yazdani, and E.A. Turley, *Hyaluronan and RHAMM in wound repair and the "cancerization" of stromal tissues.* Biomed Res Int, 2014. 2014: p. 103923.
149. Tolle, L.B. and T.J. Standiford, *Danger-associated molecular patterns (DAMPs) in acute lung injury.* J Pathol, 2013. 229(2): p. 145-56.
150. Turley, E.A., P.W. Noble, and L.Y. Bourguignon, *Signaling properties of hyaluronan receptors.* J Biol Chem, 2002. 277(7): p. 4589-92.
151. van Rongen, E., H.T. Madhuizen, C.H. Tan, S.K. Durham, and M.J. Gijbels, *Early and late effects of fractionated irradiation and the kinetics of repair in rat lung.* Radiother Oncol, 1990. 17(4): p. 323-37.
152. Volmer, J.B., L.F. Thompson, and M.R. Blackburn, *Ecto-5'-nucleotidase (CD73)-mediated adenosine production is tissue protective in a model of bleomycin-induced lung injury.* J Immunol, 2006. 176(7): p. 4449-58.
153. Ward, E.R., L.W. Hedlund, W.C. Kurylo, C.T. Wheeler, G.P. Cofer, M.W. Dewhirst, L.B. Marks, and Z. Vujaskovic, *Proton and hyperpolarized helium magnetic resonance imaging of radiation-induced lung injury in rats.* Int J Radiat Oncol Biol Phys, 2004. 58(5): p. 1562-9.

154. Weber, C.E., N.Y. Li, P.Y. Wai, and P.C. Kuo, *Epithelial-mesenchymal transition, TGF-beta, and osteopontin in wound healing and tissue remodeling after injury.* J Burn Care Res, 2012. 33(3): p. 311-8.
155. Weigel, P.H., V.C. Hascall, and M. Tammi, *Hyaluronan synthases.* J Biol Chem, 1997. 272(22): p. 13997-4000.
156. Westbury, C.B. and J.R. Yarnold, *Radiation fibrosis--current clinical and therapeutic perspectives.* Clin Oncol (R Coll Radiol), 2012. 24(10): p. 657-72.
157. Westermann, W., R. Schobl, E.P. Rieber, and K.H. Frank, *Th2 cells as effectors in postirradiation pulmonary damage preceding fibrosis in the rat.* Int J Radiat Biol, 1999. 75(5): p. 629-38.
158. Wilkinson, T.S., S. Potter-Perigo, C. Tsoi, L.C. Altman, and T.N. Wight, *Pro- and anti-inflammatory factors cooperate to control hyaluronan synthesis in lung fibroblasts.* Am J Respir Cell Mol Biol, 2004. 31(1): p. 92-9.
159. Willers, H., C.G. Azzoli, W.L. Santivasi, and F. Xia, *Basic mechanisms of therapeutic resistance to radiation and chemotherapy in lung cancer.* Cancer J, 2013. 19(3): p. 200-7.
160. Williams, J.P., C.J. Johnston, and J.N. Finkelstein, *Treatment for radiation-induced pulmonary late effects: spoiled for choice or looking in the wrong direction?* Curr Drug Targets, 2010. 11(11): p. 1386-94.
161. Willis, B.C., R.M. duBois, and Z. Borok, *Epithelial origin of myofibroblasts during fibrosis in the lung.* Proc Am Thorac Soc, 2006. 3(4): p. 377-82.
162. Wing, K. and S. Sakaguchi, *Regulatory T cells exert checks and balances on self tolerance and autoimmunity.* Nat Immunol, 2010. 11(1): p. 7-13.
163. Wynn, T.A., *Integrating mechanisms of pulmonary fibrosis.* J Exp Med, 2011. 208(7): p. 1339-50.
164. Wynn, T.A. and L. Barron, *Macrophages: master regulators of inflammation and fibrosis.* Semin Liver Dis, 2010. 30(3): p. 245-57.
165. Wynn, T.A. and T.R. Ramalingam, *Mechanisms of fibrosis: therapeutic translation for fibrotic disease.* Nat Med, 2012. 18(7): p. 1028-40.
166. Xiong, S., R. Guo, Z. Yang, L. Xu, et al., *Treg depletion attenuates irradiation-induced pulmonary fibrosis by reducing fibrocyte accumulation, inducing Th17 response, and shifting IFN-gamma, IL-12/IL-4, IL-5 balance.* Immunobiology, 2015. 220(11): p. 1284-91.
167. Yegutkin, G.G., *Nucleotide- and nucleoside-converting ectoenzymes: Important modulators of purinergic signalling cascade.* Biochim Biophys Acta, 2008. 1783(5): p. 673-94.
168. Yegutkin, G.G., F. Marttila-Ichihara, M. Karikoski, J. Niemela, J.P. Laurila, K. Elima, S. Jalkanen, and M. Salmi, *Altered purinergic signaling in CD73-deficient mice inhibits tumor progression.* Eur J Immunol, 2011. 41(5): p. 1231-41.
169. Young, H.W., J.G. Molina, D. Dimina, H. Zhong, M. Jacobson, L.N. Chan, T.S. Chan, J.J. Lee, and M.R. Blackburn, *A3 adenosine receptor signaling contributes to airway inflammation and mucus production in adenosine deaminase-deficient mice.* J Immunol, 2004. 173(2): p. 1380-9.
170. Zaman, A., Z. Cui, J.P. Foley, H. Zhao, P.C. Grimm, H.M. Delisser, and R.C. Savani, *Expression and role of the hyaluronan receptor RHAMM in inflammation after bleomycin injury.* Am J Respir Cell Mol Biol, 2005. 33(5): p. 447-54.
171. Zhang, H., G. Han, H. Liu, J. Chen, X. Ji, F. Zhou, Y. Zhou, and C. Xie, *The development of classically and alternatively activated macrophages has different effects on the varied stages of radiation-induced pulmonary injury in mice.* J Radiat Res, 2011. 52(6): p. 717-26.
172. Zhang, J.G., L. Hepburn, G. Cruz, R.A. Borman, and K.L. Clark, *The role of adenosine A2A and A2B receptors in the regulation of TNF-alpha production by human monocytes.* Biochem Pharmacol, 2005. 69(6): p. 883-9.
173. Zhou, Y., J.N. Murthy, D. Zeng, L. Belardinelli, and M.R. Blackburn, *Alterations in adenosine metabolism and signaling in patients with chronic obstructive pulmonary disease and idiopathic pulmonary fibrosis.* PLoS One, 2010. 5(2): p. e9224.

174. Zhou, Y., D.J. Schneider, E. Morschl, L. Song, M. Pedroza, H. Karmouty-Quintana, T. Le, C.X. Sun, and M.R. Blackburn, *Distinct roles for the A2B adenosine receptor in acute and chronic stages of bleomycin-induced lung injury.* J Immunol, 2011. 186(2): p. 1097-106.

7 List of Abbreviations

ADA	adenosine deaminase
$ADA^{-/-}$	ADA knockout
ADORA1	adenosine receptor 1
ADORA2A	adenosine receptor 2A
$ADORA2A^{-/-}$	ADORA2A knockout
ADORA2B	adenosine receptor 2B
$ADORA2B^{-/-}$	ADORA2B knockout
ADORA3	adenosine receptor 3
$ADORA3^{-/-}$	ADORA3 knockout
ADP	adenosine diphosphate
AMP	adenosine monophosphate
ARG1	arginase-1
ATP	adenosine triphosphate
BAL(F)	bronchoalveolar lavage (fluid)
BLM	bleomycin
CCL-2	macrophage chemoattractant protein-1
CD39	ectonucleoside triphosphate diphosphohydrolase-1
CD73	ecto-5′-nucleotidase
$CD73^{-/-}$	CD73 knockout
COPD	chronic abstructive pulmonary disease
CSF-1	colony-stimulatin factor 1
DAMP	danger associated molecule pattern
ECM	extracellular matrix
EMT	epithelial-mesenchymal transition
ENT	equilibrative nucleoside transporter
FoxP3	forkhead-box-protein P3
HA	hyaluronan
Has1-3	HA synthase 1-3
HMGB1	high mobility group box 1 protein
HMW	high molecular weight
HSP70	heat-shock protein 70
HYAL	hyaluronidase
i.p.	intraperitoneal
i.t.	intratracheal
i.v.	intravenous
IL-1	interleukin 1 (or any other number)
INF-γ	interferon-gamma
iNOS	inducible nitric oxide synthase
IPF	idiopathic pulmonary fibrosis
IR	ionizing radiation
LMW	low molecular weight
MCP-1	macrophage chemoattractant protein-1
M-CSF	macrophage-colony stimulating factor

MHCII	major histocombatibility complex class II
MIP-1β/2	macrophage inflammatory protein-1beta/-2
MMR	macrophage mannose receptor
NF-κB	nuclear factor kappa-light-chain-enhancer of activated B cells
NOS	nitric oxide species
OPN	osteopontin
PDGF	platelet derived growth factor
PEG-ADA	pegylated ADA
QPCR	quantitative real-time PCR
RAG2	recombination activating gene 2
RANTES	regulated on activation, normal T cell expressed and secreted
RHAMM	receptor for HA-mediated motility
RILF	radiation-induced lung fibrosis
ROS	reactive oxygen species
RT	radiotherapy
TBI	total body irradiation
TGFβ	transforming growth factor beta
TLR	toll-like receptor
TNFα	tumor necrosis factor alpha
WTI	whole thorax irradiation
α-SMA	alpha smooth muscle actin

8 List of Figures

9 Curriculum vitae

Der Lebenslauf ist aus Gründen des Datenschutzes nicht enthalten.

Der Lebenslauf ist aus Gründen des Datenschutzes nicht enthalten.

Der Lebenslauf ist aus Gründen des Datenschutzes nicht enthalten.

10 Declarations

Erklärung:

Hiermit erkläre ich, gem. § 6 Abs. 2, g der Promotionsordnung der Fakultät für Biologie zur Erlangung der Dr. rer. nat., dass ich das Arbeitsgebiet, dem das Thema *„Role of radiation-induced immune changes for normal tissue toxicity with a focus on CD73/adenosine signaling and macrophages“* zuzuordnen ist, in Forschung und Lehre vertrete und den Antrag von *Simone de Leve* befürworte.

Essen, den _____ _____ _____

Name des wissenschaftl. Betreuers/Mitglieds der Universität Duisburg-Essen	Unterschrift des wissenschaftl. Betreuers/Mitglieds der Universität Duisburg-Essen

Erklärung:

Hiermit erkläre ich, gem. § 7 Abs. 2, d und f der Promotionsordnung der Fakultät für Biologie zur Erlangung des Dr. rer. nat., dass ich die vorliegende Dissertation selbständig verfasst und mich keiner anderen als der angegebenen Hilfsmittel bedient habe und alle wörtlich oder inhaltlich übernommenen Stellen als solche gekennzeichnet habe.

Essen, den _____ _____

Unterschrift der Doktorandin

Erklärung:

Hiermit erkläre ich, gem. § 7 Abs. 2, e und g der Promotionsordnung der Fakultät für Biologie zur Erlangung des Dr. rer. nat., dass ich keine anderen Promotionen bzw. Promotionsversuche in der Vergangenheit durchgeführt habe, dass diese Arbeit von keiner anderen Fakultät abgelehnt worden ist, und dass ich die Dissertation nur in diesem Verfahren einreiche.

Essen, den _____ _____

Unterschrift der Doktorandin